MAXIMIZING LOCOMOTOR RECOVERY AFTER STROKE

RICHARDS C.L.[1], MALOUIN F.[1] AND DEAN C.[2]

[1]Département de réadaptation et Centre interdisciplinaire de recherche en réadaptation et intégration sociale (CIRRIS), Université Laval et l'Institut de réadaptation en déficience physique de Québec, Qc., Canada; [2]School of Physiotherapy, University of Sydney, NSW, Australia.

INTRODUCTION

Given the limited rehabilitation available to stroke victims, an effective therapeutic approach is imperative. Many studies support a task-oriented approach provided early and with sufficient intensity to promote locomotor recovery[1,2]. Gait speed at discharge from rehabilitation, however, is often insufficient to promote independence[3,4] and follow-up out-patient rehabilitation is rarely offered. We undertook two studies to examine the potential for further locomotor recovery in individuals with chronic stroke. The first examined the effectiveness of a task-related circuit training class while the second investigated the effects of an individualized task-related exercise program designed to improve ankle power generation at "pushoff"[5]. The exercise programs for both studies were inspired by the practice intense Australian motor relearning approach[6].

MATERIALS AND METHODS

The first study, a randomized controlled pilot trial, evaluated the efficacy of a task-related circuit training exercise class for persons with chronic stroke (0.6–3.2 years after stroke). Twelve subjects were randomized into the experimental (EXP) or the control (CTL) group. Both groups participated in 1-hour of task-related training 3 times a week for 4 weeks. Sessions were organized as a circuit training exercise class. The EXP group completed practice at a series of 10 workstations designed to strengthen the muscles in the affected leg in a functionally relevant way and in addition participated in walking races and relays with other members of the group. For the CTL group, the organization and delivery of the training was similar except that the workstations were designed to improve training of the affected upper limb. Performance was evaluated with both clinical and laboratory measures made immediately after therapy and 2 months later to assess retention. Using a multiple single case design, the second study evaluated the effects of individualized task-related exercise designed to improve plantarflexor "push-off". Four subjects with chronic stroke (0.9–2.1 years after stroke; age: 49–70 years) received therapy 3 times a week for 1 hour for 3 weeks.

RESULTS

In the first study, analysis of change scores showed the EXP group to perform significantly better than the control group in the 6-minute walk test and walking speed. The increase in distance walked during the 6-minute walk test for the EXP group ranged from 14.5–91.1 M immediately after therapy and 16.8–82.4 M, 2 months later, compared with ranges of –2.4–8.7 and –4.3–8.3 M for the CTL group. Walking speed (without assistive devices) improved 3.2–21.2 cm/s. No significant differences were found between the groups in grip strength or dexterity measures over the immediate or retention periods. In study two, all 4 subjects improved their preferred walking speed and walking endurance and these improvements were associated with improved power generation at the ankle at "pushoff" and at the hip at "pulloff". The endurance impairment of about 25%, as measured by the 6-minute walk test, in these patients with good pre-therapy walking speeds (78–142 cm/s) improved 21.2–28.5% after the intense training program, more than the preferred walking speed (10–17%).

DISCUSSION AND CONCLUSION

These studies[4,5] confirm the potential for locomotor recovery of individuals in the chronic phase of stroke and their capacity to collaborate in relatively intense exercise. They also indicate that a specific task-related and intense approach can promote substantial change with as little as 9–12 one-hour sessions over a 3–4 week period on an out-patient basis. Both the circuit training and the individualized approaches were shown to be effective with the amount of practice required in the training sessions. An important finding was that gait speed alone tended to underestimate the magnitude of the locomotor deficit revealed by the endurance-related measures. While gait speed improved in both studies, the magnitude of the improvement was larger for the endurance measures, even in the subjects who walked at near-normal velocities prior to therapy. These results suggest the need for periodic tune-up sessions for individuals with chronic stroke to maximize their locomotor potential and emphasize the need to consider endurance as a limiting factor that is likely related to intensity and type of practice.

This work was supported by grants from the FRSQ and Fonds en réadaptation de l'Université Laval.

REFERENCES

1–RICHARDS C.L. et al. (1993)- *Arch. Phys. Med. Rehabil.* 74:612–620.

2– KWAKKEL G. et al. (1999)- *Lancet* 354:191–196.

3– PERRY J. et al. (1995)-*Stroke* 26:982–989.

4–RICHARDS C.L. et al. (1999)- *Clin. Geriatric Med.* 15:833–855.

5–DEAN C.M. et al. (2000)- *Arch. Phys. Med. Rehabil.* 81:409–417.

6–CARR J.H. and SHEPHERD R.B. (1998)- *Neurological Rehabilitation: Optimizing Motor Performance*, Oxford, Butterworth Heinemann.

CASE STUDY OF THE KINEMATICS AND KINETICS OF AN ACL DEFICIENT SUBJECT THAT EXPERIENCED "GIVING WAY" DURING A STEPPING DOWN TASK

HOUCK[1], J, YACK[2], H.J AND SNYDER[3], M.
[1]Ithaca College, 300 East River Road, Rochester, NY, [2]University of Iowa, Iowa City, IA, [3]University of Rochester, Rochester, NY

INTRODUCTION

Knee anterolateral instability includes increased anterior translation (> 5 mm) and internal rotation (>3°) and is believed to result in episodes of "giving way" during functional activities. Yet, due to difficulties tracking the femur, no studies recorded a "giving way" event during a functional activity. Serendipitously, an ACL deficient subject reported experiencing "giving way" while participating in a study utilizing a new approach to tracking the femur that significantly decreases tibiofemoral kinematic errors[1]. The purpose of this report is to compare knee kinematics and kinetics of the "giving way" trial to the other trials that the subject did not experience a "giving way" event.

METHODS

A 32 y.o. male subject weighing 88.6 kg and 1.82 m tall that ruptured his left ACL 5 ? weeks prior to testing participated in the study. Functionally the subject scored 64% on the Lysholm Scale, 57% on the Modified Noyes Questionnaire and rated his knee as 50% in response to a global question of knee function. Cybex II isokinetic strength tests suggested involved side knee extension was 75% and knee flexion was 89% of the uninvolved side. The KT-1000 measured 5 mm of anterior laxity relative to the opposite leg. The subject experienced "giving way" during a successful step down from an 8-inch curb walking at 1.24 m/s. The Optotrack motion analysis system tracked markers placed on the foot, leg, thigh and pelvis at 60 Hz. Subsequently, the position data was combined with ground reaction force and anthropometric data to estimate knee joint angles, moments and powers using the Kingait3 software (Mishac, Inc., Waterloo, CA). Published reports of the patella tendon moment arm[3] and line of action[2] were used to estimate shear forces due to the ground reaction force and patella tendon.

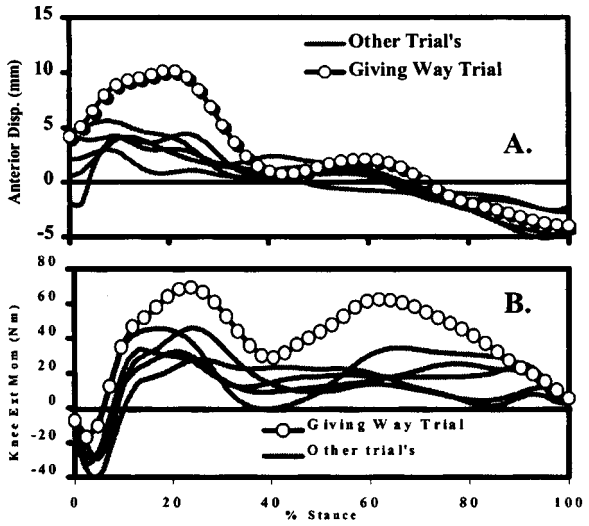

Fig.1a. Knee anterior/posterior displacement and (B) Knee sagittal plane moments across stance.

RESULTS

Peak A/P displacement was much larger during the "giving way" trial (10.1 mm) compared to the other trials (0.46 ± 0.13 mm) (Fig. 1A), however, peak external rotation was similar (4.1° vs 3.0 ± 0.8°). The increased anterior displacement occurred from 5% to 36 % of stance (Fig. 1A). Peak knee flexion was larger for the "giving way" trial (41.1º) compared to the other trials (33.1 ± 2.4º). Peak sagittal plane moment during the "giving way" trial increased relative to the other trials (69.3 Nm vs. 36.96 ± 8.27 Nm - Figure 1B). The net effect of the increased knee angles and moments are estimated by the tibial shear forces which were larger for the "giving way" trial (558.5 N vs 367.5 ± 57.5 N). In contrast to the other trials (external rotation, 2.38 ± 1.66 Nm) the transverse plane knee moments were toward internal rotation (2.09 Nm) for the "giving way" trial. Also, frontal plane knee moments for the "giving way" trial were lower relative to the other trials (5.44 Nm vs 28.05 ± 9.83 Nm).

DISCUSSION

Deviations of knee sagittal plane kinematics and moments were uniquely associated with the "giving way" trial (Fig. 1). The estimated shear forces suggest that the external loading that occurred during the "giving way" trial may have contributed to the increased anterior displacement. Higher quadriceps demand, and subsequently greater shear is results from the higher knee extension moment during the "giving way" trial. The frontal and transverse plane moments were also unique to the "giving way" trial, and therefore suggest that alterations in three dimensional joint loading may lead to higher risk of "giving way" episodes.

ACKNOWLEDGEMENT: Support was provided by NSF Grant # BES 99-02340

REFERENCES

Yack et al., Gait & Clinical Movement Analysis Conference, Rochester, Mn, April 2000.
Kellis et al., Clinical Biomechanics. 1999.
Herzog, Read. J Anat. 1993.

KINEMATICS AND KINETICS OF TOTAL KNEE REPLACEMENT PATIENTS; FLUOROSCOPY, MOTION ANALYSIS, AND FORCEPLATE DATA

DELUZIO K.J.[1], BANKS S.A.[2], COSTIGAN P.A.[1], LADOUCEUR D.[1], O'FLYNN H.[3], WYSS U.P.[1], JASTY M.[3], RUBASH H.[3], HARRIS W.H.[3]

[1]Clinical Mechanics Group, Kingston, Ontario/Canada; [2]Good Samaritan Medical Center, West Palm Beach, Fl., [3]Massachussetts General Hospital, Boston, Ma.

INTRODUCTION

Total knee replacements (TKR) have survival rates of 80–95% up to 10 years, after which the failure rate increases. One reason for these failures is excessive wear of the polyethylene articulation. New materials are being developed to address the issue of wear, but these new materials must be shown to be superior before being brought to market. Currently, new artificial knees are tested in mechanical knee simulators. However, the results of such testing are only useful if the testing protocol accurately reproduces the knee joint's kinematics and kinetics. Accurate kinematics can be obtained through fluoroscopic analysis of the knee[1] while conservative estimates of the kinetics are possible by combining motion analysis and force plate information with a simple knee model[2]. The objective of this study was to integrate the simultaneous quantification of both the kinematics and the kinetics of a total knee replacement design using fluoroscopy, motion analysis and force plate recordings during a step-up motion.

MATERIALS AND METHODS

Three consenting males with four knees implanted with the same design of primary, posterior cruciate retaining, total knee arthroplasty, participated in this study. The TKR (Miller-Galante II, Zimmer Inc, Warsaw, IN) was of low conformity in the sagittal plane offering little anterior/posterior constraint. The patients, aged 63, 63 and 79, were 5–7 years post-operative. They all ambulated without support and were able to climb stairs reciprocally. Subjects were asked to perform a single limb step-up/down maneuver while standing on a force plate imbedded in a step. They were simultaneously monitored by the motion analysis system and fluoroscopy. Fluoroscopy images were obtained at 30 Hz (Series 9800 Cardiac, OEC Medical Systems Inc., Salt Lake City, UT) and three dimensional tibio-femoral motions were obtained from the fluoroscopic images using shape matching techniques[1]. The motion analysis/forceplate system has been previously described and validated[3,4].

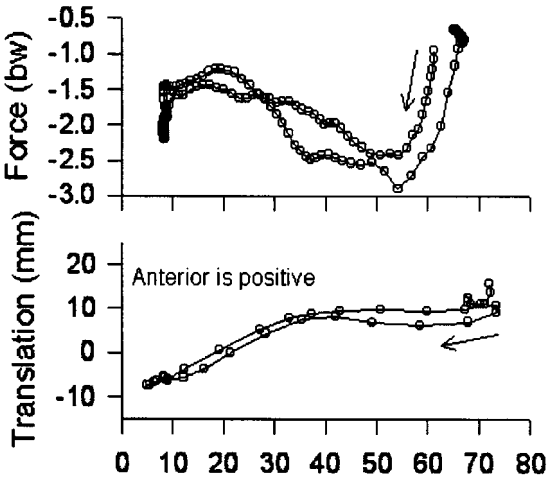

Fig. 1. Distal/Proximal Bone-on-Bone Force and Femoral translations versus flexion angle for a single patient.

RESULTS

Data for a single representative subject are shown in Figure 1. The bone-on-bone forces reached a peak of 3 times body weight at about 55° of knee flexion. This corresponded to a large net flexion moment, counter-acted by the quadriceps that acts to support the body during ascent. The forces then decreased to a minimum of just over one body weight when the knee became fully extended. The step-down phase was similar to the ascent. The translation of a point on the femur with respect to the tibia is illustrated in Figure 1. The femur translated posteriorly during ascent and reversed to follow the same path during descent.

DISCUSSION AND CONCLUSION

In general, the knee kinematics were found to be consistent with observations from previous studies[5,6]. Fluoroscopy is uniquely suited to measure the kinematics of the femoral and tibial components because the axes of rotation can be precisely defined and there is no skin motion artefact. Bone-on-bone forces are difficult to assess as they cannot yet be directly measured. The forces reported here are conservative yet they are three times higher than net forces that ignore all muscle action. Simultaneous kinematic and kinetic data provides information on the interaction between the motions and forces at the knee that is critical to understanding the limitations of current TKR designs and materials, and in developing alternatives.

REFERENCES

1-BANKS, et al. IEEE Transactions BME 43(6), 1996.
2-LI et al. J. Biomed. Eng 15, 1993.
3-COSTIGAN, et al. Med.Biol.Eng.Comp. May, 1992.
4-DELUZIO et al. J. Biomech. 26, 1992.
5-BANKS et al. J Arthroplasty 12(3) 1997.
6-BANKS et al. Am J Knee Surg fall, 1997.

A KINETIC ANALYSIS OF A STEPPING TASK FOLLOWING TOTAL KNEE ARTHROPLASTY

J. M. BYRNE, S. D. PRENTICE, W. H. GAGE
Gait and Posture Laboratory, University of Waterloo

INTRODUCTION

When conservative treatment for knee ostoearthritis (OA) ceases to adequately control knee pain a total knee arthroplasty (TKA) is frequently performed. Though pain levels and mobility improve following TKA, patients typically ambulate more slowly and generate very different knee moments then age matched controls[1]. When faced with the more challenging task of ascending stairs patients exhibit deficits in knee flexor moments and range of motion[2]. As stepping onto a raised surface occurs often during daily activities, these altered movement patterns may place patients at greater risk for falls or increase the wear on the prosthetic joint. In this study a kinetic analysis of a step-up task will be used to provide insight into the modifications seen in joint kinetics following TKA. More importantly it may also serve to highlight rehabilitation strategies that may improve patient outcomes.

METHODS

Two groups, healthy controls (3 males, 4 females, mean age 69.3) and TKA patients (2 males, 4 females, mean age 78.5) were examined. Subjects were in good health and had no neurological disorders. All patients were at least 6 months post TKA. Participants performed a total of 10 step-up trials at a height of 8''. Subjects began with both feet on a lower force plate and then stepped onto an upper force plate, finishing with both feet on the upper plate. The left and right limb each lead for half the trials. Kinematic data was collected using an OPTOTRAK system. Infrared markers were placed bilaterally at nine different locations on the lower limb and trunk. Moments at the ankle, knee and hip joints of each limb were calculated using inverse dynamics. Power and work values were then calculated to facilitate a comparison of the movement strategies used at each joint. For the purposes of analysis 3 limb groups were defined – control, surgical and non-surgical. Between limb differences at each joint were analyzed using ANOVA and post-hoc Tukey tests.

RESULTS

Work levels are shown in Figure 1 for the stance phase of each limb. In the control group, the lead limb acted to elevate the body by the application of rotational "pull-up" energy at the knee and hip. To assist with this elevation, the trail ankle provided "push-off" power. In the patient group knee energies in the surgical lead limb were significantly decreased, while at the hip significant increases in energy occurred. Non-surgical trail ankle energy also increased. When the surgical limb trailed, less push-off energy was seen at the ankle, while trail hip energies increased.

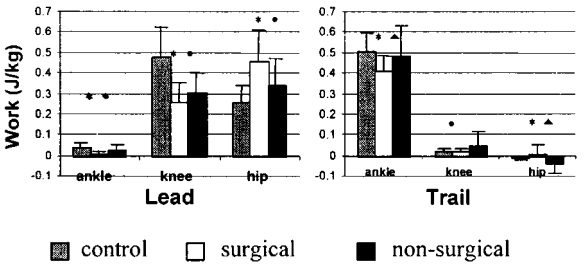

Fig. 1. Lead and trail limb work levels during the stance phase (significance between: •control/surgical, *control/non-surgical, ▲surgical/non-surgical ($p < 0.05$)).

DISCUSSION

The knee extensor mechanism is the principal contributor to pull-up during stair ascent[3]. It is not surprising then that diminished surgical lead limb knee energy is seen in individuals following TKA. Altered knee joint mechanics[2], muscle weakness or habitual gait patterns may contribute to these findings. To compensate for this decreased extensor energy and thus to enable safe completion of the task, we see increased surgical pull-up hip energy in the patient group. During stair ascent trail limb plantar flexor activity is thought to lift the body vertically[3], therefore, assisting with pull-up. Increases in non-surgical trail limb ankle energy may, therefore, be compensating for the decreased activity in the surgical lead knee. When the surgical limb trails, reductions in ankle energy levels may indicate unwillingness on part of the patient to load the surgical limb or may be an indication of altered motor control in the limb[4]. As the surgical trail knee does not (or is unable to) compensate for this decreased ankle energy it appears that the trail surgical hip provides the additional push-off energy needed. The absence of differences between the non-surgical and surgical limbs in 4 of the 6 conditions is also of interest. Factors including concomitant OA and muscle weakness may explain these differences, though further work, controlling for these factors is needed. In summary, the patient population employs compensation using healthy joints to enable successful completion of a step-up task. Maximizing the performance of these compensating joints may further enhance outcomes.

REFERENCES

1–Wilson et al. (1996) J. Arthroplasty 11:359–367.
2–Andraicchi TP (1993) J. Biomechanical Engineering 115:575-580.
3–McFadyen BJ and Winter DA (1988) J. Biomechanics 21:733-744.
4–Gage WH (1999) Unpublished MSc thesis UWaterloo Gait and Posture Labratory.

KINEMATIC AND KINETIC ANALYSES OF LEVEL GAIT AND STAIR CLIMBING IN FUNCTIONAL STROKE SURVIVORS

NADEAU S.[1,2], MCFADYEN B.J.[3,4] AND MALOUIN F.[3,4],
[1]École de réadaptation, Université de Montréal; [2]Centre de recherche, Institut de réadaptation de Montréal, (Qc), Canada; [3]Institut de réadaptation en déficience physique de Québec and [4] Université Laval.

INTRODUCTION

Level walking and stair climbing are among the locomotor tasks frequently performed in daily activities. From a mechanical point of view, these two tasks are quite different. In gait, the energy generation in the sagittal plane of motion is essentially produced by hip flexors and extensors and the ankle plantarflexors (1,2). The knee muscles are mainly used to decelerate the segments resulting in energy absorption whereas in stair ascent, the knee flexors and extensors are important energy generators. In the frontal plane, the hip abductor moment is very similar in magnitude (1.0 N.m/kg) for level gait and stair climbing. However, contrary to level gait, a concentric action of the hip abductor muscles is used to control the pelvis resulting in an important power generation during the stance phase (3). It is not well known how stroke subjects perform in stair climbing in comparison to healthy subjects. The purpose of this study was to assess the time-distance, kinematic and kinetic variables of level gait and stair climbing in a group of chronic stroke survivors and to compare their results to those of healthy subjects performing at natural speed.

MATERIAL AND METHODS

Eight adults with residual hemiparesis due to a cerebral vascular accident [mean age (SD) 49.4 (9.9) yrs] and eleven healthy subjects [55.4 (9.4) yrs] participated in the study. The stroke subjects were very functional. Their mean natural gait speed was 1.09 (0.22) m/s and their mean score on the timed “Up & Go” test was 11.0 (1.85) s revealing high functional capacities. All subjects, except one who had moderate spasticity, demonstrated a slight increase or normal tone at the ankle joint. Subjects were asked to perform at their natural speed. In the stair climbing task, subjects stood in front of the stairs before ascending. Only one stroke subject held the railing to climb the steps. Three dimensional kinematic data were obtained using the Optotrak system sampled at 75 Hz. The ground reaction forces were collected with two separate AMTI force platforms embedded in the first and second steps of the stair and in the ground for level walking. The time-distance parameters were obtained from three footswitches under each foot. The relative angles at the hip, knee and ankle joints were calculated with a Cardanic x-y-z rotation sequence. The net muscle moments of force were estimated using an inverse dynamic approach with the Kingait 3 software (Mishac Kinetics). At least three normalized cycles of level gait and stair climbing (second step) were averaged for each subject. The data examined included the time-distance parameters, the level and stair gait profiles and the main peak values of the joint angles and moments in the sagittal plane at all three joints as well as in the frontal plane at the hip joint.

RESULTS

For level gait, the time-distance parameters were not different between groups and between sides for the stroke subjects. However, the stair gait data revealed a lower mean cadence [72 (15.4) vs. 94 (12.8) step/min] and a shorter stance phase [57 (4.8) vs. 60 (1.1) %] as a percent of stride (*t*-test; $t < 0.05$) in the stroke survivors in comparison to the healthy group. Few differences were observed in the joint angle data for the stair task. In gait, a decreased plantar flexion movement at the end of the stance phase was observed on the affected side. The kinetic analysis revealed a decreased dorsiflexion moment during level gait at the beginning of the stance phase on both sides for the stroke subjects. In stair climbing, the peak knee extensor moments on the affected [0.75 Nm/kg] and non-affected sides [1.19 Nm/kg] were decreased and increased respectively in comparison to normal data [0.98 Nm/kg)]. Moreover, the hip abductor moment on the non-affected side was higher and prolonged at the end of the stance phase in comparison to healthy subjects.

DISCUSSION AND CONCLUSION

The stroke subjects in this study were clinically classified as having a very good functional recovery. This was confirmed by the level gait analysis that only revealed differences at the ankle joint. However, their stair gait performance was clearly reduced in comparison to the healthy group and detailed analysis of the data revealed evidence of the utilisation of compensatory strategies by the non-affected side. This suggests that the stair climbing task might be more useful than level walking to assess good stroke performers. Moreover, results clearly showed that the joint angle parameters taken alone were not sufficient to distinguish the stroke from the healthy subjects in stair ascent. However, it is believed that further analyses of the kinematic and kinetic data are warranted before any generalization should be done to the large population of the stroke survivors.

ACKNOWLEDGEMENTS: Financial support from NSERC. Dr. Nadeau is supported by the MRC of Canada. We acknowledged Mr. Comeau and Mr. St-Vincent for their technical support.

REFERENCES

1. McFadyen & Winter. J Biomech, 1988: 21: 733–744.
2. Livingston et al. Arch Phys Med Rehabil,1991:72:398–402.
3. Nadeau, S et al. Gait & Posture,1999; 9 (suppl 1): S60.

RELIABILITY OF LOWER LIMB NET JOINT MOMENTS IN GAIT OF CHILDREN WITH DUCHENNE MUSCULAR DYSTROPHY

EMOND M.,[1,2] GRAVEL D.,[2] GAGNON D.,[3] VANASSE M.[1] AND NADEAU S. [2]

[1]Hôpital Marie Enfant; [2]Institut de Réadaptation de Montréal; [3]Université de Sherbrooke, Canada.

INTRODUCTION

Duchenne muscular dystrophy (DMD) is a progressive disease which leads to loss of the ability to walk. Impairment of the muscular system can induce fatigue across trials during a testing session while deterioration can take place between sessions. To appreciate the effect of therapeutic interventions, it is essential to know the reliability of gait measurements. The objective of this study was to quantify the reliability of lower limb net joint moments across trials and sessions.

MATERIAL AND METHODS

Ten children with DMD (mean age 9.6 years, ranging from 7 to 13) but still able to walk independently took part in the study. Five trials at natural cadence were recorded by a three-dimensional analysis system (Peak Performance). Two evaluation sessions were conducted within a two-week interval. Net moments of force of each joint of the weaker limb were calculated with the inverse solution. The reliability of the data was evaluated using the generalizability theory,[1] a modern test theory based on the analysis of variance. It comprises two steps. The first, known as a G-study, is to find the variance components associated with the relevant factors that affect reliability. In the present study, these factors are the subjects, the trials, the sessions and their interactions. The D-study is the second step in which the results of the G-study are used to find the reliability expected for a particular design. Thus, the present study, with five trials and two sessions, constitutes the G-study and the expected reliability will be computed for a D-study, with five trials in one session. Two indices of reliability were computed. One is the dependability coefficient (ϕ), which is computed as the ratio of the subject variance to the total variance. The total variance is the sum of the subject variance and the absolute error variance. The latter includes systematic errors associated with trials and sessions as well as random errors due to interactions between subjects, trials and sessions. The maximum value of ϕ is 1 when no error is present. The second index is the standard error of measurement (SEM), which gives the stability of the variable in terms of a unit of measurement such as Nm or Nm/kg. It is computed as the square root of the absolute error variance. Because the dependability coefficient is related to the subject variance, it can be affected by the normalization procedure, thereby reducing the variability across subjects. To pinpoint this effect, the reliability will be reported for absolute (Nm) and normalized (Nm/kg) moments.

RESULTS

Table 1 gives the expected dependability coefficients and SEMs for a D-study design based on the mean of five trials in one session. The dependability coefficients are not systematically reduced by the normalization process, although a marked effect is observed for the plantarflexor moments. Except for the hip extensor moments, the SEMs of absolute moments were less than 3 Nm.

DISCUSSION AND CONCLUSION

The reliability, as expressed by the coefficient ϕ, depends on the joint moment. When low values are found, they are generally attributable to a high variance component associated with the interaction between subjects and sessions. Variance related to trials is low. The normalization markedly affects the reliability of the plantarflexor moments by reducing the subject variance. Even if low coefficients ϕ are calculated, these are not indicators of the precision of measurement and the SEM is more informative. Considering that we can be 95% confident that the true moment lies in the interval of $\pm$ two SEMs, the maximum error reaches 8.42 Nm (hip extensor moment). This value is comparable to the results reported by sensitivity analysis of moment to errors of alignment.[2]

This project was supported by FRSQ and OPPQ.

REFERENCES

1. Shavelson and Webb (1991) Generalizability Theory Newbury Park. Sage.
2. McCraw and DeVita P (1995). J Biom. 28: 985–988.

Table 1. Dependability coefficients (ϕ) and standard error of measurements (SEM) for moments expressed in absolute (Nm) and normalized (Nm/kg) units. The gait cycle locations of the peak moment values are given in parentheses.

	ϕ		SEM	
	Abs.	**Nor.**	**Abs.**	**Nor.**
Hip moment				
Extensors (10%)	0.33	0.45	4.21	0.111
Flexors (55%)	0.61	0.68	2.47	0.078
Knee moment				
Extensors/flexors (15%)	0.75	0.67	2.51	0.082
Flexors (45%)	0.53	0.33	2.59	0.091
Extensors (60%)	0.10	0.19	2.39	0.072
Ankle moment				
Dorsiflexors (5%)	0.62	0.60	0.73	0.024
Plantarflexors (50%)	0.90	0.52	2.95	0.099

NUMERICAL SIMULATION OF THE MECHANICAL RESPONSE OF CHONDROCYTES IN UNCONFINED COMPRESSION DURING CYCLIC LOADING

JOHN Z. WU AND WALTER HERZOG
Human Performance Lab., Faculty of Kinesiology, The University of Calgary, Calgary, Alberta, Canada

INTRODUCTION

Biochemical composition and mechanical properties of articular cartilage are associated with the metabolic activity of chondrocytes. Fluid pressure and stress-strain state in and around chondrocytes are important mechanical stimuli associated with remodeling, adaptation, and degeneration of articular cartilage. Experimental studies have indicated that cyclic compressive loads stimulate the biosynthetic activity of cells differently than static compressive loads. However, only the overall response of cartilage to dynamic loading has been determined to date. The purpose of the present study was to determine numerically the location- and time-dependent stress-strain state and fluid pressure distribution in chondrocytes in an unconfined, cyclic compression test.

METHODS

Articular cartilage was approximated as a macroscopically homogenized material having effective material properties. The average mechanical behaviour of cartilage was obtained using the homogenized model. The solution of the time-dependent displacement and fluid pressure fields was used as the time-dependent boundary conditions for a microscopic sub-model, to obtain the time-dependent mechanical behaviour of cells in different locations within the cartilage. Cartilage was considered to be composed of extracellular matrix and small, spherical cells. Both, cartilage matrix and cells, were treated as biphasic materials. The permeability was assumed to be deformation-dependent. Numerical tests using unconfined compression with similar configurations as in the experiments by Guilak [2] were performed. The cartilage specimen was assumed to be fixe on the bottom plate. The indentation plate on top of the specimen was assumed to be impermeable. The values for the elastic modulus, Poisson's ratio, and the initial permeability of the matrix and cells were assumed according to [3,4]. The cells used for illustration of our simulations were located at three positions within the cartilage specimen: center, surface, and bottom. The numerical tests were carried out using a prescribed cyclic load. The effects of loading frequency and loading amplitude on cell deformation were investigated using loading tests with three cyclic frequencies and two amplitudes (f = 0, 0.1, and 0.02 Hz; s_m = 0.1 and 0.2 MPa). The cyclic loading with zero frequency (f = *0* Hz) corresponds to a constant load. The magnitude of the constant load was taken as the average value for the cyclic loading conditions.

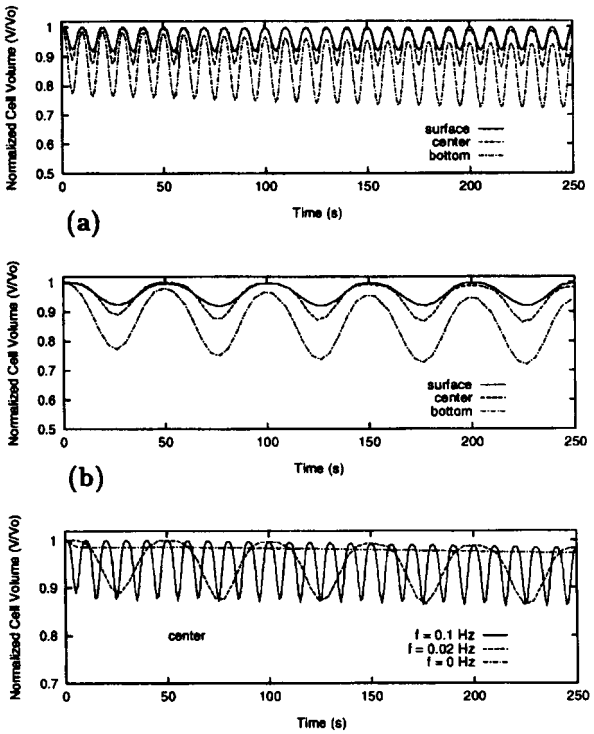

Fig. 1. Determination of cell volume as a function of location and time (with average, nominal stress sm 5 0.1 MPa). (a)-(b) æ cells at center, surface and bottom: (a) f 5 0.10 Hz; (b) f 5 0.02 Hz. (c) æ cell at center: f 5 0, 0.02, and 0.10 Hz.

RESULTS AND DISCUSSION

Changes in cell volume and cell average fluid pressure at the center, surface, and bottom were determined using constant and cyclic loading with different cyclic frequencies (f = 0.10 Hz and 0.02 Hz) (Fig. 1). For cyclic loading, the cell near the "bone-cartilage interface" experienced larger deformations (larger cyclic amplitude) than the cell near the contact surface (Figs. 1a-b). The average fluid pressure cyclic amplitude in cell near the "bone-cartilage interface" was larger than that of the cell near the contact surface (results not shown). The cell volume was predicted to decrease, on average, as a function of time for static and cyclic loading (Fig. 1c). The present simulations indicated that cells near the cartilage-bone interface would receive larger mechanical stimuli compared to those near the contact surface.

ACKNOWLEDGEMENTS: Alberta Heritage Foundation for Medical Research, the Medical Research Council of Canada, and the Arthritis Society of Canada

REFERENCES

[1] Wu J.Z., Herzog W., and Epstein J. Biomech, 32:563–572, 1999.
[2] Guilak F, J. Biomech., Vol. 28, pp. 1529–1541, 1995.
[3] Jones WR, Ting-Beall HP, Lee GM, Kelley SS, Hochmuth RM, and Guilak F, Trans. ORS, 22:1:199, 1997. [4] Shin D and Athanasiou KA Trans. ORS, 22:1:152, 1997.

STRETCHING AND INTERLEUKIN-1∃ INDUCE STROMELYSIN IN RABBIT TENDON CELLS

ARCHAMBAULT J.[1], TSUZAKI M.[2], HERZOG W.[1], BANES A.[2]

[1]Human Performance Laboratory, Faculty of Kinesiology, University of Calgary, Canada; [2]Department of Orthopaedics, University of North Carolina, Chapel Hill, NC, USA

INTRODUCTION

Occurrence of repetitive motion injuries is thought to depend on exposure to excessive mechanical loads and individual factors such as systematic illness[1]. Thus, tendons may be injured either through mechanical or biochemical events. We evaluated the expression and production of cyclooxygenase-2 (COX-2) and matrix metalloproteinases (MMPs) by rabbit paratenon cells exposed to stretching and interleukin-1∃(IL-1∃). We hypothesized that IL-1∃ would be a more powerful stimulus for COX-2 and MMP expression than would mechanical load, but that a combination of both would be more powerful than either one alone.

MATERIALS AND METHODS

Fibroblasts were isolated from the paratenon of the Achilles tendon of 5–7 month old male NZW rabbits. Four experimental conditions were used to investigate how tendon cells responded to mechanical and biochemical stimuli: control (C), stretch (S), interleukin (IL) and stretch + interleukin (S+IL). Stretched samples were subjected to one of two, 6 hour strain protocols. One group received 2% biaxial elongation at 1.25 Hz, and a second group received 5% elongation at 0.33 Hz. Interleukin treated samples were incubated with 1nM IL-1∃. Stretch + interleukin samples were incubated with IL-1∃ and subjected to one of the two strain protocols. Cell number, gene expression and protein production were evaluated 24 hours after the start of the treatments. Total cellular RNA was isolated, then subjected to polymerase chain reaction for 25 cycles. The following genes were evaluated: COX-2, collagenase-1 (MMP-1), stromelysin-1 (MMP-3), type I collagen and ∃-actin. The amount of proMMP-3 protein released into the culture supernatant fluid was quantified in duplicate samples with a rabbit-specific ELISA (Amersham Pharmacia Biotech, UK) then normalized to cell number. Differences between experimental treatments were evaluated with a Kruskal-Wallis non-parametric ANOVA. Experiments were repeated twice.

RESULTS

Interleukin-1∃ treated cells expressed MMP-3; control samples did not (Fig. 1). The supernatant fluid of cells treated with IL-1∃ contained 16 times more proMMP-3 protein than that of control cells (Fig. 2). The gene expression of MMP-3 was also induced by the 5% stretching protocol, but not by the 2% protocol. The supernatant fluid of cells stretched by 5% contained 3 times more proMMP-3 protein than unstretched cells or cells stretched by 2%. The combined treatment of 5% elongation and IL-1∃ resulted in a 20-fold increase in protein levels over control cells. The gene expression of MMP-1 was similar to that of MMP-3. The expression of COX-2 was slightly upregulated by

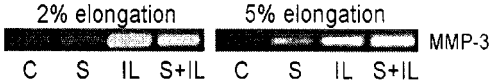

Fig. 1. Gene expression of stromelysin (MMP-3).

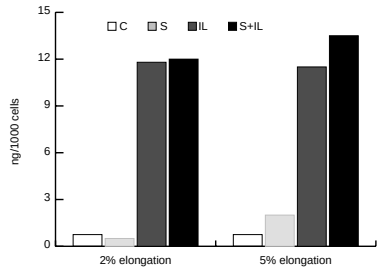

Fig. 2. Stromelysin present in supernatant fluid.

IL-1∃ treatment, but not by stretching. The expression of collagen I and ∃-actin did not change with the experimental treatments.

DISCUSSION AND CONCLUSIONS

Treatment of tendon cells with IL-1∃ dramatically increased stromelysin expression and production. Upregulation of stromelysin by IL-1∃ occurs in other connective tissues, and has been shown to result in matrix destruction[2]. Rabbit tendon cells responded to one mechanical load regimen (5% elongation) with a modest increase in MMP-3 expression and production. If enough force and strain are applied to a tendon *in vivo*, its cells may produce enzymes that can degrade matrix. If an inflammatory cytokine is present locally, such as during a systemic disease, the production of degradative enzymes may be amplified.

ACKNOWLEDGEMENTS: NSERC, AHFMR, NIH

REFERENCES

1–MACKINNON et al. (1997) - *J Hand Surg* 22A:2–18.
2–MURPHY et al. (1991) - *Br J Rheum* 30(S1):25–31.

TENSEGRITY MODEL TO DESCRIBE THE COUPLING BETWEEN ELASTIC ENERGY AND DEFORMATION OF CELLS TWISTED BY MAGNETIC PROBES

S. WENDLING[1], P. CAÑADAS[1], V. LAURENT[2], E. PLANUS[2], R. FODIL[2], C. ODDOU[1], D. ISABEY[1]

[1]Laboratoire de Mécanique Physique, CNRS ESA-7052; [2]INSERM U492, Faculté de Médecine, Université Paris-XII Val de Marne, 94010 Créteil.

INTRODUCTION

Shape adaptation and resistance to deformation of living tissues involve physical and physiological properties of cellular units. The high adaptability of the cells which change their shape when the support is distorted and tend to get stiffer as external stress is increased (stiffening response) has been pointed out by many authors [1,2]. Spatial re-arrangement of cytoskeleton elements has been proposed to be the underlying mechanism of cellular shape and stiffness adaptability, as recently shown on the basis of tensegrity model [3,4]. However, pertinent factors and critical conditions governing cell non-linear behavior are still not clearly understood. In the present study, we attempted to characterize non linearity by analyzing the elastic energy as a function of the overall strain using both the theoretical 30-element tensegrity model and experimental results obtained by twisting magnetic cytometry coupled to microscopic study of the structure in cultured epithelial cells.

METHODS

The 30-element tensegrity structure is composed of a continuous network of 24 pre-stretched elastic cables compressing a discontinuous network of 6 rigid struts. The internal tension (or prestress) of this tensegrity structure is defined by the persistent strain of the elastic cables at reference state (before deformation). This tensegrity structure was anchored to a rigid substratum through the three nodes located in the basal plane. During torsion, the three nodes, which define the superior plane, were constrained to rotate around the k-axis normal to both basal and superior planes. During extension, the three nodes of the superior plane were constrained to a linear translation along the k-axis. The unknown elastic recoil forces of the tensegrity structure were calculated using a linear incremental method, in which the force equilibrium equations are numerically solved at each node. The normalized elastic energy of the structure E_n^* was deduced from the product elastic forces times the overall deformation of the structure divided by the elastic energy of an individual cable at 100% strain. The overall deformation of the structure was calculated from the angular or linear displacement between the superior and basal planes divided by their distance before deformation. Twisting magnetic cytometry experiments were performed in A549 human epithelial cells using RGD-coated ferromagnetic beads (diameter: 4.5 µm) linked to integrins, magnetized then submitted to magnetic torque [50–150 pN.µm], treated or not with cytochalasine D which tends to depolymerize actin filaments thus altering prestress level.

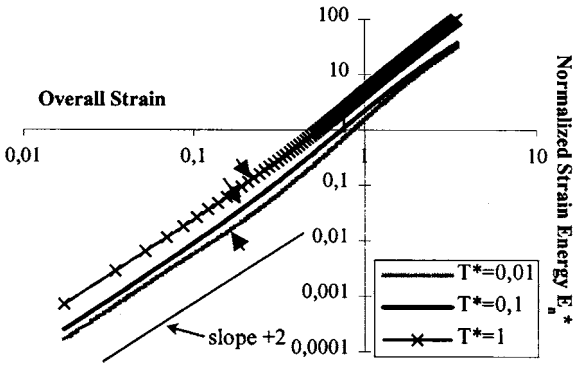

Energy-Strain relationships of a twisted tensegrity structure

RESULTS

Theoretical results obtained with the tensegrity structure show that the normalized elastic energy increases with both overall strain and internal tension T^* of elastic cables (3 T^* values tested below).

For the different values tested of internal tension, the strain energy increases proportionally with the squared strain of the structure (slope$=+2$) at small deformation (strain$<$10%) while this dependency is increased (slope$>+2$) at large deformation (strain$>$30%). The exact value of strain corresponding to this low to high transition in E_n^* strain-dependency appears slightly lowered at lower prestress (see arrows). Cells measured at two different levels of prestress induced by treatment with cytochalasine D revealed a similar E_n^* strain-dependency.

DISCUSSION AND CONCLUSION

The theoretical results allow to predict a strain range (10%-30%) beyond which the E_n^* strain-dependency will be increased likely to the increased contribution of spatial rearrangement. Note that small prestress values at given overall deformation could facilitate spatial rearrangement which could explain the earlier transition (in terms of strain) toward stronger E_n^* strain-dependency. Energy-Strain measurements in cultured cells tend to support these conclusions. For instance, cytochalasine D treatment does not abolishes the stiffening response nor the structural arrangement.

REFERENCES

1–N. Wang et al., *Science*, 260, pp. 1124–1127, (1993).
2–O. Thoumine et al., *Exp. Cell Res*., 219, pp. 427–441, (1995).
3–M.F. Coughlin et al., *J. Biomech. Eng*., 120, pp. 770–777, (1998).
4–S. Wendling et al., *J. Th. Biol*., 196, pp. 309–325, (1999).

AN ULTRASOUND METHOD TO INVESTIGATE SOFT TISSUE REACTION TO BIOMATERIAL

ABOU YOUNES F[1], POTEL C[2], DE BELLEVAL JF[1], GHERBEZZA J-M, BONAN C[3], DEVAUCHELLE B[3], GREBE R[1]

[1]Université de technologie de Compiègne, Centre de Royallieu, BP. 20529–60205 Compiegne; [2]IUT de l'Aisne, Département OGP de Soissons, 15 avenue François Mitterrand, Les Terrasses du Mail, 02 880 CUFFIES; [3]Service de chirurgie Maxillofaciale, Hopital du Nord, place Victor Pauchet, 80054 Amiens Cedex

INTRODUCTION

Resorbable biomaterials become more and more important in osteosyntheses as e.g. performed in maxillo-facial surgery. The success of this kind of surgery depends on the kind and degree of tissue response to the resulting injury and the properties of the used biomaterial. So the availability of a method that allows to investigate tissue reactions and bone tolerance due to the bioresorbable material is of great interest [1]. The method should therefor be based on noninvasive procedures as e.g. US- and MRI-investigations.

Previous studies have demonstrated that the contact between tissue and implant has an effect on the elasticity of both tissue and biomaterial [2]. We present here an approach by which changes in mechanical properties of implants and surrounding tissue can be detected and followed up. Our method is based on a ultrasound transducer used in A-scan mode integrated in a specially developed echo-signal acquisition and processing hard-/software environment.

MATERIALS AND METHODS

The chain of acquisition is build up from a 5 MHz ultrasonic transducer with a 2.7mm focal spot, a pulse echo generator with 70V peak output and a digital oscilloscope connected via a RS232 interface to an IBM compatible laptop. To enable portability together with adequate acoustic coupling and precise displacement of the transducer a special handheld transducer-device has been developed.

The transducer is placed perpendicular to the surface of the specimen, at a distance equal to its focal length. Then it is moved stepwise forward towards the surface, in 1mm steps. At every position an averaged echo signal is acquired and stored. Thus, the tissue is investigated down to a depth of about 25mm. In previous studies, depths of up to 7mm have been evaluated only [3,4].

The echo signals resulting from successive acquisitions are matched and fused (Fig. 1). A sliding window is used for the subsequent FFT. For every window the characteristic frequency and attenuation is calculated as proposed in [3].

To test and validate our method we have proceeded in two phases:

Phantom studies: Agar-agar gel of different density has been used to produce flat cylinders exhibiting different mechanical properties. They have combined to piles mimicking properties of subsequent layers of tissue.

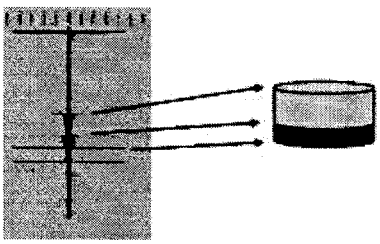

Fig. 1. Echo from a double layer structure as a model for the interface between layers of different soft tissue.

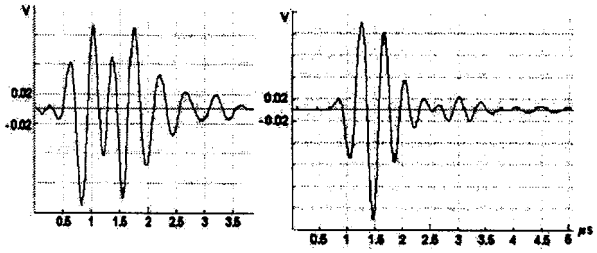

Fig. 2. Echo of a soft (left) and a hard (right) phantom.

In vitro studies: This phase has been realized on chicken legs with implanted prosthesis.

The influence of mechanical properties on the acquired signals becomes evident by comparison of the echos from the interfaces of different phantoms with the surrounding water. As can be stated from Figure 2 the echos reflected from phantoms made from soft agar-agar are longer in duration and slightly smaller in amplitude as those from harder ones. This goes well together with our according computer models and simulation (not shown) and holds also for the evaluation of the weaker reflections from inside the phantoms.

CONCLUSION

The first results show that our method provides a noninvasive low cost tool to identify and qualify changes in prosthesis mechanical properties as well as in the surrounding tissue.

REFERENCES

S.S. Kohles et al. Ultrasonically determined elasticity and cortical density in canine femora after hip arthroplasty. Journal of biomechanics. Vol 27, No 2, 1994, PP 137–144.

R.B. Ashman et al. A continuous wave technique of the elastic properties of cortical bone. Journal of biomechanics. Vol 17, No 5, 1984, PP 349–361.

C. Guittet et al. In vivo high-frequency ultrasonic characterization of human dermis, IEEE transactions on biomedical engineering. Vol 46, No 6, 1999, pp. 740–746.

Z. Sun et al. Automatic ultrasound determination of thermal coagulation front during laser tissue heating. IEEE transactions on ultrasonics. Vol 16, No 5, 1999, pp.1134–1146.

FEMOROTIBIAL CONTACT ANALYSIS FOR ANATOMIC DESIGNS OF TKA USING A NON-LINEAR RIGID-BODY-SPRING MODEL

NUÑO N.[1] AND AHMED A.M.[2]

[1]DEIS, Faculty of Engineering, University of Bologna, Bologna, Italy; [2]Department of Mechanical Engineering, McGill University, Montreal, Canada.

INTRODUCTION

The aim of the study was a three-dimensional parametric femorotibial contact analysis for "anatomic" designs of Total Knee Arthroplasty (TKA) components based on recent measurements of the geometry of the natural articular surfaces[1]. It was planned to use an extension of the rigid-body-spring model[2], where the non-linear material behaviour of the tibial polyethylene component is taken into account.

NON-LINEAR RIGID-BODY-SPRING MODEL

The rigid femoral component indents the deformable ultra-high molecular weight polyethylene (UHMWPE) tibial component (fixed to a rigid foundation), which is discretized by a series of spring elements. The sagittal and frontal profiles of the bearing surfaces, based on measurements of the femoral condyles[1], are shown in Figure 1(a,b); r_1=19.2 mm, r_2=35.8 mm, (r_1/r_2=0.54), $\alpha_1=\alpha_2$=30.4°. In the frontal plane R=21.0 mm, β=30° and the components are conforming. $N \times M$ non-linear springs equally spaced ($\varepsilon=d$=0.5 mm) are used. Poisson's ratio ν was taken as 0.4, and the non-linear modulus of elasticity, $E(\varepsilon)$, from the results of relaxation tests[3] of irradiated UHMWPE at 37°C.

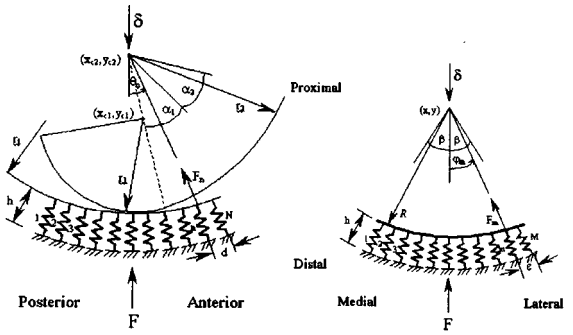

Fig. 1. (a) Sagittal plane; (b) Frontal plane.

Analogous to the case when the deformable material is linearly elastic[4], the spring stiffness per unit area is

$$k_{n,m} = \left[1-\nu E\epsilon_{n,m}\right] / \left[1+2\nu h\right]$$

where $E\epsilon_{n,m}$ is the non-linear modulus of elasticity, $\epsilon_{n,m} = \delta_{n,m}/h$ is the strain and h=10 mm. The compression of spring (n,m) is given by

$$\delta_{n,m} = \delta \cos\theta_n \cos\varphi_m.$$

The vertical force F is the vertical component of the resultants of the $N \times M$ forces created by each compressed spring

$$F_{n,m} = k_{n,m}\delta_{n,m}\epsilon d$$

and

$$F = \sum_{n=1}^{N}\sum_{n=1}^{M} F_{n,m}\cos\theta_n \cos\varphi_m$$

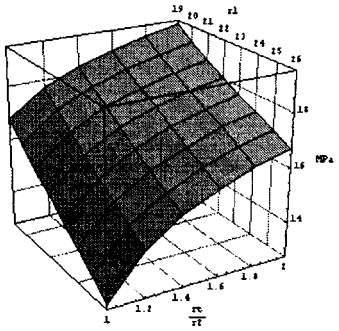

Fig. 2. Peak contact stresses.

The knee flexed at 45° was analyzed for a femorotibial compressive load of 4.25 times body weight of 750 N.

RESULTS

An increase in the ratio r_1/r_2 increased the contact area, thus decreased the peak contact stresses. The parameters r_1 and r_2 were varied up to 35% from their initial values to remain close to the natural geometry. The maximum increase in the contact area was achieved by increasing r_1. Figure 2 shows the effect of varying r_1 and the femorotibial conformity on the peak contact stresses; e.g. as r_1 increased from 19 to 26 mm, the peak stresses decreased by up to 24% for r_t/r_2=1. When increasing r_t/r_2 (decreasing femorotibial conformity in the sagittal plane) the peak stresses increased by up to 30% for r_1 kept at 26 mm. The effect of varying r_1 and the radius of curvature R of the femoral and tibial components in the frontal plane on the peak contact stresses for a constant femorotibial conformity, r_t/r_2=1, was also investigated. For any r_1 considered (19 to 26 mm) increasing R from 15 to 35 mm decreased the peak stress by 41%.

DISCUSSION AND CONCLUSION

The RBSM method was found useful to analyze contact including the non-linear behaviour of the UHMWPE in an efficient way in comparison with finite element analysis which requires large computational effort. The analysis provided results pertinent to the deisgn of anatomic femorotibial components from the point of view of contact conditions.

REFERENCES

1–NUÑO N. and AHMED A.M. (1998)-Proc. of Medit. Conf. on Medical and Biological Engng and Computing.

2–KAWAI T. (1980)-*Inter. J. for Numerical Methods in Engng, 16*, 81–120.

3–WALDMAN S.D. and BRYANT J.T. (1994)-*J. of Applied Biomaterials, 5*, 333–338.

4–BLANKEVOORT L. et al. (1991)-*J.Biomech. 24*, 1019–1031.

ANTHROPOMETRIC AND SENSORY FACTORS INFLUENCE PERCEPTION OF FOOTWEAR COMFORT

HAU A., STEFANYSHYN D.J. AND NIGG B.M.
Human Performance Laboratory, University of Calgary, Canada

INTRODUCTION

The most common injuries amongst military personnel are overuse injuries to the lower extremities[1]. It has been shown that using basketball shoes for military training reduces the incidence of overuse injuries to the feet compared to combat boots[2]. Furthermore, shock absorbing inserts have been shown to reduce the incidence of pain in the Achilles tendon, calves, and back[3]. It is speculated that comfortable shoe inserts reduce fatigue and therefore injury frequency[4]. However, comfort is subject-specific and to date there is little knowledge about the relationship between subject characteristics, footwear material and shape, and comfort. Therefore, the purpose of this study was to determine anthropometric and sensory factors that are related to differences in comfort perception.

MATERIALS AND METHODS

103 military personnel (7 female, 96 male) with an average age 27 ($\pm$ 7.1) years, height 174.5 ($\pm$ 7.0) cm, and weight 81.7 ($\pm$10.2) kg volunteered in this study and gave informed consent. All subjects participated in the regular military training and did not have any injuries or pain at the time of the study. Subject characteristics including foot shape, leg alignment, and sensitivity were measured for each subject. Seven different footwear conditions were used: combat boots without any inserts and combat boots with six pairs of inserts different in material and shape (Table 1). The subjects were asked to walk in their boots on different surfaces (pavement, grass, gravel, and concrete) and to give a comfort rating for each of the seven footwear conditions tested in a randomly selected order. Comfort was rated using a visual scale. The left end of the visual scale was labeled 'not comfortable' and corresponded to a comfort rating 0, the right end was labeled 'very comfortable' corresponding to a comfort rating 10. To determine the effect of each subject characteristic, the subjects with the ten lowest values and the subjects with the ten highest values were selected for each of the subject characteristics. The differences between comfort ratings (Δ_C) for pairs of inserts that differed in only one material property or shape characteristic were then compared for the low and the high group of each subject characteristic. MANOVA analysis and student-t tests ($\alpha = 0.05$) were performed to detect significant differences in comfort perception between these groups of subjects.

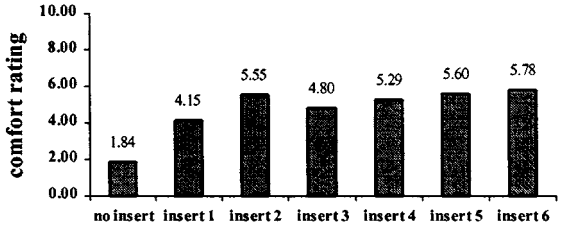

Fig. 1. Mean comfort ratings for all footwear conditions.

Table 1. Material and shape of the shoe inserts.

			Material		Elasticity	
No	**Arch**	**Heel shape**	**Heel**	**Forefoot**	**Heel**	**Forefoot**
1	high	spherical	hard	hard	elastic	elastic
2	high	spherical	soft	soft	elastic	elastic
3	high	spherical	soft	soft	viscous	viscous
4	high	spherical	soft	soft	viscous	elastic
5	low	spherical	soft	soft	viscous	elastic
6	high	flat	soft	soft	elastic	elastic

RESULTS

Analysis of variance showed a significant difference between average comfort ratings of all inserts ($p < .001$). The combat boots without inserts were rated significantly lower than all insert conditions ($p < .001$). The rating for the hard insert, insert 1, was lower than all other inserts ($p < .036$). The elastic insert, insert 2, was rated higher than the viscous insert, insert 3 ($p = .016$) and the elastic forefoot insert, insert 4 higher than the viscous forefoot insert, insert 3 ($p = .015$) (Fig. 1).

No significant differences between comfort ratings of different groups based on subject characteristics have been found but some trends could be observed. In general, more sensitive subjects distinguished more between the hard and the soft insert ($\Delta_C = 2.2$) compared to less sensitive subjects ($\Delta_C = 0.3$). More sensitive subjects to vibration stimuli at 30 Hz preferred the soft insert ($\Delta_C = 0.9$) whereas less sensitive subjects preferred the hard insert ($\Delta_C = 1.1$). More sensitive subjects to vibration stimuli at 125 Hz preferred the high arch insert ($\Delta_C = 0.8$) whereas less sensitive subjects preferred the low arch insert ($\Delta_C = 1.2$). Subjects with small Q-angles, subjects with poorly aligned subtalar joints and subjects sensitive to vibration stimuli at 30 Hz preferred the elastic insert ($\Delta_C = 1.9$, $\Delta_C = 1.9$, $\Delta_C = 1.5$).

DISCUSSION AND CONCLUSION

The comfort ratings for the tested conditions reflect the differences in hardness between the conditions very well. Soft inserts might reduce the amplitude and frequency of the impact signal. Less sensitive subjects to vibration stimuli might not detect this change and thus not distinguish between the soft and the hard inserts. The fact that the largest differences between insert conditions were between the soft and the hard inserts might be an indicator that the hardness of a shoe is the predominant factor for comfort perception. In general, tactile and vibration sensitivity and foot and leg alignment seem to be related to comfort perception of different footwear modifications. However, it is speculated that static measurements might not be sufficient to fully predict comfort perception and that task-specific dynamic variables such as kinematic and kinetic variables as well as EMG characteristics should be included for future studies.

REFERENCES

1–ROSS J. (1993)-*Mil. Med.*-158(6) 410–415.
2–MILGROM C. et al. (1992)-*Clin. Orthop.* 189–192.
3–FAUNO P. et al. (1993)-*Int. J. Sports Med.*-14(5) 288–290.
4–NIGG B.M. et al. (1999)-*Med. Sci. Sports Exerc.* 31(7) Suppl.-421–428.

THE RELATIONSHIP OF BAREFOOT TO INSHOE PRESSURE DISTRIBUTON

NASS, D.[1], HENNIG, E. M.[1], FISCHER, B.[2]
[1]*Biomechanics Laboratory, University of Essen, Germany;*
[2]*Biomechanics Laboratory, University of Santa Catarina, Brasil*

INTRODUCTION

Pressure distribution analyses during standing and walking are used more and more by running shoe stores, to advice customers and recommend specific running shoe models for the runners foot anatomy. Only little information exists about the predictability of the plantar pressure during running in a shoe against plantar pressure information from barefoot standing and walking. The purpose of this study was to evaluate whether plantar pressure distribution in a running shoe can be predicted by barefoot pressures at half and full body weight standing or using peak pressures from barefoot walking.

MATERIALS AND METHODS

21 male runners participated in the study (BW 73 kg, SD 8.0). For the inshoe measurements the subjects perfomed five running trails (3.3 m/sec) in 13 different commercially available running shoes. In each shoe condition five repetitive running trials were collected. Running speed was controlled by a photocell arrangement. Pressure data were taken during right foot ground contact, using a HALM PD-16 pressure distribution unit (Halm GmbH, Frankfurt, Germany). Eight single piezoelectric transducers were positioned at palpated anatomical locations underneath the medial and lateral heel, the medial and lateral midfoot, the metartasal heads I, III and V and the hallux. For a comparison of the inshoe with the barefoot data the two heel and midfoot peak pressure were averaged, resulting in single peak pressure informations for the heel and midfoot. After calculating the mean pressures for the five trials in each shoe condition, these mean values were averaged for each subject across the 13 shoe conditions. The running condition is indicated with the letter **R**. For the barefoot measurements data collection was perfomed using a capacitive pressure distribution platform with a resolution of 2 sensors/cm^2 (EMED, FO1, Novel GMbH, München). All subjects were tested in three experimental conditions. Data were collected during half (**RH**) and full body weight standing (**RF**) as well as walking (**RW**) with the right foot across the platform.

Fig. 1. Correlation coefficients (r) for peak pressure values during running R vs. RH, RF and RW.

Table 1. Mean peak pressure values (kPa)

	RH	RF	W	R
Heel	115	165	417	947
	(38)	(50)	(99)	(160)
Midfoot	14	50	49	325
	(26)	(48)	(58)	(92)
Metatarsal head V	67	120	184	333
	(34)	(70)	(116)	(126)
Metatarsal head III	86	134	354	535
	(32)	(40)	(117)	(140)
Metatarsal head I	57	115	283	774
	(30)	(121)	(142)	(252)
Hallux	34	112	454	516
	(33)	(87)	(182)	(150)

Because of increased variability during walking five repetitive trials were performed for this experimental condition. Peak pressures were evaluated for 6 anatomical locations, the heel, the midfoot, the metatarsal heads I, III and V and the hallux.

RESULTS

The following table presents the mean pressure values for all subjects in the four conditions. As expected the peak pressure values increase with the load under the foot. As summarized in Table 1, for all experimental conditions the highest pressure values were found under the heel, followed by the third metatarsal head. Only during barefoot walking the second highest pressure is present under the hallux. The lowest pressure values are always below the midfoot region. To investigate possible predictors from the barefoot conditions towards running inside of athletic shoes, regression analyses were performed.

The regression analyses showed for the midfoot and the first metatarsal head region low, but significant correlations between the peak pressures in the barefoot against the in-shoe running conditions (Fig. 1). For barefoot walking, a medium correlation was also present for the heel region.

DISCUSSION AND CONCLUSION

The pressure values, found for the four experimental conditions, are similar to those, reported in the literature. (Cavanagh et al. 1987, Hennig, 1993, 1995). Only for the half body weight standing condition significant correlations were found against the midfoot pressures during running in shoes. It is surprising that the individual foot anatomy do not find its expression in similar pressure patterns across all experimental conditions. The pressures under the heel during walking were found to be the best predictors of peak pressures during running. Therefore it can be presumed that the dynamics of the walking pattern may be similar to foot to ground contacts in running.

The regression analyses showed that the plantar pressure analysis from barefoot standing and walking has a very limited value for predicting in-shoe pressures during running. The highest determination coefficient under the heel was only $r^2=0.38$. Under all other foot regions the common variance for the barefoot against the running pressures was always lower than 32 %. For three of the six analyzed anatomical regions no significant correlations were found at all. Therefore it can be concluded that the analyses of plantar pressures during barefoot standing and walking are no suitable methods to predict inshoe pressure patterns during running in running footwear.

REFERENCES

CAVANAGH, P.R. et al. (1987)-Pressure distribution under the symptom-free feet during barefoot standing Foot & Ankle-262–276.

HENNIG, E.M. et al. (1993)-Die Dreipunktunterstützung des Fusses-Z. Orthop.-279–284.

HENNIG, E.M. et al. (1995)-In-shoe pressure distribution for running in various types of footware- J Appl Biom-299–310.

FOOT SLAP DURING RUNNING IN CHILDREN

SCHEPENS B.[1,2], WILLEMS P.A.[1] & HEGLUND N.C.[1]
[1]Unité de réadaptation, Université Catholique de Louvain, Belgium, [2]Current address: Département de physiologie, Université de Montréal, Canada.

INTRODUCTION

During running, at the beginning of the ground contact phase, there is a peak in the vertical force (see upper left panel of figure), which is thought to be due to the rapid deceleration of the foot and lower leg during heel strike. This phenomenon has been observed[1] but never quantified in adults. Furthermore, since young children have relatively lightweight limbs, they should have a smaller foot slap. Here we report the effect of speed and age on the occurrence and magnitude of foot slap.

MATERIALS AND METHODS

The vertical force was measured, using a platform 6 m long and 0.4 m wide, in fifty-one children 2 to 16 years old and in six adults running at different speeds[2]. In most cases, two trials per subject were recorded in each velocity class of 1 km/h, for a total of 1979 runs.

RESULTS

The upper left panel of the figure shows the vertical force as a function of time for a 2 year-old running at 7.9 km/h.

In the other panels the open symbols represent the maximum force during foot slap (f_{slap}), and the closed symbols represent the maximum force due to the acceleration of the center of mass (f_{cm}) as a function of speed in each age group. At low speeds the vertical force tracings are relatively smooth, without a prominent peak. The insets in the figure show the fraction of the steps displaying a foot slap (as determined by eye) as a function of speed. With increasing speed, the f_{slap} becomes relatively more important, particularly in the children. At all ages, f_{cm} ranges from less than two times body weight (at speeds lower than 11 km/h) up to more than three times the body weight (at speeds higher than 25 km/h). In two year-old children, the magnitude of f_{slap} is always larger than f_{cm}. On the contrary, in adults (with the exception of the very highest speeds) f_{cm} is always larger than f_{slap}. During growth, f_{slap} at a given speed is progressively reduced, and after the age of 12 it is almost the same as in adults.

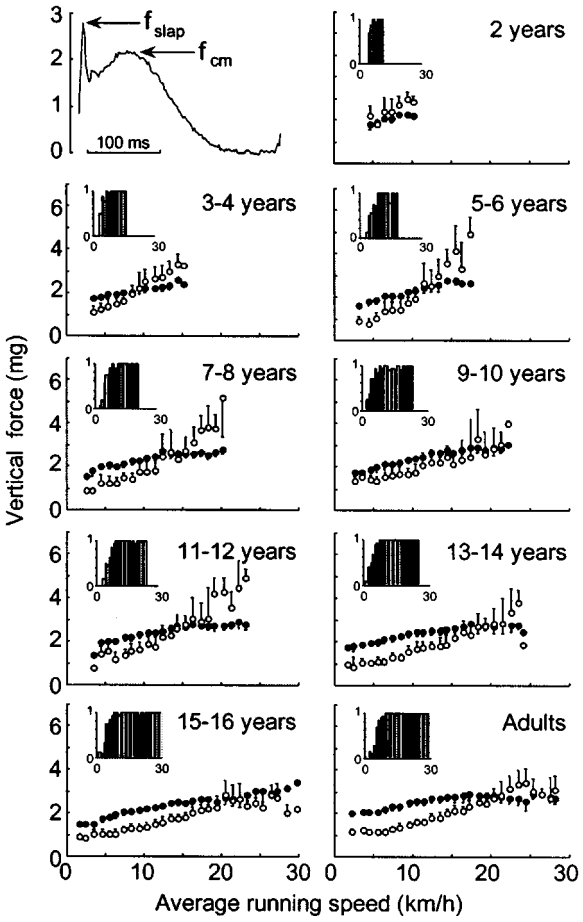

DISCUSSION AND CONCLUSION

Characteristics of the landing phase change with age; young subjects seem to be unable to lessen the impact of the foot on the ground. The muscular contraction of the pre-tibial muscles as well as the ankle and knee motion seem to play an important role in the shock absorption at initial floor contact[3]. The capacity to develop strength is relatively smaller in children than in young adults, and could be due to a lack in motor control during voluntary muscle contraction[4]. The higher peak force during landing might thus be attributed in part to a lower ability to control ankle and knee movements, and muscular contraction of the pre-tibial muscles, at initial contact.

REFERENCES

1– Cavanagh et al. (1980) *J. Biomech.* 13:397–406.
2– Schepens et al. (1998) *J. Physiol.* 509:927–940.
3– Simon et al., (1981) *J. Biomech.* 14:817–822.
4– Kanehisa et al., (1995) *Int. J. Sport. Med.* 16:54–60.

THREE-DIMENSIONAL KINEMATICS OF HUMAN KNEE DURING GAIT USING A JOINT AVERAGING COORDINATE SYSTEM METHOD

MUN J.H.[1], FREEMAN J.[2], CHOI W.S.[1] AND RIM K.[1,2]
[1]The Department of Biomedical Engineering; [2]The Department of Mechanical Engineering, The University of Iowa, Iowa City, Iowa 52242, USA.

INTRODUCTION

In experimental clinical gait analysis, random and systematic errors caused by skin movement, skeletal deformation and equipment errors[1–4] make it impossible to achieve error-free kinematic data. Averaging methods have been used to improve estimates of body segment orientation. Previous methods involve averaging either the Euler-Bryant angles[3], or averaging of test trials[2], with neither technique being theoretically sound. A new method, the Joint Averaging Coordinate System (JACS) is the topic of this study. The JACS method determines multiple transformations, and consequently Euler-Bryant angles for the joint. The angles are then averaged to determine the orientation of the joint. The JACS method provides quantitatively better results by reducing the effects of random error.

MATERIAL AND METHODS

The JACS method uses each marker on a segment as the origin of a local coordinate system. The method determines the transformation between that marker origin and the global coordinate system by using a standard three-marker technique[4]. By cyclically permuting the order of each three-marker combination, many transformations can be computed for the segment. For example, using a five-marker system, with the markers labeled from $\mathbf{P_1}$ to $\mathbf{P_5}$, the thirty marker combination permutations listed in Table 1 are possible, while excluding mirror-image combinations.

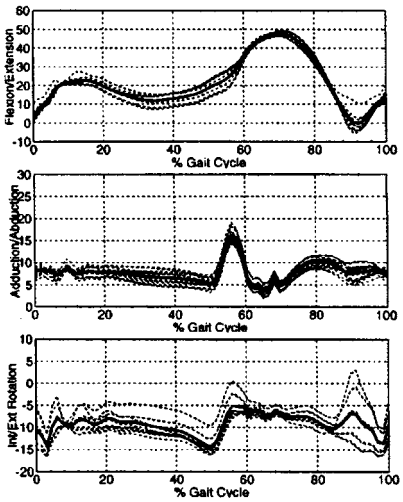

Fig. 1. Comparison of relative rotation angles.

Table 1: Five marker permutation combinations.

Origin	**Marker Point Combination**					
P_1	$P_1P_5P_4$	$P_1P_5P_3$	$P_1P_5P_2$	$P_1P_4P_3$	$P_1P_4P_2$	$P_1P_3P_2$
P_2	$P_2P_1P_5$	$P_2P_1P_4$	$P_2P_1P_3$	$P_2P_5P_4$	$P_2P_5P_3$	$P_2P_4P_3$
P_3	$P_3P_2P_1$	$P_3P_2P_5$	$P_3P_2P_4$	$P_3P_1P_5$	$P_3P_1P_4$	$P_3P_5P_4$
P_4	$P_4P_3P_2$	$P_4P_3P_1$	$P_4P_3P_5$	$P_4P_2P_1$	$P_4P_2P_5$	$P_4P_1P_5$
P_5	$P_5P_4P_3$	$P_5P_4P_2$	$P_5P_4P_1$	$P_5P_3P_2$	$P_5P_3P_1$	$P_5P_2P_1$

The JACS method uses a constant transformation matrix to transform the orientation matrix determined for each marker combination to the Grood and Suntay[5] reference frame at the knee joint. Each of the constant transformation matrices is determined from the standing calibration position prior to the gait experiment. If the segment moved with rigid body motion, the results of every transformation to the knee coordinate system would be identical. However, random and systematic errors in the marker locations lead to differences between the individual transformations.

The JACS method then determines the three Bryant angles associated with each of the transformations with respect to the knee joint reference frame. These angles are then averaged to determine segment orientation. Finally, the flexion/extension, adduction/abduction, and internal/external rotation angles are determined from the relative orientation of the leg segments.

RESULTS

Experimental gait data from a healthy male with a free walking speed of 1.4 m/sec was used for the inverse kinematic analysis. During gait, the thigh segment was tracked using five anatomical skin markers, while the shank segment was tracked using three markers. The relative motions between the femur and tibia segments in terms of flexion/extension, adduction/abduction and external/internal rotations are shown in Figure 1. The dark solid line in the figure represents the JACS results, while the dotted lines represent each of the transformed knee joint angles prior to averaging. Variations shown in the joint angles depend on the permutation sequence of the skin markers, as given in Table 1.

DISCUSSION AND CONCLUSION

The JACS method is a statistical technique to reduce experimental error for a single gait trial without any additional experimental measurements or cost. The method provides quantitatively better results by averaging random errors of the body segment orientation.

REFERENCES

1–CAPPELLO, A. et al.-(1997)-Hum Mov Sci, v.16, 259–274.
2–KADABA, M. et al.-(1990)-J Ortho Res. v.8, 383–392.
3–PANJABI, M. et al.-(1993)-J Ortho Res, v.11, 525–536, 1993.
4–VAUGHAN, C. et al.-(1992)-*Dynamics of Human Gait*.
5–GROOD, E. et al.-(1983)-J Bio Eng; v.105, 136–144.

COMPARISON OF METHODS TO DETERMINE MECHANICAL ENERGY EXPENDITURE OF WALKING AT VARIOUS VELOCITIES

SEMENIUK, K.M. AND ROBERTSON, D.G.E.
School of Human Kinetics, University of Ottawa, Canada.

INTRODUCTION

Two experimental techniques have dominated the literature concerning the estimation of mechanical energy expenditure (MEE) in human motion. The first method, the absolute power method (APM), is a kinetic based approach that utilizes inverse dynamics to determine MEE from the net moments and powers. The absolute work method (AWM), is a kinematic approach which determines MEE from the changes in kinetic and potential energy of the segments. Although classical mechanics implies that these two methods should produce similar results, differences have been determined with the AWM underestimating the APM[1,2]. As well, a theoretical analysis has been performed proving the validity of the APM as the best estimate of MEE and the invalidity of the AWM except in a limited number of situations[1]. The purpose of this study was to compare the MEE results of the APM and AWM of normal walking over a range of velocities and to investigate the relationship between MEE and walking velocity.

MATERIAL AND METHODS

Ten healthy and active subjects (5 female and 5 male) were required to walk at five velocities: 40% below normal (B40), 20% below normal (B20), normal, 20% above normal (A20) and 40% above normal (A40). The normal walking condition was the velocity the subjects achieved when given the instructions to walk as naturally as possible. Overall average required velocities ranged from 0.85 to 1.99 m/s. Velocities were determined by two photoelectric Micro Switches (Honeywell) placed 6.5 m apart in the middle of a 14 m walkway. Five trials of each walking condition were gathered from all subjects. Acceptable trials were those with no visible stride modifications and that fell within a range of $\pm$2.5% of the required velocity. A single video camera (Panasonic AG-456UP) recorded the two-dimensional (2D) movement of one complete stride of the right side of the body. Walking was considered symmetrical with the movement occurring predominantly in the sagittal plane of motion[2,4]. Motion analysis of a 7 segment rigid body model was achieved with the Ariel Performance Analysis System (APAS). The x and y coordinate data were smoothed using a 4[th] order, zero-lag, low-pass Butterworth filter with the cutoff frequencies determined by residual analysis. Ground reaction forces were obtained with a force platform (Kistler) at a sampling rate of 200 Hz. All kinematic and MEE calculations were derived using Biomech Motion Analysis software[4]. Statistical analysis included repeated measures analysis of variance, Games and Howell *post hoc* testing and curve fitting techniques using the method of least-squares to examine the relationship between MEE and walking velocity.

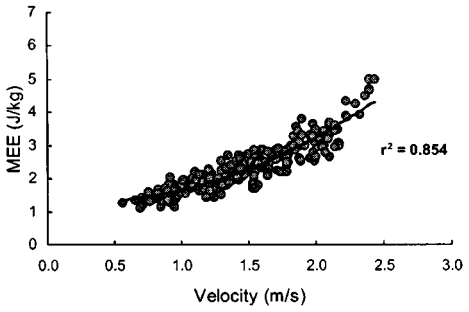

Fig. 1. Normalized MEE results of the APM (n = 250).

RESULTS

The repeated measures ANOVA found that there was no significant difference between the MEE results of the APM and AWM. The AWM, with mean normalized MEE results ranging from 1.54 to 4.26 J/kg, overestimated the APM, with results ranging from 1.50 to 3.32 J/kg. Using the APM, a significant difference was determined between all walking conditions except between A20 and A40. The AWM failed to differentiate between any of the individual walking conditions. Furthermore, variation increased within the AWM results as walking velocity increased. This was evident in the curve estimation results. Even though all normalized MEE trial results from both methods were significantly represented by a second-order polynomial ($P \leq 0.001$), the AWM ($r^2 = 0.769$) demonstrated a larger variability than the APM ($r^2 = 0.854$) whose values are shown in Figure 1.

DISCUSSION AND CONCLUSION

Contradicting previous research[1,2], no significant difference was found between the two methods with the mean normalized results of the AWM actually overestimating the APM. This similarity might be due to the fact that the analysis was undertaken in 2D. By taking into account only one side of the body, anti-symmetrical movements which reduce the MEE calculations of the AWM would not have been as great as a 3D analysis of both sides of the body[1,2]. However, this is not inferring that the AWM is as valid as the APM when it comes to deriving MEE of walking in 2D. The APM is still a more valid method since it was able to significantly determine differences between the majority of the individual walking conditions. As well, the variability in the velocity of walking can be accounted for by approximately 9% more with the MEE using the APM than using the AWM. Furthermore, the APM allows one to gain an understanding of the causes of the movement because of the calculations of the net moments of force and powers at each joint. In fact, ensemble averaged net moment and power curves displayed characteristic patterns in which the magnitude increased in proportion to the velocity change with the shape of the curves remaining the same[3].

REFERENCES

1–ALESHINSKY SY (1986a-e). *J. Biomech.* 19:287–315.
2–CALDWELL GE and FORRESTER LW (1992). *Med. Sci. Sports Exerc*. 24:1396–1412.
3–WINTER DA (1991). *The biomechanics and motor control of human gait: normal, elderly and pathological*.
4–ROBERTSON DGE *www.health.uottawa.ca/csb/software.*

SIMULTANEOUS PERFORMANCE OF POSITIVE AND NEGATIVE EXTERNAL MECHANICAL WORK IN HUMAN WALKING

DONELAN J.M.[1]*, KUO A.D.[2] AND KRAM R.[1]

*[1]Dept. of Integrative Biology, University of California, Berkeley, CA, 94720–3140 USA; [2]Dept. of Mechanical Engineering and Applied Mechanics, University of Michigan, Ann Arbor, MI, 48109–2125 USA. *E-mail: mdonelan@uclink4.berkeley.edu*

INTRODUCTION

The work performed against external forces is a major component of the total mechanical work performed in walking. Traditional measures of external work are based on the sum of ground reaction forces acting on the feet1. However, during the double support phase, the legs push against each other in the fore-aft and medio-lateral directions2,3. Thus, the leading leg may perform negative external work while simultaneously the trailing leg performs positive external work. We measured the mechanical work performed against external forces by each leg individually during human walking. We hypothesized that this would reveal a substantial amount of external mechanical work that has been overlooked by Cavagna's traditional method.

MATERIALS AND METHODS

We measured the three components of the individual foot-ground reaction forces as 10 subjects (5 male, 5 female, body mass 68.9612.2 kg; mean 6 S.D.) walked across two force platforms mounted in succession near the midpoint of our walkway. Subjects walked at six different randomized speeds (0.75, 1.00, 1.25, 1.50, 1.75 and 2.00 m/s).

We calculated the power generated against external forces by the trailing and leading legs from the dot product of the ground reaction force acting under each leg and the center of mass velocity. We calculated the components of the instantaneous center of mass velocity using the time-integrals of the center of mass accelerations determined from the summed ground reaction forces1. We calculated the external work performed by each leg to overcome the external forces from the time-integral of the powers generated by the trailing and leading legs. We then calculated the positive and negative external mechanical work performed by a leg by summing the positive increments and negative decrements in the external work, respectively. External mechanical work has traditionally been calculated from the change in mechanical energy of the center of mass[1]. This is equivalent to summing the individual foot-ground reaction forces before calculating power or to summing the instantaneous powers generated by each leg before integrating to determine work.

RESULTS

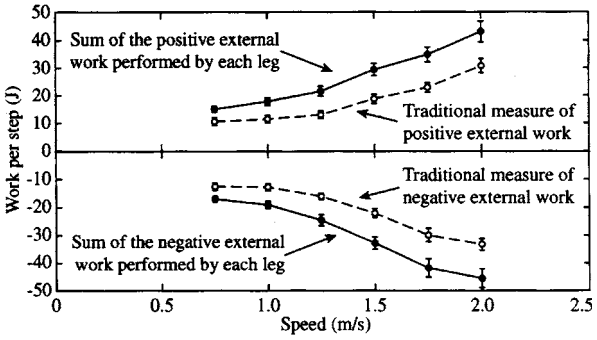

Fig. 1. External mechanical work per step vs. speed (n=10). On average, the sum of the external work performed by each leg was 48% greater than traditional measures.

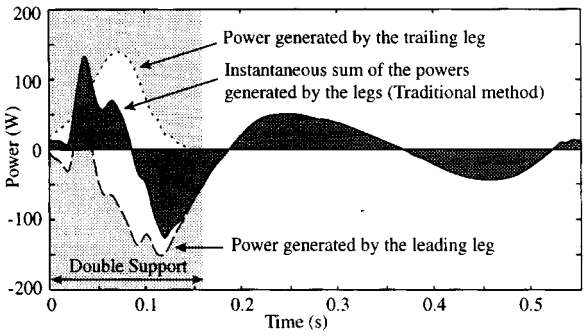

Fig. 2. External mechanical power traces from a typical trial at 1.25 m/s. Traditional measures substantially underestimated total external mechanical work because during double support, the leading leg predominately generated negative power while simultaneously, the trailing leg generated positive power. The difference between the shaded and un-shaded areas under the power-time curves indicates differences in measured work.

DISCUSSION AND CONCLUSION

Calculating work from the sum of the work performed by each leg reveals a substantial amount of external mechanical work that has been overlooked by the traditional method. While remaining simple, our present method provides insight into individual leg function and brings us closer to more complete measures of the total mechanical work in walking.

This work was supported in part by an NSERC fellowship to JMD, NIH, NSF and Whitaker grants to ADK and a NIH grant to RK.

REFERENCES

1–Cavagna G.A. (1975)-J. Appl. Physiol. 174–179.
2–Alexander R.M. (1983)-Animal Mechanics.
3–Winter D.A. (1990)-Biomechanics and Motor Control of Human Movement.

ADAPTATION OF THE GAIT INITIATION PROCESS FOR STEPPING ON TO A NEW LEVEL DURING A SINGLE STEP

GELAT T.[1] AND BRENIERE Y. [1]

[1]*Laboratoire de Physiologie du Mouvement INSERM U-483, Université Paris-Sud, Bat 441, 91405 Orsay Cedex, France*

INTRODUCTION

During the gait initiation in level walking, the anticipatory postural adjustments (APA) which precede heel off consist of a forward fall of the whole body and their duration depends on the intended gait velocity[1] related to the step length. The present study examines the adaptation of the gait initiation process for stepping on to a new level compared to level walking during a single step[2]. We analyzed dynamics of the centre of mass (CM) of the body in the sagittal plane. During stepping on to a new level, the main question: is APA duration influenced by the final height of the CM when the single step length is given? More generally, we wanted to know if the organization of the CM forward dynamics, well described during gait initiation in level walking[1], changed when stepping on to a new level.

MATERIALS AND METHODS

Five subjects aged from 23 to 39 participated in the experiment. From a stable posture on a force plate, the subjects had to execute a single forward step with the right foot at natural speed. We used a triangular force plate (2 m each side) equipped with strain gauges which measured the ground reaction forces along the antero-posterior (Rx), lateral and vertical (Rz) axes. Only Rx and Rz were used to calculate the respective accelerations of the CM from Newton's law. The movement was performed in five experimental conditions (C1, C2, C3, C4 and C5). C1 was a level walking task. The other conditions (stair conditions) required to step on to a new level which was a rigid box fixed to the force plate; its height was 8 cm in C2, 16 cm in C3, 24 cm in C4 and 32 cm in C5. In all conditions, the step length was fixed to the subject's foot length. Seven trials for each condition were recorded. To detect the onset of the stepping leg movement, i.e. the heel off (tHO), we used a mono-axial accelerometer fixed to the heel of this leg.

The following variables were analysed in the five conditions: duration of APA, corresponding to the time between the instant of the first variation of the centre of pressure along the antero-posterior axis and tHO; forward velocity of the CM at tHO (VxHO), at the instants of toe off (VxTO) and foot contact (VxFC) of the stepping leg and its maximal value (Vxmax); vertical displacement of the CM (Δz). Vx and Δz were calculated respectively by a simple and double integration from the acceleration data.

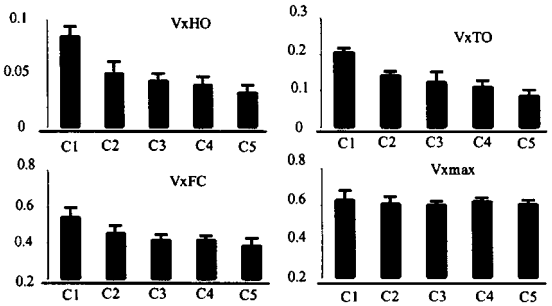

Fig. 1. Mean of Vx ($m.s^{-1}$) at tHO, tTO, tFC and maximal value during the five conditions.

RESULTS

The main result was that APA duration was longer ($p<.05$) in C1 than in the stair conditions for which no significant difference was found. We noted that VxHO was clearly higher ($p<.01$) in C1 than in the stair conditions and that the same tendency was observed for VxTO and VxFC (Fig. 1). By contrast, no significant difference was found for Vxmax between the five conditions (Fig. 1).

In all stair conditions, the majority of body lift (90% of the final height) occurred only after tFC.

DISCUSSION AND CONCLUSION

Results clearly showed that the organization of the CM forward dynamics changed when confronted by the initiation of stepping on to a new level. Regardless of the step height, Vx was not only reduced at tHO but also up to tFC. Given that Vxmax was similar in all conditions (because of the same step length contraints), it can be suggested that the CM forward dynamics is organized in a sequential mode during the initiation of stepping on to a new level. As the majority of body lift occurred after tFC, it can be hypothesized that the forward velocity of the CM and implicitly its displacement were smaller at this instant to optimize the mechanical advantage of knee extension offered by the placement of the leading limb on the step[3]. Another hypothesis may be proposed from the following consideration: even if the vertical position of the CM at foot contact is very far from its final value, what is crucial for the success of the task is to clear the edge of the new level. In this way, reduction of the forward disequilibrium of the body up to foot contact could be intended to facilitate the clearance of the new level. Further investigations are required to examine the validity of the two hypotheses.

REFERENCES

1–Brenière, Y. et al. (1987) J. Mot. Behav., 19: 62–76.
2–Dietrich, G. et al. (1994) Hum. Mov. Sci., 13: 195–210.
3–Mc Fadyen, B. and Winter, DA. (1988) J. Biomech, 21: 733–744.

3D KNEE GAIT AT DIFFERENT SPEEDS

OAKLEY P.A. AND COSTIGAN P.A.
Queen's University, Kingston, ON, Canada.

INTRODUCTION

The purpose of many gait studies is for comparison, whether between groups (ie. Patient-normal/gender/age) or within groups (ie. Clinical intervention/pre and post-op). It has long been known that changes in gait speed are a common feature of locomotion,[1] and that there is a range of comfortable speeds.[2] Therefore, a dilemma exists because regardless of the measure obtained for comparison, 'every feature of walking changes when walking speed changes,'[3] so a speed difference may explain all or part of the gait differences.[4] The purpose of this study was to quantify the changes in 3D knee gait parameters throughout normal gait speeds.

MATERIAL AND METHODS

Twenty young, healthy males and females volunteered for this study. The group had a mean 177cm height, 71kg weight, and 24 year age. All subjects had their right legs instrumented and an optoelectric motion analysis system tracked the active markers while the subjects walked over a force plate imbedded in the floor. The data was sampled at 50 Hz, filtered,[5] processed using the Q-GAIT system,[6] and normalized by body mass. Each subject performed five walking trials at their self-selected cadence as well as, by metronome, 15% and 30% above and below that. This data represents 500 individual trials. All measures are along or about the posterior-anterior (PA), lateral-medial (LM), and distal-proximal (DP) axes.

RESULTS

Cadences ranged from 80 to 147 steps/min and were correlated with velocity (r=0.90). Using cadence, linear regressions predicting angles (A: Deg), forces (F: N/kg), moments (M: Nm/kg), and absorption (abs)/ generation (gen) powers (P: W/kg) at specific gait events (Table 1) were computed. The percentage changes from baseline cadence (100%) are shown in Table 2.

DISCUSSION AND CONCLUSION

These results pertain only to young, healthy normal subjects walking within the cadence range. In general, covariances were low for angles and high for kinetics. In fact, r values ranged from 0.5 to 0.87 for the kinetics shown.

Interestingly, Table 2 illustrates how some gait parameter values changed by as much as 80% with only a 30% change in cadence. Only those parameters showing a strong relationship to cadence are presented, although knowing which parameters did not relate to speed is also important. For example, no adduction moment parameters changed with changes in gait speed. This study provides a complete presentation of 3D knee gait speed influences and uniquely quantifies these changes. This data may serve as a useful tool for other researchers.

REFERENCES

1–Grieve et al. (1966)-Ergonomics, 5, 379–399.
2–Murray et al. (1966)-Am J Phys Med, 45, 8–24.
3–Inman et al. (1981)-Williams & Wilkins, Balt.
4–Oatis (1995)-In: Craik et al. Mosby, St Louis.
5–Winter (1979)-Wiley, New York.
6–Costigan et al. (1992)-Med Biol Eng Comp 30, 343–350.

Table 1. Linear regressions.

Parameter	r^2	b_1	b_0	SE
A-Max stance flexion	0.20	0.110	8.379	5.28
A-Max swing flexion	0.14	0.068	54.91	4.05
F-Min PA at heel strike	0.72	–0.018	0.841	0.27
F-Max PA	0.48	0.019	1.660	0.49
F-Max LM at push off	0.31	0.004	–0.195	0.15
F-Min DP	0.46	–0.034	–6.339	0.88
F-Max DP at midstance	0.50	0.003	–9.513	0.84
M-Min LM at heelstrike	0.69	–0.006	0.300	0.10
M-Max LM at wt acc	0.50	0.007	–0.093	0.16
P-Max PA absorption	0.25	0.001	–0.096	0.06
P-LM gen at heelstrike	0.50	–0.013	0.823	0.31
P-LM abs at weight acc	0.58	0.015	–1.010	0.32
P-LM gen after wt acc	0.63	–0.010	0.645	0.19
P-Max LM absorption	0.67	0.025	–1.329	0.43
P-LM abs latter stance	0.76	0.020	–1.284	0.27

$Y = b_1X + b_0$; Y=gait measure; X=cadence (steps/min)

Table 2. Percentage change from baseline (100%).

Parameter	70	85	100	115	130
A-Max stance flexion	–23	–12	0	6	12
A-Max swing flexion	–7	–2	0	0	–1
F-Min PA at heel strike	–50	–25	0	26	45
F-Max PA	–20	–12	0	8	8
F-Max LM at push off	–50	–22	0	31	63
F-Min DP	–12	–6	0	7	10
F-Max DP at midstance	10	15	0	–16	–24
M-Min LM at heelstrike	–53	–28	0	21	37
M-Max LM at wt acc	–39	–20	0	15	30
P-Max PA absorption	–57	–26	0	21	62
P-LM gen at heelstrike	–68	–40	0	30	43
P-LM abs at weight acc	–65	–34	0	43	72
P-LM gen after wt acc	–66	–41	0	40	82
P-Max LM absorption	–50	–31	0	29	52
P-LM abs latter stance	–58	–29	0	30	62

CLASSIFYING LIFT TECHNIQUE USING A CLUSTER ANALYIS APPROACH

ALBERT WJ[1], STEVENSON JM[2], COSTIGAN PA[2] AND SMITH JT[2]

[1]University of New Brunswick, Fredericton, NB, Canada;
[2]Queen's University, Kingston, Ontario, Canada

INTRODUCTION

One of the major suggestions for reducing injuries, especially to the lower back, in manual material handling (MMH) occupations is the adoption of a 'correct' lifting technique[1]. Typically, lifting technique is defined by the posture assumed at the start of the lift (squat or stoop)[2] with more recent investigations focusing on coordination of movements[3]. Surprisingly few studies have investigated the lifting technique of experienced manual material handlers. These studies reveal, however, that workers use methods other than those recommended during training[4]. The purpose of this study was to identify the lifting technique used by an experienced industrial population and to provide a method for classifying their technique based on the entire lifting profile.

METHODOLOGY

Experienced workers primarily involved in handling nylon bobbins (between 4 and 12 kg) were recruited from a local manufacturing plant. Workers were included in the study if their jobs required them to lift between 5,000 and 7,000 kg per day and they had not complained of lower back pain requiring medical treatment or change in activity for over a year. A freestyle sagittal box lift task was performed in a lift envelope from the floor to the subject's shoulder height and the motion was recorded using the Fastrak™ electromagnetic motion system. The sensors of the Fastrak™ system tracked motion of the wrist and thoracic, lumbar and sacral spine in six spatial co-ordinates, three linear and three angular. Data on 108 subjects were used in the present study.

In order to describe specific types of lift, motion patterns were grouped according to the shapes of the co-ordinate curves and their derivatives. A separate analysis was performed on each of three combinations of curves. The first combination, describing 'Posture', included curves for sacrum height, trunk angle and wrist-to-sacrum distance. The second combination, 'Velocity', consisted of the velocity curves for the vertical wrist movement and the S1, L1 and T1 flexion. The third combination described 'Segment Bend' and included the orientation angles of the entire thoracic and lumbar segments and their associated velocity curves.

Each cluster analysis was performed on a matrix of curves, one row per subject, each row containing curve values at regular intervals in normalized time, the separate curves in the combination strung end to end. Using a hierarchical divisive clustering algorithm[5,6] provided in the S-Plus analysis package, two clusters were considered sufficient to divide the subjects into extreme groups determined by the clustering tree. Therefore in each analysis (Posture, Velocity and Segment Bend), each subject was assigned to either Group 1 or Group 2. Those subjects who did not maintain consistent group membership across the three analyses were reassigned to a new group, Group 3.

Table 1. Initial group by Cluster Analysis and final group assignment.

N	Posture Analysis	Velocity Analysis	Segment Bend Analysis	Final Group
29	1	1	1	1
33	2	2	2	2
3	1	1	2	3
12	2	1	1	3
7	2	1	2	3
24	2	2	1	3

RESULTS

The assignment of subjects to Groups 1 and 2 was compared across the three analyses (Table 1). Sixty-two of the 108 subjects were assigned to the same group in each of the three analyses. Of the 62 subjects, 29 fell consistently in Group 1 while 33 always fell in Group 2. The remaining 46 inconsistent subjects constituted Group 3.

DISCUSSION AND CONCLUSIONS

Cluster analysis provides a method for separating experienced lifters into groups according to the kinematics of their lifting motion using eleven motion curves. For easier discussion the groups were labeled according to their starting lifting posture: 'Squat' and 'Stoop' for Groups 1 and 2, respectively. The Stoop Posture group demonstrated larger T1, L1 and L5/S1 extension velocities over the first 40% of the lift. The motion was led by extension at the sacrum with the lumbar and thoracic segments lagging slightly behind. The Squat Posture group demonstrated pronounced T1, L1 and L5/S1 flexion velocities during the first 20% of the lift prior to the extension of the segments. This may be a result of the knee extending well in advance of the trunk[4]. The thoracic and lumbar bend velocities were also slower in the Squat Posture Group with the peak velocities occurring later in the lift. The majority of the subjects classified in Group 3 had a lifting posture with a large degree of trunk flexion with varying degrees of knee bend. Group 3 differed from the Stoop Posture group in having slower trunk segment extension velocities.

The clustering methodology has provided a strategy for classifying lifting techniques according to their dynamic motion curves. Further studies are being conducted on changes to the groupings with increased load demands.

REFERENCES

1–Snook SH et al. (1978). *J. Occ. Med. 20(7)*:478–481.
2–Lueopongsak, N et al. (1997). *Scand. J. Rehabil. Med. 29*:57–64.
3–Scholz JP et al. (1995). *Phys. Therapy 75(2)*:133–134.
4–Kuorinka I et al. (1994). *Ergon. 37(4)*:655–661.
5–Kaufman, L and Rousseeuw, PJ (1990). Finding groups in data. An introduction to cluster analysis NY: Wiley & Sons.
6–Macnaughton-Smith P (1964). *Nature 202*:1034–1035.

EFFECT OF CONTAINER CHARACTERISTICS ON THE KINEMATICS AND KINETICS OF FREESTYLE LIFTING

DELISLE, A.[1], GAGNON, M.[2], DESJARDINS, P.[2]
[1]Institut de recherche en santé et sécurité du travail du Québec, Canada; [2]Département de Kinésiologie, Université de Montréal, Canada.

INTRODUCTION

Manual materials handling has long been related to low-back pain. The training of workers to safe lifting has led to comparison of stoop vs squat lifting of boxes with handles. Unfortunately, little is known about what happens in freestyle lifting of containers with varying characteristics. This study compared the effect of asymmetrical lifting of symmetrical and asymmetrical containers (load asymmetry effect), and the asymmetrical lifting of a symmetrical cylinder (load format effect).

MATERIAL AND METHODS

Ten healthy male subjects (mean age 23 yr; range 21–31 yr) with little experience had to lift three 15–kg containers 49 times in one session and once one month later. Subjects lifted the containers using their self-selected strategy. The lift started from a low shelf (0.22 m) in front of the subject and ended on a higher shelf (1.0 m), 1.6 m and 90º to the left. Two containers were identical boxes (0.40 × 0.40 × 0.40 m), one with a symmetrical load and the other with its center of gravity offset by 0.08 m to the right. The other container was a cylinder 0.81 m long with a diameter of 0.33 m. The three containers were presented to the subjects in a continuous manner and in random order. Four sequences were analyzed (1, 25, 49, 50), for a total of 12 lifts per subject. A new force plate (2.4 m × 2.4 m) was used to measure ground reaction forces along with a 3D videographic system to capture the motion of the subjects. A 3D dynamic model of the whole body was used to compute the L5/S1 joint moment. Several kinetics and kinematics variables were also computed for the analyses. All the analyses were done for the phase of movement where the container was completely supported by the subject. Analyses of variance with repeated measures were applied (p#0.1) with Greenhouse-Geisser and Bonferroni adjustments.

RESULTS

The load asymmetry had little effect on the parameters used to compare the conditions, whereas the load format showed important effects. Generally, the handling of the cylinder, as compared to the boxes, involved smaller loading on the L5/S1 joint (Table 1). Interestingly, when the load was picked up, the lateral bending moment at L5/S1 was smaller for the cylinder. The mechanical work done on the cylinder was larger, whereas the work done on the subject's center of gravity while handling the cylinder was smaller.

Table 1. Mean (std. dev.) L5/S 1 joint moments and integrals, and mechanical work.

	Sym. Box (1)	Asy. Box (2)	Cylinder (3)
Moments at pickup (Nm)			
Extensor	214 (35)	210 (33)	207 (27)
Torsion	14 (10)	15 (12)	13 (10)
Lat. bending	34 (26)[3]	29 (21)	15 (10)[1]
Moment integrals (Nms)			
Extensor	276 (76)[3]	278 (78)	259 (75)[1]
Left torsion	13 (9)[2]	10 (8)[1]	13 (9)
Right torsion	–12 (6)	–14 (9)	–12 (6)
Right lat. bending	21 (17)[2]	13 (12)[1]	22 (14)
Left lat. bending	–23 (16)	–31 (21)	–19 (10)
Mechanical work (J)			
Container's c.g.	130 (11)[3]	127 (14)	143 (15)[1]
Subject's c.g.	271 (110)[3]	259 (108)	201 (96)[1]

DISCUSSION AND CONCLUSION

Previous reports have shown that lifting asymmetrical loads resulted in smaller preferred weight of lift[1] and that holding of asymmetrical loads had large effects on lumbar load[2]. However, an important difference with these studies is that boxes in the current study did not have any handles, so subjects often adopted asymmetrical hand positions. Moreover, subjects were free to tilt the containers while transferring them. Hand positions and container maneuvers probably explain why little difference was observed due to load asymmetry, and why somewhat larger asymmetrical loadings were observed for the boxes as compared to the cylinder. As for the cylinder, it is important to mention that the inner part of the cylinder's ends were empty so that it allowed easy gripping. Therefore, subjects had to flex themselves to a lesser extent in order to grab the cylinder, and so the work on the subject's center of gravity was smaller. The format of the cylinder probably reduced the lever arm with L5/S1 joint and explains the smaller integral of the extensor moment over time. In conclusion, it appears that some simple maneuvers with the box can counterbalance the effect of load asymmetry.

REFERENCES

1–MITAL and FARD (1986)-Ergonomics 29: 1263–1272.
2–HAFEZ and JÄGER (1997)-Proceedings of the 13[th] Triennial Congress of the IEA, Tampere, Finland: 506–508.

THE EFFECTS OF REPEATED SPINE FLEXION ON THE FLEXION-RELAXATION RESPONSE

MCNORTON S.[1], POTVIN J.[2], DICKEY J.[1]
[1]University of Guelph, [2]University of Windsor

INTRODUCTION

The flexion-relaxation (FR) response of the trunk extensor muscles was first reported by Floyd and Silver[1] and has been the focus of a number of studies on acute trunk loading[2]. However, while we know that ligaments can creep with prolonged/repeated loading, little is known about the effects of repeated flexion loading on the FR response. The primary purpose of this research was to examine the effect of repeated spinal loading on lumbar spine mechanics and the FR response for male and female subjects, with and without a hand held load.

MATERIAL AND METHODS

The volunteer subject group consisted of 15 males and 15 females, both with no known history of low-back pain. All measurements were made using an electromyography collection system as well as a 3Space electromagnetic transducer. Ag/AgCl surface electrodes were used to detect the muscle activity. A timer program was used to keep the movement pace of each subject consistent across trials. Isometric maximum voluntary contractions (MVCs) of the trunk muscles were performed in a test contraction apparatus.

The electrodes were attached bilaterally to the subject at the levels of L4/L5 and T9. The 3Space source was attached to the subject at the sacrum while the sensor was attached on the spine at the level of T6. Next, MVC trials were collected, for EMG normalization, using a LABVIEW program. The experimental procedure was as follows: the subject locked their knees and flexed forward, as far as possible, 10 times consecutively with no load. Next, the subject flexed forward 10 times with a 4.5 kg load in their hands. This was followed by the subject flexing 60 times with a 2.3 kg load held in their hands. Next, the subject flexed 10 more times with the 4.5kg load and then finished with 10 repetitions without a load in their hands.

The kinematic data (20 Hz) and raw EMG data (1000 Hz) data were synchronized. Raw EMG signals were rectified, low pass filtered (6 Hz), normalized to MVC and then every 50th sample was used to match with the 3SPACE data. Each set of 10 trials was separated as one of four conditions (Pre No Load, Pre Load, Post Load, Post No Load). For each flexion trial, EMG was used to determine the start and end times for flexion-relaxation. The following statistics were calculated: maximum flexion angle (2_{MAX}), flexion angle at FR (2_{FR}), FR angle as a percentage of maximum ($\%2_{FR}$) and average EMG ampltudes during FR. Averages were taken across the 10 repeated trials for each variable and subject. A three-way repeated measures ANOVA (time, load, gender) was used to determine expermental effects.

RESULTS

FR was observed in 24 of 30 subjects. There was no significant effect of gender or load on $\%2_{FR}$ but there was a significant increase ($p < 0.05$) associated with repetitive loading (time) with values increasing from $90.4 \pm 8.6\%$ (pre) to $93.0 \pm 9.3\%$ (post). In addition, 2_{FR} demonstrated a relative increase of 5.8% over time ($p < 0.05$) and males were found to have 2_{FR} angles that were 18.8% higher than females ($p < 0.05$). It was also found that when resistance was added, the maximum flexion angle increased significantly ($p < 0.05$) and this effect was larger for the pre condition. Average lumbar EMG amplitudes were generally less than 2% during FR. Bilateral Thoracic EMG amplitudes during FR were observed to increase from approximately 8.5 %MVC to 12 %MVC with the addition of the load ($p < 0.5$ for both sides).

DISCUSSION AND CONCLUSION

The results of this study indicate that repeated spine flexion does have an effect on the FR response, as it was observed to increase both the absolute angle and the percentage of maximum at which FR occured. This was likely due to some creep of the passive extensor tissues of the spine, in response to the repeated loading. Load did appear to increase maximum flexion angles (likely due to the increased strain on passive extensor tissues), and the effects of repetitive flexion on FR was more pronounced in the condition where no load was held by the subjects. Male subjects demonstrated higher maximum flexion angles and angles at FR but the FR angle, as a percentage of maximum, were very similar to female values.

This study has provided some new evidence about the effect of repeated spinal loading on lumbar spine mechanics in healthy subjects. Future studies should look to repeat the experiment using subject groups of different ages to see if the results from this study are generalizable to a larger population. More studies need to be done looking at the exact roles of the erector spinae muscles and ligaments during full flexion to help provide more conclusive evidence as to why this phenomenon occurs. In addition, further studies should determine how spinal impairment interacts with repetitive flexion to affect the flexion relaxation response.

REFERENCES

1–FLOYD W, SILVER P (1955) *J. Phys.*, 129:184–203.
2–KIPPERS V, PARKER A (1984) *Spine*, 9(7):740–745.

MUSCULAR MODELING: RELATIONSHIP BETWEEN POSTURAL DEFAULT AND SPINE OVERLOADING.

POMERO V.[1], VITAL J-M.[2], LAVASTE F.[1], IMBERT G.[1], SKALLI W.[1]

[1]Laboratoire de Biomécanique, ENSAM, Paris; [2]CHU Tripôde, Bordeaux, France.

INTRODUCTION

Relationship between postural default and spine overloading is not well investigated yet. Postural default yields an increase of the net reaction at a given vertebral level, but quantification of muscular regulation to avoid spine overload is not fully understood. A muscular regulation model was developed [1] to investigate this regulation process. The objectives of the present study is to use this muscular model in order to compare spine loads and muscular recruitment between a volunteer with no spinal pathology and an unbalanced patient with a sagittal default.

MATERIALS AND METHOD

Two subjects participated to the study: A patient(age: 65, height: 1.70m, weight: 55kg), and a volunteer(age: 29, height: 1.82m, weight: 67kg). Location of the gravity line and net reaction at the L3/L4 level was quantified using sagittal radiographs of the spine and ground pressure measurements (RS Scan - Footscan Pro) in the same referential. Muscular geometry in the L3/L4 disc plane was obtained from MRI (Philips Medical Systems – Gyroscan NT) of the thoraco-lumbar region. Maximum muscle stress for flexors and extensors was estimated using CYBEX device. All measurements (except MRI) were performed for both subjects in erect posture. Muscular pattern and inter-vertebral spinal loads were then quantified for both subjects, using our existing muscular model. This model is based on the assumption that muscles act to prevent excessive spinal loads; a multicriteria regulation process (taking into account antagonist activity) yields a distribution of net reaction into individual muscular forces and spine loads. For the patient, a first simulation was performed emphasizing the spine protection criteria (case 1), and a second one considered a maximum muscular stress level close to that found for the normal volunteer (15N/cm^2, case 2).

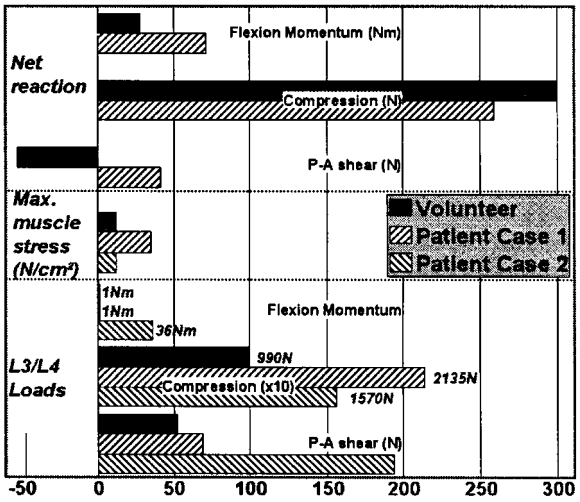

Fig. 1. Comparison of net reaction, maximum muscle stress and L3/L4 loads for the volunteer and the patient.

RESULTS

For the patient and the volunteer, gravity line in sagittal plane was respectively 90 mm in front of the center of the L3/L4 disc and 25 mm behind, while L3/L4 plane inclination from horizontal was respectively 9° and 0°. This resulted in the net reaction at disc center (L3/L4) in the plane of the disc for patient and volunteer presented in Figure 1. Patient extensors maximum stress was found very low compared to volunteer (Extensors: 54Nm vs. 317Nm; Flexors: 83Nm vs. 139Nm). As for the simulation results, we found that for both subjects, the erector spinae group was the highest group activated, but at a different level (patient: 35N/cm^2; volunteer: 12N/cm^2). For the normal patient, other muscles were all activated under 5N/cm^2, while the patient presented activation over 20N/cm^2 for the internal oblicus, the quadratus lumborum and the latissimus dorsi. Nevertheless, with a different muscular expense, both succeeded in regulating spinal loading of the L3/L4 vertebral joint, except for compression (Fig. 1). However, limitation of patient's extensors muscular stress to 15N/cm^2 yielded a decrease of compression, but a drastic increase of the spinal loads: 195N for P-A shear and 36Nm for flexion.

DISCUSSION AND CONCLUSION

Our muscular model suggested that because of the postural default, the patient had a higher net momentum in the joint compared to the normal volunteer. As a result, either the muscular system needed stronger activation, yielding a higher joint compression and probably also a muscle fatigue in such an activation level, or the spinal loads increased to a higher level.

REFERENCE

1–Pomero V., Lavaste F., Imbert G., Skalli W. (1999): " Estimation of spinal loads ", XXIVème Congrès de la Société de Biomécanique, Beaune, France.

ASSESSMENT OF SUBJECT MOTION IN A TRUNK POSITIONING APPARATUS FOR SCOLIOSIS MEASUREMENT

PONCET P.[1], RONSKY J.L.[2], DANSEREAU J.[3,4], ZERNICKE R.F.[1,2].

[1]Department of Surgery, University of Calgary, Calgary, Alberta, Canada; [2]Department of Mechanical and Manufacturing Engineering, University of Calgary, Calgary, Alberta, Canada; [3]Research Centre, Sainte-Justine Hospital, Montreal, Quebec, Canada; [4]Department of Mechanical Engineering, Ecole Polytechnique, Montreal, Quebec, Canada.

INTRODUCTION

Multiple imaging systems (laser-scanning[1], stereo-radiography[2]) are used to quantify trunk surface topography and underlying bone geometry (spine and rib cage) so as to assess relations between torso-surface asymmetry and spinal deformity[3]. A custom patient-positioning apparatus consisted of stabilizing devices to maintain a patient's posture and segmental positions to ensure a suitably stationary patient during data acquisitions with the imaging systems was designed. To test the effectiveness of the positioning device in stabilizing subject posture and to study the influence of breathing on torso displacement, trunk motions were assessed with a video motion analysis system.

MATERIAL AND METHODS

The positioning system comprised two components (Fig. 1). The upper part consisted of two arm rests and a cutaneous contact adjusted at the base of the neck (above C7) and attached to the frame with an articulated arm that was locked in position. The lower part of the positioning system included two cutaneous contacts that touched at two points of the subject's lower back and attached to the frame with an adjustable telescopic tube and ball joint. The main role of the three cutaneous contacts was to minimize body sway and axial rotation, while arm support helped stabilize the patient's upper body. Trunk motions of 5 healthy normal subjects were assessed with a video motion analysis system (Expert Vision, Motion Analysis Corp., Santa Rosa, CA). Nine reflective markers were attached to the torso, the subject positioned in the apparatus, and 30-s trials of the subject position were recorded for: normal breathing, holding breath, with and without the positioning system. The three-dimensional displacements of the reflective markers attached were measured relative to their initial position.

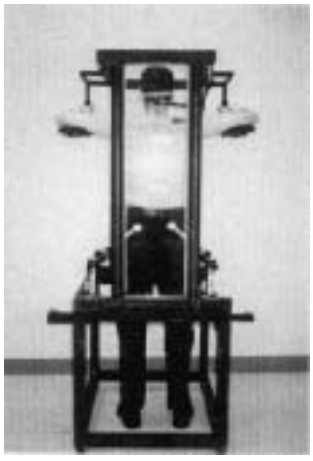

Fig. 1. Positioning apparatus.

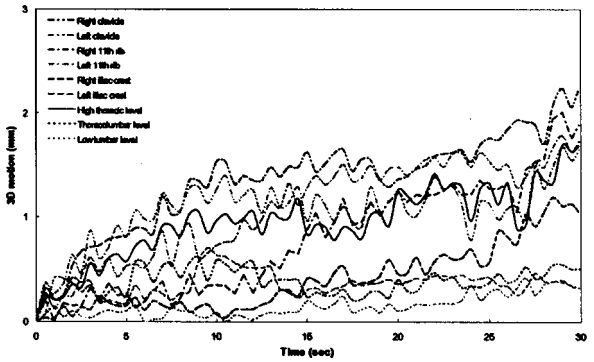

Fig. 2. Typical 3D displacement of 9 reflective markers attached to a representative subject's torso.

RESULTS

Subject sway with normal breathing during standing (17 mm) was substantially reduced with the positioning system (9 mm). Holding breath within the positioning device reduced movement to less than 3 mm (Fig. 2). The neck cutaneous contact alone, surprisingly, was more effective than the arm rests, minimizing the motion by half of 17 mm.

DISCUSSION AND CONCLUSION

Subject movement during data acquisition is minimized with the positioning device and with holding breathing. The positioning device provides consistent inter-subject positioning without distorting typical posture.

REFERENCES

1–Poncet et al. (2000), *CMBBE* (In press).
2–Dansereau et al. (1990), *Société Canadienne de Génie Mécanique*, 2:61–4.
3–Theologis et al. (1997), *Spine*, 22:1223–1228.

COMPUTER SIMULATION OF COLORADO INSTRUMENTATION OF THE SCOLIOTIC SPINE: PRELIMINARY RESULTS

VERNIEST F. [1,2,3], PETIT Y. [1,2], CHOPIN D. [4], GODILLON-MAQUINGHEN A-P.[3], DRAZETIC P.[3], AUBIN C-É [1,2]

[1]Research Center, Sainte-Justine Hospital, Montréal, Canada; [2]Mechanical Eng. Dept., École Polytechnique de Montréal, Canada; [3]LAMIH, Université de Valenciennes et du Hainaut Cambrésis, France; [4] nstitut Calot, Berck sur Mer, France.

INTRODUCTION

Surgical instrumentation of the scoliotic spine is a complex procedure involving many parameters to determine pre- and intra-operatively such as the spinal segment to instrument, the number, position and size of hooks/screws, the rod shape and size, etc. Despite a large number of clinical publications, there is no consensus on the operative protocol and surgery's outcome may differ accordingly. The objective of this study is to develop and assess a biomechanical model to predict the effect of the Colorado instrumentation of the scoliotic spine as a function of pre-operative geometry and surgical planning.

METHODS

The spine geometry of one patient lying on the operative table was first calculated using two radiographs and an intra-operative 3D reconstruction algorithm[1]. The biomechanical model of the patient's spine was then defined using the flexible mechanism approach developed by Poulin et al.[2] (Fig. 1). The model was generated from the 3D geometric data, using a graphic interface developed on Matlab. The mechanical properties were calculated from published data[2].

The boundary conditions were defined by fixing all degrees of freedom of the rod, which is defined at its final shape and position. We considered each element of the instrumentation as rigid (non-deformable) body. The screws or hooks were rigidly constrained to their instrumented vertebrae.

The simulation was defined in two steps: (1) the links between the screws and the rod were made using translation joints to bring progressively the screws close to the rod's mooring point; (2) a translational motion was imposed on the nuts through the screws' axes, leading the clips to their end point to complete the reduction. Simulation results were assessed by comparison of the Cobb angle and the 3D position of reconstructed and simulated geometries.

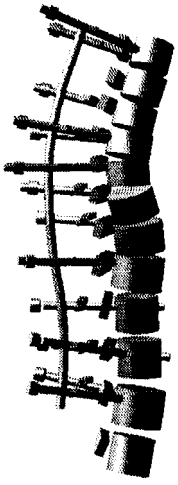

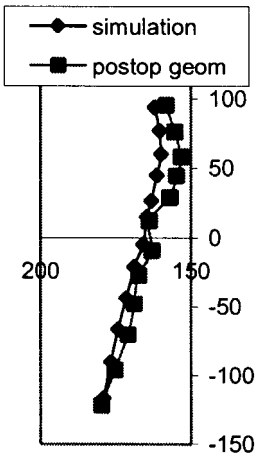

Fig. 1. *(left)* Lateral view of instrumented patient's spine model.
Fig. 2. *(right)* Post-op and simulated PA spinal geometry.

RESULTS

Preliminary simulation results show a difference between simulated and 3D reconstructed post-op geometry of the spine of 2° in the frontal plane for the Cobb angle, 5° in the sagittal plane for the kyphosis angle and of $4{,}7 \pm 2{,}3$ mm for the 3D position of vertebra centroids. The maximum distance (7 mm) was observed at the apex of the instrumented spinal segment. Figure 2 is showing the post-op spinal geometry of the patient's spine, as well as the simulated spine.

CONCLUSION

These preliminary results show that the Colorado surgical technique can be modeled adequately using the pre-operative geometric data and limited simulation strategy parameters. This study is still in progress: simulation mechanisms will be refined and more cases will be simulated in order to confirm these results and validate this new approach. This simulation method has the potential to become a powerful tool for surgeons in the planning of Colorado instrumentation to predict and improve the surgery's outcome.

REFERENCES

[1]–F. Cheriet, S. Delorme, J. Dansereau, C.É. Aubin, J.A. de Guise, H. Labelle, Reconstruction radiographique peropératoire de la colonne vertébrale scoliotique, Annales de Chirurgie, 53:8, 808–815, 1999.

[2]–F. Poulin, C.E. Aubin, I.A.F. Stokes, M. Gardner, Morse, H. Labelle, Modélisation biomécanique de l'instrumentation du rachis scoliotique à l'aide de mécanismes flexibles: étude de faisabilité, Annales de Chirurgie, 52:8 761–767, 1998.

BIOMECHANICAL MODELING OF SPINAL GROWTH MODULATION FOR THE STUDY OF SCOLIOTIC DEFORMITIES

VILLEMURE I.[1,2], AUBIN C.-E.[2,3], DANSEREAU J.[2,3], AND LABELLE H.[1,2]

[1]Biomedical Eng Inst, University of Montreal; [2]Research Center, Sainte-Justine Hospital, Montreal; [3]Mech Eng Dept, Ecole Polytechnique, Montreal, Canada.

INTRODUCTION

Adolescent idiopathic scoliosis is a complex tridimensional deformity of the spine and rib cage. While its etiology and pathogenesis are still not well understood, it is generally recognized that scoliosis mostly progresses during adolescent growth spurt within a biomechanical cycle sequentially involving postural instability of the trunk, asymmetrical loading of the spine, vertebral growth modulation and development of scoliotic deformities [1,2,3]. Very few biomechanical models of the scoliotic spine include the potential of vertebral growth modulation during scoliosis progression. This study intended to develop a modeling approach incorporating spinal growth modulation of the thoracic and lumbar spine in order to adequately simulate the progression of scoliotic deformities.

MATERIAL AND METHODS

Based on experimental and clinical observations, the model of bone growth modulation was formulated with variables integrating: 1) time t in terms of quasi-static iterations; 2) a biomechanical stimulus of growth modulation, defined as internal forces F and related to bone mechanical properties E; 3) a sensitivity factor to the biomechanical stimulus. The global formulation consists in an iterative procedure over t, sequentially integrating a growth component G, an external loading and the resultant growth modulation component mc = G(EF). This procedure was integrated into a finite element model of the thoracic and lumbar spine [4], which was refined to enable a representative distribution of internal forces in the vertebral bodies. G was specified from vertebral growth rate (0.8 (thor) and 1.1 (lumb) mm/yr.) obtained in the literature while the growth modulation components mc were determined based on internal forces directly calculated from the simulations of the model in response to the loading. A first simulation was made using the personalized geometry of a mild scoliotic patient (Cobb = 17), allowing qualitative assessment of scoliotic deformities evolving over 12 months (cycles) in response to apical moments corresponding to a 15 mm eccentricity of the patient's gravity line in the coronal plane. Scoliotic descriptors (Cobb angle, kyphosis, wedging angle of the thoracic apex and its angular orientation, vertebral axial rotation) were evaluated for each growth cycle.

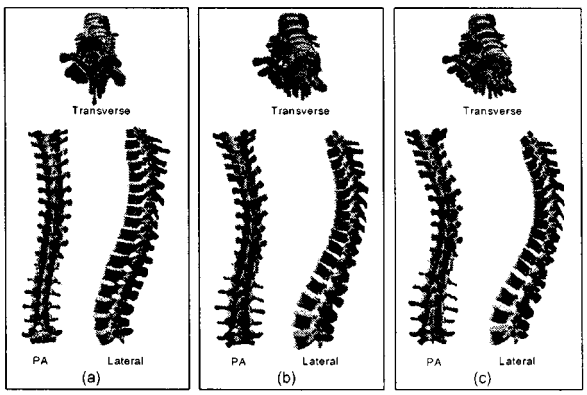

Fig. 1. a) initial configuration; b) simulation at the 6th month; c) simulation at the 12th month.

RESULTS

Frontal, sagittal and transverse spinal views corresponded to clinically observable scoliotic spinal configurations (Fig. 1). In the model simulations, the thoracic Cobb angle and kyphosis increased non-linearly from the first to last growth cycle (17º to 34º and 37º to 48º respectively). At the thoracic apex, the wedging angle evolved from 3.1º to 7.7º with a 16º angular displacement of this deformity towards the local frontal plane. Concomitantly, the apex rotated from 7º to 13º towards the convexity.

DISCUSSION AND CONCLUSION

The simulation adequately reproduces a progressing thoracic scoliotic curve while the increased kyphosis represents a possible condition although a thoracic hypokyphosis is frequently reported in the literature. Evolution of vertebral wedging and axial rotation of the thoracic apex is in agreement with clinical and experimental observations reported with curve progression. Overall, the developed model adequately represents the self-sustaining progression of vertebral and spinal scoliotic deformities. The model is however limited by the actual state of knowledge on growth modulation. Nevertheless, this study demonstrates the feasibility of the modeling approach and, compared to other biomechanical studies of scoliosis, it achieves a more complete representation of the scoliotic spine by incorporating vertebral growth modulation.

The original finite element model was developed in collaboration with the ÉNSAM, Paris.

REFERENCES

1–BURWELL R.G. et al. (1992), Acta Orthop Belg, 58, 33–58.
2–PERDRIOLLE R. et al. (1993), Spine, 18, 343–349.
3–ROAF R. (1966), Scoliosis, E. & S. Livingstone Ltd., Edinburgh, 147pp.
4–AUBIN C.-É. et al. (1995), Ann Chir, 49, 749–761.

AID FOR CONTOUR DETECTION OF INTERVERTEBRAL DISK CONSTITUENTS FROM MRI SIGNAL ANALYSIS

ESTIVALÈZES É.[1], SALES DE GAUZY J.[2] AND SÉVELY A.[3]
[1]INSERM U518; [2]Hôpital des Enfants; [3]CHU Purpan, Toulouse, France

INTRODUCTION

Imagery techniques such as radiography, computer tomography or magnetic resonance are widely used in the field of biomechanics to obtain *in vivo* geometrical data of patient[1,2,3].

MRI is supposed nowadays to be a non-invasive technique and appropriate to visualize soft tissue. However, images obtained from this technique are visualized in gray scale and it is sometimes difficult to determine to the naked eye the contour of the different structures and particularly for images of intervertebral disk. Indeed, the frontiers between the different parts of an intervertebral disk, nucleus pulposus and annulus fibrosus, are not easy to determine. The main objective of this work was to obtain an operator independent imaging tool to treat MRI scans of intervertebral disk. So an analysis of the MRI signal was done on a lumbar spine to detect precisely the different constituents of the intervertebral disk.

MATERIALS AND METHODS

The MRI was performed on a 11 year old volunteer boy with no known spine problems.

The MRI images reviewed were obtained on a Siemens Magneton Vision 1.5 Tesla. Turbo spin echo T2 sagittal and coronal images were obtained through the lumbar spine using standard protocols. Slice thicknesses on sagittal and coronal images were 4 mm with steps of 4 mm. The repetition time was TR 3500, the echo time was 132 and the pixel matrix was 512 $\times$ 512 with a pixel size of 0.5859 mm.

Each image, being coded with ACR-NEMA 2.0, was decoded, then the MRI signal intensity was extracted for each pixel of the region of interest. The position of each pixel, with respect to the reference coordinate frame attached to the IRM table, and the corresponding MRI signal intensity were stored in an ASCII file.

This file was exported in Microsoft®Excel and plotted as 3D graphic.

RESULTS

The MRI signal intensity was extracted from a 100 mm $\times$ 100 mm part of the original MRI scan represented by Fig. 1-a. Values were plotted via Microsoft®Excel with the surface graphical type tool, each color corresponds to a MRI signal intensity ranging from 0 to 850 with a pitch of 50.

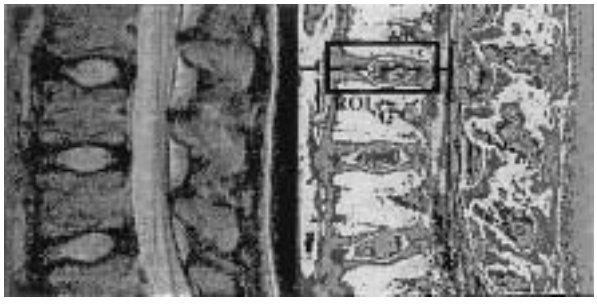

5th MRI sagittal scan (a) 5th MRI signal intensity (b).

Fig. 1. Display of a part of the 5th sagittal scan before (a) and after treatment of MRI signal intensity (b).

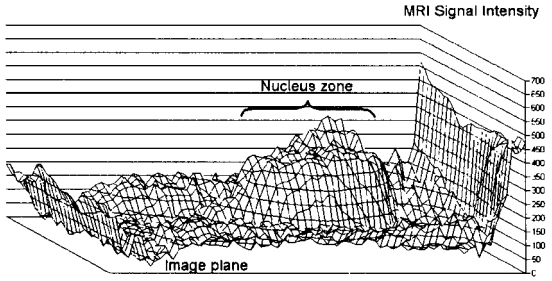

Fig. 2. Variation of the signal intensity in the reduced region of interest (ROI) corresponding to the intervertebral disk.

When all data are plotted, it is interesting to reduce the region of interest to focalize specifically on the intervertebral disk (Fig. 1-b.). Figure 2 displays the variation of the signal intensity in the ROI rectangular zone including an intervertebral disk.

DISCUSSION AND CONCLUSION

The range of the MRI signal intensity of the zone including the disk varies from 0 to 450. Values of the signal intensity between 0 and 150 seem to represent the annulus fibrosus, when values between 150 and 450 seem to represent the nucleus pulposus.

Actually, this observation is confirmed by the analysis of the curve representing the signal intensity versus the line (dash point on Figure 1) cutting the disk in two parts; the slope is very smooth for values between 0 and 150 and steeper between 150 and 450.

Generally classical imaging techniques use in an empirical manner the center and the width of the gray scale of the image, available in imaging software, to obtain a better contrasted image and consequently, the results are operator dependent. In this work, the use of MRI signal intensity to determine the different constituent of the intervertebral disk is relevant thus enabling an operator independent.

Furthermore, this method could be applied to improve in vivo measurements of disk entities like disk height, disk bulge, disk degeneration,…

REFERENCES

1–Boos N. et al., Spine, 21(5):563–570 1996.
2–Balderson R. A. et al., Spine, 23(1):54–59 1998.
3–Smith B. M. T. et al., Spine, 23(19):2074–2080 1998.

BIOMECANIQUE OSTEOARTICULAIRE

F. LAVASTE
ENSAM, Laboratoire de Biomécanique, Paris

INTRODUCTION

La modélisation du corps humain en 17 segments corporels principaux, tête, cou, thorax, abdomen, bassin . . . fait apparaître des liaisons entre ces segments appelées encore articulations intersegmentaires. On dénombre ainsi 14 articulations principales ou intersegmentaires.

L'articulation intersegmentaire aij relie deux segments adjacents Si et Sj. Elle permet la mobilité de Si par rapport à Sj, elle permet également le transfert des efforts de Si vers Sj ou Sj vers Si. La commande des mouvements de Si par rapport à Sj est assurée par les muscles articulaires. Lorsque l'articulation est défaillante, cas de lésions traumatiques ou dégénératives, la restauration de l'articulation peut être assurée par une prothèse articulaire.

L'objet de la biomécanique ostéoarticulaire est d'analyser la cinématique articulaire, de simuler le comportement mécanique de l'articulation, d'aider à la conception des prothèses articulaire.

La démarche utilisée reste la même quelque soit l'articulation étudiée, dans cet exposé nous traiterons plus spécifiquement de l'articulation intervertébrale, en abordant successivement la cinématique intervertébrale aux différents niveaux de la colonne, la modélisation géométrique et mécanique des segments vertébraux, l'aide à la conception des implants rachidiens.

ANALYSE CINEMATIQUE

La cinématique intervertébrale est bi ou tridimensionnelle selon le type de mouvement. Les analyses cinématiques peuvent être conduites *in vivo* ou in-vitro à l'aide de l'imagerie médicale ou de procédés optoélectronique ou ultrasonique ou magnétique. Les résultats font apparître de grandes variations de mobilités selon les étages vertébraux et les mouvements. A titre d'exemples l'amplitude de mobilité principale en rotation axiale droite gauche est de 70 degrés en C_1C_2 alors qu'elle n'est que de quelques degrés (5 degrés) en L_1L_2.

MODELISATION GEOMETRIQUE ET MECANIQUE

La modélisation géométrique personalisée s'est largement dévelopée ces cinq dernières années à partir de l'imagerie médicale et plus particulièrement à partir de la stéréoradiographie. La précision de ces reconstructions 3D par stéréoradiographies est voisine de celle obtenue à l'aide de coupes scanner millimétriques. La modélisation mécanique fait intervenir les caractéristiques mécanique des différents composants de l'articulation. Ces caractéristiques sont en général extraites de la bibliographie internationale (caractéristiques mécanique du tissu osseux, ligamentaire, discal. . .). Cependant dans certains cas il est nécessaire d'introduire des caractéristiques mécaniques personnalisées (modélisations des colonnes scoliotiques) pou simuler de façon fine le comportement mécanique.

La dernière étape de la modélisation consiste à valider le modèle géométrique et mécanique soit en se référant à des résultats bibliographiques soit en comparant les résultats de la simulation à des résultats d'expérimentation *in vitro* ou à des résultats obtenus dans le cadre d'examens cliniques.

CONCEPTION DES IMPLANTS

Les modèles articulaires validés sont alors utilisés pour améliorer la connaissance du comportement mécanique articulaire en faisant varier les différents paramètres du modèle. Ces modèles sont également utilisé pour aider à la conception des implants ou prothèses articulaires en introduisant dans le modèle ostéoarticulaire une modélisation paramètrée de l'implant destiné à restaurer la fonctionnalité de l'articulation.

Il est ainsi possible de valider sur le plan mécanique la conception de l'implant.

CONCLUSION

En conclusion les analyses expérimentales *in vitro* conjuguées aux observations cliniques et complétées par les modélisations géométriques et mécaniques, permettent une connaissance plus fine de la biomécanique ostéoarticulaire et apportent une contribution spécifique dans le traitement des pathologies articulaires.

MECHANICAL PROPERTIES OF EPITHELIAL CELLS EVALUATED BY MICROASPIRATION AND MAGNETOCYTOMETRY

LAURENT V.[1], PLANUS E.[1], ISABEY D.[1], LACOMBE C.[2], BUCHERER C.[2]

[1]INSERM U492, Physiopathologie et Thérapeutique Respiratoires, Faculté de Médecine, Paris 12, Créteil, France; [2]Unité de Biorhéologie, Université Paris 6 et LBHP CNRS ESA 7057, Paris, France.

INTRODUCTION

Cell mechanical properties play a major role in cellular functions such as adherence, migration, invasion and proliferation. A variety of micromanipulation techniques can be used for mechanical measurements in living cells. Data obtained with these techniques are scattered and are supposed to depend primarily on the technique employed and to a lesser extent from the type of cell used. To evaluate these assumptions, we compare quantitatively the results given by two techniques: aspiration through micropipette (microaspiration) and magnetic twisting cytometry (magnetocytometry) on the same epithelial cells treated or not with a drug depolymerizing actin filaments.

MATERIAL AND METHODS

For aspiration experiments, epithelial cells A549 were trypsinized and suspended in a culture medium with HEPES. In some experiments, cells were treated with cytochalasin D which is known to alter polymerization of actin filaments. Micropipette experiments consist of aspirating one single cell in a micropipette (3.8 µm mean diameter) under a well controlled aspiration pressure (198 Pa in mean). Cellular responses were analyzed with a viscoelastic Kelvin model during microaspiration (untreated cells), a Maxwell model (treated cells) and with a Voigt model (untreated and treated cells) during magnetocytometry, as classically proposed (1,2,3,4).

RESULTS

Results for microaspiration are given in Table 1 and Figures 1, 2 whereas Table 2 and Figure 3 give results for magnetocytometry.

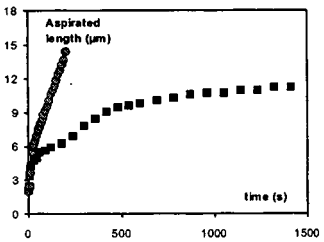

Fig. 1. Aspirated length as a function of time for a untreated cell (■) and a cell treated with cytochalasin D () (5 µg/ml) in a 6 µm pipette diameter under an aspiration pressure of 235 Pa.

Table 1. Experimental characteristics and mechanical parameters obtained by micromanipulation on 13 epithelial cells.

	Mean	SD
Pipette diameter 2Rp (µm)	3.8	0.2
Cell diameter 2Rc (µm)	15.4	1.6
Ratio Rc/Rp	4.0	0.4
Aspiration pressure (Pa)	198	6
Aspiration time (s)	1500	400
Rigidity modulus K_1 (Pa)	49	18
Rigidity modulus K_2 (Pa)	296	112
Viscosity modulus µ (kPa.s)	12.9	5.1

Fig. 2. Deformations in a 6 µm pipette diameter and under an aspiration pressure of 235 Pa of a non treated cell on the left, and of a cell treated with cytochalasin D on the right. Corresponding values of rigidity and viscosity of treated cells are 180 Pa and 13.2 kPa respectively.

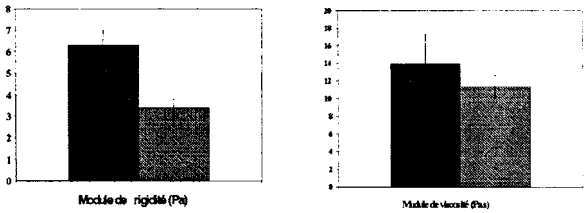

Fig. 3. Rigidity (on the left) and viscosity (on the right) moduli evaluated by magnetocytometry on 5 wells before (in black) and after treatment with cytochalasin D (in grey) (1 µg/ml).

Table 2. Experimental characteristics and mechanical parameters obtained by micromanipulation on 5 wells containing approximately 50 000 cells.

	Mean	SD
Shear stress (Pa)	3.4	0.1
Bead rotation angle (°)	31.3	2.7
Rigidity modulus E (Pa)	6.3	0.7
Viscosity modulus µ (Pa.s)	13.9	3.4

DISCUSSION AND CONCLUSION

First, values of rigidity and viscosity moduli obtained with the two techniques are quite different, depending on the mode, the amplitude and the duration of the applied stress. Viscosity modulus is three orders of magnitude greater during microaspiration compared to magnetocytometry, likely due to the long time of aspiration. Secondly, the actin cytoskeleton seems to play an important role in the cellular viscoelastic response evaluated by both techniques, as shown by the smaller values of rigidity measured after cytochalasine D treatment. Thirdly, more elaborated rheological models are required, notably concerning the magnetocytometry data, in an attempt to reconcile the discrepancies obtained with the two techniques.

REFERENCES

1–Sato, M., Theret, D.P., Wheeler, L.T., Ohshima, N., Nerem R.M. (1990), *J. Biomech. Eng*., 112, 3, 263–268.

2–Schmid-Schönbein, G.W., Sung, K.L., Tözeren, H., Skalak, R., Chien, S. (1981), *Biophys. J.*, 36, 1, 243–256.

3–Theret, D.P., Levesque, M.J., Sato, M., Nerem, R., Wheeler, M.T. (1988), *J. Biomech. Eng*., 110, 3, 190–199.

4–Wang, N., Butler, J.P., Ingber, D.E., (1993), *Science*, 260, 1124–1127.

PLASMATIC, INTERSTITIAL AND INTRA-CELLULAR FLUID MONITORING IN DIALYZED PATIENTS BY IMPEDANCE SPECTROSCOPY

FENECH M[1]., MAASRANI M[2]. AND JAFFRIN M.Y[1],
[1]UMR CNRS 6600, Technological University of Compiegne, 60205, Compiegne, France, [2] Université Islamique du Liban.

INTRODUCTION

Multifrequency impedance spectroscopy has been proposed for the non invasive monitoring of extra (ECW) and intracellular (ICW) water volumes during dialysis[1] . In addition continuous measurement of hematocrit in the blood line feeding the hemodialyser gives access to plasma volume variations and, by difference between ECW and plasma volumes, to interstitial volume. Fluid transfer monitoring between these compartments may be useful for preventing vascular disorders such as hypotension.

MATERIAL AND METHODS

Data were collected on pediatric patients (12–21 yr) and on 6 older adults (44–72 yr), each one monitored three times over a one month interval, using a multifrequency impedancemeter XITRON 4200 (5–1000 Khz) and an optical device (Crit-Line) for measuring hematocrit. Blood pressure was continuously monitored by an automatic pressure recorder.

ECW and ICW volumes were calculated with the help of Hanai's mixture conductivity theory to account for the presence of non conducting elements, fat bones and cells (at low frequency) in the tissues. Values of ECW and ICW resistivities were taken from De Lorenzo et al.[2] Plasma volume variations were deducted from hematocrit using mass conservation and invariance of red cell volume. The interstitial volume was calculated as the difference between ECW and plasma volumes.

RESULTS

The ECW volume was found to decrease during dialysis due to ultrafiltration (UF). In the younger patients, the ECW decrease represented, on the average, 95% of weight loss against 45% in older patients. The contribution of ICW to ultrafiltration must therefore be less in younger patients.

A change in UF rate during dialysis induces a corresponding change in the rate of ECW decay (Fig. 1). The variation of plasmatic ΔVP, intracellular ΔICW, interstitial ΔVL, extracellular ΔECW and ultrafiltered UF volumes; of an adult patient is represented in Figure 2. The drop in plasma volume (0.7 l) is much less that the ultrafiltered volume (3 l), due to vascular refilling from interstitial (1.4 l) and ICW (0.9 l).

Hypotension was not observed in patients in whom the various compartments contributed about equally to the weight loss such as in Figure 2, while it was observed more often in patients with irregular volume patterns.

CONCLUSION

The combination of continuous hematocrit and blood pressure measurements with bio-impedance spectroscopy gives complete information on the amount and origin of vascular refilling in a patient and can serve as a guide to prevent hypotension during a dialysis treatment and could help to predict the dry weight.

The main difficulty lies in the correct calculation of ECW and ICW volumes using an electrical model of tissues. We had to recalculate ICW volumes from impedance data as the direct calculation by the XITRON 4200 was incorrect.

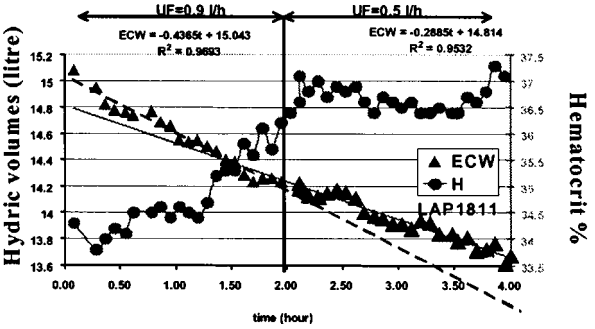

Fig. 1. Influence of a change of UF on the rate of ECW decay and hematocrit for patient LAP 1811.

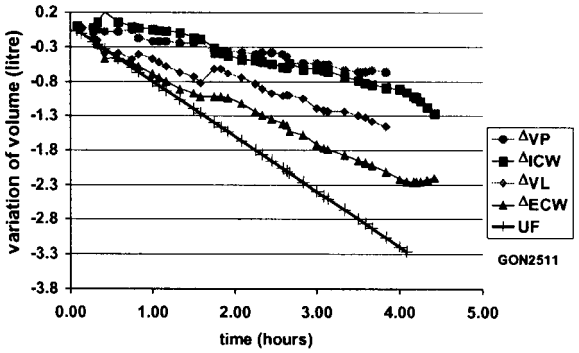

Fig. 2. Variation of various hydric volumes for patient GON2501.

REFERENCES

1–MEIJER J., de VRIES P., GOOVAERTS, H. et al. Measurement of transcellular fluid shift during hemodialysis. Med. & Biol. Eng. & Comput., 1989, 27, pp. 147–158.

2–De LORENZO A., ANDREOLI. A, MATTHIE, J. , WITHERS P : Predicting body cell mass with bioimpedance by using theoretical methods: a technical review. J. Appl. Physiol., 82(5), pp. 1542–1558, 1997.

ARTERIAL WALL REMODELING USING AN *EX VIVO* ARTERY SUPPORT SYSTEM

ZULLIGER M.[1], MONTORZI-THORELL G.[1], FRIEDEZ P.[1], KRETZERS L.[2], LARIK V.[2], MEISTER J.J.[1] AND STERGIOPULOS N.[1]

[1]Biomechanical Engineering Laboratory, Swiss Federal Institute of Technology, Lausanne, Switzerland; [2]Bukken Research Center, Maastrecht, Netherlands.

INTRODUCTION

Large arteries remodel rapidly in response to changes in blood pressure. For example, within 3 to 5 days after inducing hypertension in rats by aortic banding, aortic wall thickness already reaches 50% of its final value [1]. In order to achieve better control over biomechanical parameters driving remodeling than is possible in animal models, our team has developed an *ex vivo* artery support system (EVASS) based on the one developed by Dr. A. Tedgui. EVASS allows mean pressure and flow in blood vessels of 2 to 10 mm diameter to be controlled while keeping arteries alive for up to 7 days.

MATERIALS AND METHODS

A high-resolution ultrasound device (NIUS 02, Omega Electronics SA) is used to measure internal diameter and wall thickness of the artery. Thus by changing pressure, pressure-diameter curves can be recorded providing information on arterial geometry and distensibility. The fact that the system is easy to access provides advantages in manipulation and drug administration over *in vivo* models. In the present work, we study right internal porcine carotid arteries taken from the slaughterhouse.

Study of non-pulsatile and pulsatile pressure effects

Three groups of arteries were perfused for 1, 3 and 8 days respectively under non-pulsatile conditions at 100 mmHg (NPP1, 3, & 8). A fourth groups was cultured for 3 days while subjected to a sinusoidal pulsatile pressure ranging from 75 to 125 mmHg (PP3). Non-pulsatile flow was set to expose the arterial lumen to approximately 1 dyn/cm^2 of wall shear stress in all four groups. Pressure-diameter curves were recorded on the first and last day for all groups.

Study of flow effects on injured arteries

Intimal hyperplasia was introduced by injuring the arterial wall intima with an inflated catheter balloon. The arteries were split in two groups according to perfusion flow; a high flow group (80 ml/min) and a low flow group (2 ml/min).

RESULTS

Study of non-pulsatile and pulsatile pressure effects

The geometry of the vessels showed no significant changes in all cases except the internal diameter of the arteries without pulsatile pressure which increased slightly over the 3 and 8 day periods.

Distensibility of the arteries at mean culture pressure (100 mmHg) showed an increase over 3 and 8 days in the non-pulsatile pressure groups, the difference after 8 days being significant (paired *t*-test, $p = 0.00857$). In the 3 day pulsatile pressure group, distensibility remained almost unchanged (paired *t*-test, $p = 0.858$) (Fig. 1).

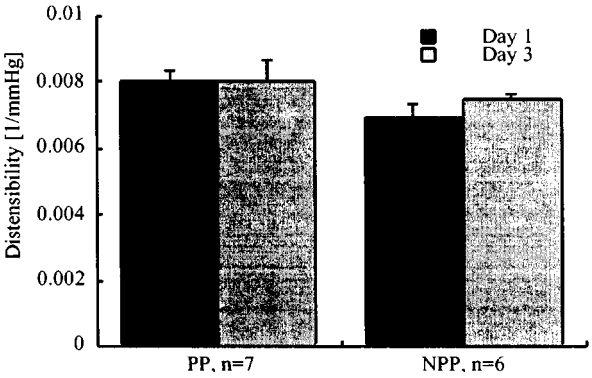

Fig. 1. The distensibility of arteries after 3 days of culture: left bars indicate the values for the group cultured with pulsatile pressure (PP, 75–125 mmHg) at days 1 and 3, right bars show the same for arteries subjected to a static pressure (NPP, 100 mmHg). A clear increase in distensibility is observed for the non-pulsatile group.

Study of flow effects on injured arteries

Histology of these arteries after four days reveled that the low flow group was subject to neointimal proliferation while the high flow group showed no formation of this kind. Further, the new tissue formed in the low pressure group lacked nuclei, which leads to the assumption that mostly matricial tissue is formed. Absence of smooth muscle cells in this area was further confirmed by the fact that immunocytochemestry showed low alfa-actin content.

DISCUSSION AND CONCLUSIONS

Study of non-pulsatile and pulsatile pressure effects

Lack of pulsatile pressure leads directly to changes in the mechanical properties of arteries within 3 days.

Study of flow effects on injured arteries

High flow rates suppress neointimal proliferation in balloon catheter injured arteries. These findings are in accordance with those of *in vivo* animal models[2] as well of those of *in vitro* models[3].

We conclude, that the *in vitro* system presented is a useful research tool for the arterial wall remodeling and that it is capable of producing results with *in vivo* significance

REFERENCES

[1]–S. Q. Liu and Y. C. Fung (1989) J Biomech Eng 111: 325–335.

[2]–T. R. Kohler and A. Jawien (1992) Arterioscler Thromb 12: 963–971.

[3]–R. Voisard, V. Jensch, R. Baur, M. Hoher and V. Hombach (1995) Coron Artery Dis 6: 657–665.

EXPERIMENTAL STUDY OF CONFINED JET: THE MITRAL VALVE REGURGITATION

SANCHEZ L.[1], PERRAULT R.[1], COISNE D.[2] AND MORIN G.[1]
[1]L.E.A., UMR 6609, Boulevard 3, Téléport 2, BP 179, 86960 FUTUROSCOPE Cedex; [2]C.H.R.U. de Poitiers, 86 000 Poitiers.

INTRODUCTION

The use, by cardiologists, of the two dimensions Doppler colour echocardiography has become a routine method for judging the severity of mitral regurgitation. So the flow description of confined jets appears to be of great importance for this phenomenon approach. Indeed, a lot of studies made by medical research deal with blood flow through different orifices such as cardiac valves. Unfortunately, recent studies have demonstrated complex relations between jet characteristics and ejected volume. In this study, the fluid mechanics theory (turbulence) and PIV measurement methods are combined to study the problem of unsteady confined jet.

MATERIAL AND METHODS

In order to sketch heart, it has been represented by 2 rooms separated by perforated wall, modelling mitral valve. The upstream room represents the left ventricle with the highest pressures in heart according to cardiac cycle. Downstream the orifice, the low pressure room is the left atrium. This experimental heart model is realised with cylindrical pipe in transparent Plexiglas with an inner diameter of 40 mm, immersed in water tank in order to minimise optical distortions. A pump, governed by a synthetizer-signal generator, provides physiological pressures conditions, where any curve can be produced by 48 steps with adjustable levels. Then, a flow meter gives reference values of flow rate just downstream of the pump. To perform PIV measurement techniques, we use a see-through fluid seeded with silica particles (10µm) and its blood like viscosity is 3,5cp at 20°C. In parallel, a numerical study has been performed, using the same geometrical, pressure drops and unsteady conditions.

RESULTS

In this study, we try to point out the results concerning the influence of the orifice shape on jet behavior when it is described only in terms of velocity values and of geometrical parameters, these ones being the more accessible and helpful for the cardiologists. Concerning the jet shape, as described in DeGroff [1] study, we observe the convergence zone with isovelocity surface area. Then, downstream the orifice, the jet is composed of the potential core, followed by the transition zone and at least a fully developed jet zone, as explained by Risso [2]. On Figure 1, in transition zone, axial velocity component decreases along the axis, due to lateral confinement and turbulent diffusion, which

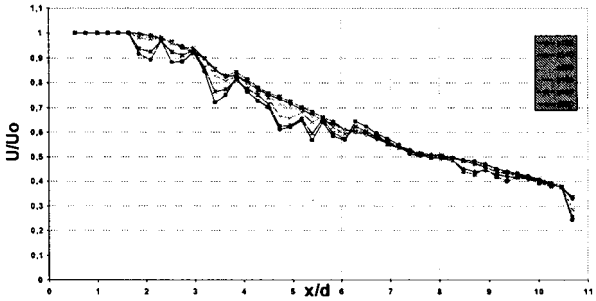

Fig. 1. Mean velocities on axial component for several pressure values.

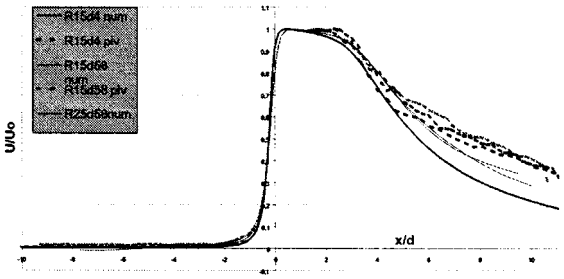

Fig. 2. Axial dimensionless velocities in experimental and numerical results.

contribute to the existence of swirling systems, and redistribute jet energy. As main results, this velocity decay and the flow shape are independent of pressure drop for systolic peak conditions. In Figure 2, a comparison is made between experimental and numerical simulations. We observe a great similitude between both results. Over a short distance of about 3d, axial velocity remains constant just downstream the orifice. This potential core length reaches to Risso's values.

DISCUSSION AND CONCLUSION

The fact that pressure drop do not influence jet flow shape is noticeable. In addition, the lateral confinement effect is shown. Characteristics of confined jet are found with a specific fluid and for unsteady *in vivo* flow conditions. The heart representation is not perfect, but results obtained agree with medical results.

REFERENCES

[1]–DeGroff: "Evaluating isovelocity surface area flow convergence method with finite element modelling." Journal of the American Society of Echocardiography, 1998, vol. 11, pp. 809–818.

[2]–Risso: "Diffusive turbulence in a confined jet experiment." J. Fluid Mech. (1997), vol. 337, pp. 233–261.

IN VIVO PREDICTION OF PLAQUE RUPTURE LOCATION BEFORE HUMAN CORONARY ANGIOPLASTY

LAGACHE M.[1], FINET G.[2], TEPPAZ P.[3], OHAYON J.[1].

[1] *LaMaCo, ESIGEC, Bourget du lac, France.*, [2] *Hôpital Cardio-vasculaire, Lyon, France,* [3] *IRCM Montreal, Quebec, Canada.*

INTRODUCTION

This, *in vivo*, study was designed to test the hypothesis that a computational structural analysis of atherosclerotic vessel, before angioplasty, can be used to predict plaque fracture location before balloon pressurization. Computational analysis of a coronary with atherosclerotic plaque require the knowledge of: a) the rheological properties of coronary's constituents (adventicia, media, fibrous plaque. . ., b) the geometrical stress-free configuration (no internal and external stress). Recent investigations have shown that unloaded normal [4] and pathologic [3] coronaries are no stress-free, and the residual stresses are no negligible. However, the present study doesn't take into account these residual stresses.

METHODS

2.1 ATP protocol

For our simulation, the stress-free configuration of the pathological coronary is identified to unloaded passive physiological state (in vivo passive artery with no luminal pressure). To evaluate the unloaded configuration, we performed an in vivo intravascular ultrasound (IVUS) imaging. The cross-sections of coronaries were acquired during the end-diastole, and after intravenous injection of adenosine triphosphate (ATP). This injection of 40 mg of ATP produces a brief atrio-ventricular block with a significant decrease of diastolic blood pressure. The normal pressure at the end diastole was about 80 mm Hg (10.4 kPa), whereas the pressure was less than 25 mm Hg (3.25 kPa) after the ATP injection. After ATP injection, we notice a significant modification of the cross-section of the coronary. There is a significant change of the vessel geometry after ATP injection. So, the intravascular ultrasound imaging performed after ATP injection provided a geometrical configuration closed to the passive physiological unloaded state. Several in vivo intravascular ultrasound observations were performed: a) for physiological pressure, 80 to 120 mm Hg (10.4 to 15.6 kPa): b) for low endoluminal pressure, after ATP injection (Pressure about 20 mm Hg, 2.6 kPa): c) after angioplasty with intend to visualize the rupture location.

2.2 Mechanical modeling

a) Materials. Although it is possible to perform solution with non-linear elastic behavior, little data regarding non-linear properties of atherosclerotic vessels are available. So we choose to assume an elastic behavior for each components of the vessel. Nevertheless, both the plaque and the artery are modeled as orthotropic material. Due to the structure of each component, every material are assumed as transverse isotropic materials, with (r, z) plane as isotropic plane. Consequently, each material is completely described by a set of five material properties. The values of Young's modulus, Poisson's ratio and shear modulus are taken from literature [1]. Lipidic and calcified plaque are assumed to be nearly incompressible ($\nu = 0.4999$) and isotropic.

b) Load. For angioplasty simulation, an endoluminal pressure was applied to the coronary. During the angioplasty, the balloon's diameter was less than the diameter of the unloaded balloon. So, the load applied to the coronary is the internal balloon pressure.

c) Finite element modeling. Mechanical calculation is performed by using finite element analysis (FEA). The finite element meshes are built by using ANSYS 5.3 software on a Sun Sparc station (Ultra 1). Due to the diversity of models, the number of elements is different from a model to an other. Nevertheless, the range of number of elements is 800 to 1200 and the range of nodes is about 700 to 1100. The element size has been chosen to have reasonable time computation. Plane strain assumption has been chosen because radial dimension of the atherosclerotic plaque was less than axial length. These plane strain elements are used with large strain formulation. Finite element problems are solved by using ANSYS 5.3 software.

RESULTS

Generally the high stress location were locate on the inner wall of the coronary. We notice that the most of fracture sites, caused by angioplasty, occurred at or near a region of high $\sigma_{\theta\theta}$ (Fig. 3). This work prove that FEA, with ATP protocol and in vivo intravascular ultrasound imaging is an efficient tool for prediction of plaque rupture location, before angioplasty. Although rupture sites were accurately identified in this study, there was no evaluation of the balloon inflation pressure needed to fracture the atherosclerotic plaque. However, to improve this prediction of rupture location we need to have more information about biomechanical behavior of human atherosclerotic tissues.

REFERENCES

[1]–Loree & al.: Effects of fibrous cap thickness on peak circimferential stress in model atherosclerotic vessels; Circulation research, Vol. 71, N° 4, 1992.

[2]–Lee & al.: Computational structural analysis based on intravascular ultrasound imaging before *in vitro* angioplasty: Prediction of plaque fracture locations; JACC, Vol. 21, N° 3, pp. 777–82, 1993.

[3]–P. Teppaz: Comportement mécanique de la plaque composite d'athérome et simulations numériques de l'angioplastie dans les coronaires humaines, Thèse de m'écanique de l'univ. de Savoie, (1999).

[4]–Chuong & al.: On residual stresses in arteries; J. Biomech. Eng., vol. 109, 189–192 (1986).

EFFECT OF SYSTOLIC DURATION ON TRANSVALVULAR PRESSURE GRADIENT

KADEM L.[1], PIBAROT P. [2,3], DUMESNIL J.G.[2], MOURET F.[1],GARITEY V.[1], DURAND L.G.[2], RIEU R.[1]

[1]Laboratoire de Biomécanique Cardiovasculaire, Ecole Supérieure de Mécanique de Marseille, Université de La Méditerranée - (I.R.P.H.E) -CNRS UMR 6594, France; [2]Laboratoire de génie biomédical, Institut de Recherches Cliniques de Montreal, Montreal, Quebec, Canada; [3]Quebec Heart Institute, Laval Hospital, Ste Foy, Quebec, Canada.

INTRODUCTION

In the context of aortic stenosis, the pressure gradient across the aortic valve is an important element to consider because it reveals the severity of the stenosis, and it directly influences the systolic wall stress imposed on the left ventricle which in turn is the main determinant factor of left ventricular hypertrophy. It is therefore important to identify and evaluate the hemodynamic factors determining the transvalvular gradient.

From the expression of Effective Orifice Area (EOA), that represents the area of the flow section at minimal pressure downstream the aortic valve, given by a combination of the continuity equation and the modified Bernoulli equation[1]:

$$EOA = \frac{Q_{mean}}{50\sqrt{\Delta P_{mean}}}$$

we can express the transvalvular gradient under the form:

$$\Delta P_{mean} = \left(\frac{V_e}{50\ EOA\ D_e}\right)^2$$

where: ΔP_{mean} mean transvalvular gradient
Q_{mean} mean transvalvular flow
V_e stroke volume
D_e systolic duration

From a theoretical standpoint, it appears that, for a given stroke volume and valvular area, the pressure gradient is inversely proportional to the systolic duration.

The aim of this study is to confirm this theoretical equation using an *in vitro* model of the left ventricular circulation and to assess if the variation in transvalvular gradient due to the changes in systolic duration is clinically significant.

MATERIAL AND METHODS

To perform the *in vitro* study, we use a simple activation pulse duplicator[2]. It is composed of silicone-made, anatomically shaped models of left heart cavities.

The ventricular model is activated by a pump in order to reproduce physiological flow conditions.

Experimental conditions are:

Heart rate	65 beats per minute
Stroke volume	75 ml
Systolic duration	250; 300; 350; 400; 450 ms.

In this study, we test several rigid stenotic orifices of varying size (0.50; 0.75; 1.00; 1.50 cm^2) and geometry (cicular, ovoid, star) and Medtronic Mosaïc bioprotheses (size: 21 mm and 25 mm), under the aforementioned hemodynamic conditions.

The transvalvular gradient across the aortic valve is measured by catheter and by continuous-wave Doppler-echocardiography.

RESULTS

Figure 1 shows the theoretical relationship between the mean transvalvular gradient and the systolic duration for a given stroke volume (80 ml) and valvular area (0.80 cm^2). When the systolic duration increases from 250 to 450 msec, the gradient decreases by 44 mmHg (–64 %). The *in vitro* validation study is still ongoing and the final results will be available within a few months.

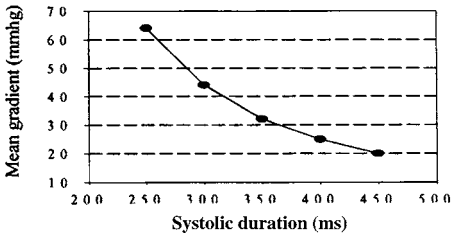

Fig. 1 Theoretical relationship between mean transvalvular gradient and the systolic duration. V_e = 80 ml; EOA= 0.80 cm^2.

DISCUSSION AND CONCLUSION

We expect that an increase in systolic duration will significantly reduce the transvalvular pressure gradient for a given valvular area and stroke volume. We also expect that the magnitude of gradient reduction associated with the increase in systolic duration will be significant from a clinical standpoint. If this hypothesis is confirmed, this study could be used to recommend the use of specific treatments aiming at the lengthening of the systolic duration in order to reduce the left ventricular wall stress.

REFERENCES

1–Dumesnil et Yoganathan (1991). Theoretical and practical differences between the Gorlin formula and continuity equation for calculating aortic and mitral valve area. The American Journal of Cardiology 67: 1268–1272.

2–Garitey et al. (1995). Ventricular flow dynamics past bileaflet prothetic heart valves. International Journal of Artificial Organs 7: 380–391.

EFFECT OF SOMATOTYPES ON STANDING POSTURE

NAULT M-L.[1,2], HINSE S.[1,2], ALLARD P.[1,2], LE BLANC R.[2] AND LABELLE H.[2,3]

[1]Department of Kinesiology, University of Montreal, Canada, Research Centre, Sainte-Justine Hospital, Canada, [3]Orthopedic Surgery, Sainte-Justine Hospital, Canada

INTRODUCTION

Height and weight have been identified as important factors affecting quiet standing stability[1] but no one has addressed body morphology as a global factor. Using anthropometric measurements, subjects can be classified according to their body composition and structure. The aim of this study was to test the hypothesis that standing posture equilibrium is influenced by different morphologic somatotypes. in able-bodied girls

MATERIAL AND METHODS

A total of 43 able-bodied girls having a mean age of 13,8±2,2 years participated in this study. Somatotypes measurements were taken to determine their endomorphic, mesomorphic or ectomorphic characteristics[2]. Then, subjects were ask to stand still on a AMTI platform for 64s with a sampling frequency of 64 Hz. Their feet were spaced by about 23 cm and their arms hanged loosely. Three trials were performed with eyes open condition. The mean position of the center of pressure (COP) in the antero-posterior and medio-lateral directions, the sway area, its minor and major axes, total displacement and average speed of the COP were calculated. Afterwards, subjects were grouped according to their somatotypes, with 15 endomorphs, 12 mesomorphs and 16 ectomorphs. Univariate analyses were carried out with $p < 0,05$. Post hoc Tuckey tests for unequal samples were performed between the groups to determine significant differences.

RESULTS

There was no statistical difference in age, height and weight among the groups and for each one, the dominant somatotype component was statistically significant from the other two. The sway area was statistically larger for the ectomorphs (236,9 ± 134,3 mm^2) than for the endomorphs (137,7 ± 71,4 mm^2) as shown in Figure 1. The minor axis was longer for the ectomorphs (8,1 ± 2,9 mm) than for the endomorphs (5,7 ± 2,2 mm) illustrated in Figure 2. The parameters related to the distance and average speed (medio-lateral, antero-posterior and resultant) were not statistically different. There was also no significant differences between the mesomorphic group and the other two groups, this for all parameters.

DISCUSSION AND CONCLUSION

The greater standing instability in the ectomorphic group can be explained in part by a low mesomorphic component witch was at 2,7 (0,7) compared to 3,7 (1,5) the endomorphs and 4,9 (1,2) for the mesomorphs. The height of the center of mass also influence standing stability. Using the reaction board method[3], mean position in ectomorphic girls was located 7,7 cm higher compared to the other girls. These findings may also be of importance to sport related activities such gymnastics and dance were balance is primordial as well as in the pathological conditions.

Ectomorphic girls displayed a larger sway area than the ectomorphic subjects. Morphology should be considered when assessing standing posture in both able-bodied subjects and patients.

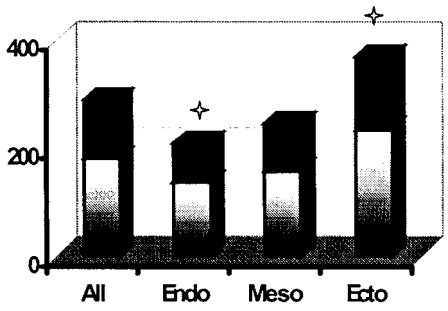

Fig. 1. Surface area delimited by COP (mm^2).

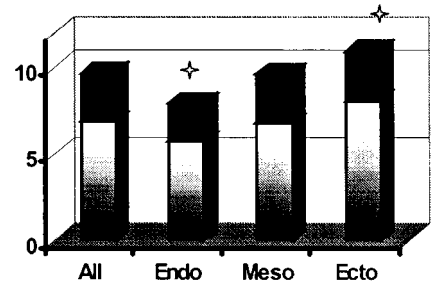

Fig. 2. Minor axis of the ellipse delimited by COP (mm).

REFERENCES

1–Bessineton J-C. et al. (1976)-*Agressologie*-49–54.
2–Carter J-E-L. et al. (1990)-Cambridge university press, 503p.
3–Pearshall D-J. et al. (1994)-*Sports Med*.-126–140.

THE VENOUS PUMP DURING STANDING

DAVID A. WINTER, AFTAB E. PATLA, RICHARD HUGHSON, STEPHEN PERRY, ANDREW BETIK

Dept. of Kinesiology, University of Waterloo, Waterloo, Ontario N2L 3G1

INTRODUCTION

During normal walking the cyclical activity of the calf muscles is more than adequate to massage the veins and achieve venous pump action. However, during standing the modulation of plantarflexor force may not be sufficient for adequate venous return. These same muscles are responsible for sagittal plane balance, and the demands of balance require small plantaflexor changes which may be in conflict with venous return demands. In pathologies, such as diabetes, the problems of inadequate circulation conflicts with the associated neuropathy which compromises balance. The goal of this initial research is to quantify the biomechanical variables that influence venous return during standing in healthy young adults.

METHODS

Eight adult subjects were asked to stand with one foot on a force plate which recorded the centre-of-pressure (COP). Using techniques described by Tschakovsky, et al.(1) the venous return velocity, Λ, was measured with a doppler flowmeter on the Popliteal vein; the flowmeter also gave the vein's diameter, d. Venous return, $V_r = Ad^2\Lambda/4$ ml/s. Integration of V_r over each minute yielded venous return in ml/min. A strain guage manometer around the calf muscles yielded the volume (%) of the calf chamber decreases and were also a measure of the venous return. The leg and foot volume was measured so that the flow could be reported in ml/min/100ml body tissue. Subjects initially were prone, then stood quietly for 2 min., then leaned with the COP 4 cm forward, then leaned back with COP 4 cm back, then with small sways ($\pm$ 2 cm) and large sways ($\pm$ 4 cm). Data were collected at 20 Hz.

RESULTS

The venous return was in "squirts" as shown in Fig. 1 along with the calf volume and COP oscillations for a small sway trial. Between sways the flow dropped sharply to zero until the COP moved forward again, and during each squirt the calf volume was seen to decrease. The magnitude of calf muscle force fluctuation was reflected in the RMS of the COP. The onset of each squirt was correlated with the COP fluctuations such that its onset occurred 50 ms after the maximum rate of change of COP. Table 1 summarizes the COP mean and RMS measures and venous return (as measured by the calf volume decreases) for each of the five posture conditions. The mean COP for each subject was relative to his/her resting position which was reported as 0 cm. On the average each subjects COP during quiet stance was 5 cm anterior of the ankle.

DISCUSSION AND CONCLUSION

The biomechanical variable that most influences venous return is the RMS of COP. Thus, the fluctuations in the muscle forces rather than the level of the average muscle force is what correlates well with the venous return. The voluntary forward lean has some influence on the venous return compared with the backward lean posture. The venous return as measured from the doppler flowmeter was not consistent over each two minute trial because it was very sensitive to the direction of the probe over the Popliteal vein; the probe had to be hand held while the subject swayed. However, the volume measures of each squirt that was recorded correlated well with the decrease in volume of the calf muscle during the period of each squirt. Future directions of this research will focus on pathologies of inadequate lower limb circulation such as diabetes.

Table 1. Venous return and COP for five postures.

Posture	Venous return ml/min/100ml		Mean COP (cm)		RMS COP (cm)	
	Avg.	S.D.	Avg.	S.D.	Avg.	S.D.
Quiet Stance	0.83	0.34	0	0	0.18	0.07
Bkward Lean	1.17	0.67	–4.11	0.79	0.29	0.17
Fwd. Lean	1.72	1.00	3.55	0.97	0.24	0.12
Small Sway	6.57	4.31	0.53	2.62	1.52	0.11
Large Sway	10.08	3.24	1.38	3.24	3.60	0.17

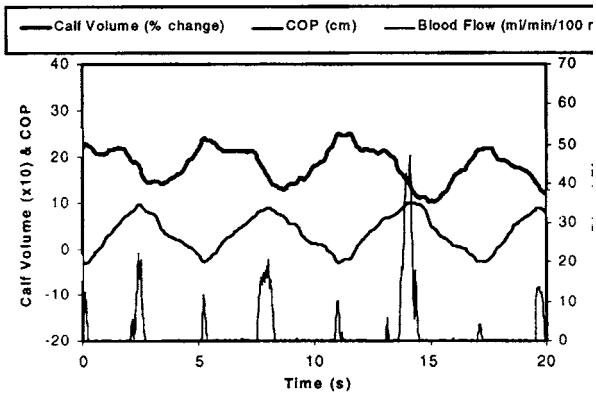

Fig. 1. Calf volume, COP and doppler venous flow during a small sway trial.

REFERENCE

1–Tschakovsky, et al. J.Appl. Physiol. 79:713–719, 1995.

DOES BODY BALANCE STABILITY DEPEND ON POSTURAL CHAIN MOBILITY OR STABILITY AREA?

KANTOR E., POUPARD L., LE BOZEC S. AND BOUISSET S.
Laboratoire de Physiologie du Mouvement, Université Paris-Sud, 91405 ORSAY, France

INTRODUCTION

It has been shown that the respiratory shifting of thoracic and abdominal masses is more or less completely compensated for by the antiphasic displacements of other parts of the body. Indeed the compensation is more efficient in standing than in sitting posture[1,2]. From a biomechanical standpoint, sitting provides a larger support base than standing, but fewer parts of the body are free to be accelerated. This is why, it has been proposed that body balance stability depends on dynamic mobility of the postural chain[3]. The aim of this study is to examine body balance stability related to respiratory perturbation, when subjects were standing and sitting with two different ischio-femoral contacts.

MATERIALS AND METHODS

Subjects were normally standing (Sta) and sitting on a rigid stool with a full (100% Sit) and one third (30% Sit) ischio-femoral contact. In the 100% Sit the pelvis mobility is known to be less than in the 30% Sit condition. The centre of pressure displacement (Sway Path: SP) along the antero-posterior axis was recorded continuously on a triangular force plate.

Eight adults were examined. They were asked to perform five successive blocks of 25s. quiet breathing (QB) and five ones of deep breathing (DB), in each of the three postures. The differences between the means were compared using the Student *t*-test.

RESULTS

For both respiratory conditions, the sway path showed that the mean values were significantly higher for the 100% Sit and 30% Sit than for the Sta condition (Table 1and Table 2). The mean values were higher, but not significantly, when the subjects were sitting with a full than with a one third ischio-femoral contact.

It was observed that if the 30% Sit value is between the Sta and 100% Sit values; the differences are not significant owing to the intermediate postural condition this corresponds to. It could also be noticed that SP values are higher in DB than in QB when the subjects are sitting. But the differences were not significant.

DISCUSSION AND CONCLUSION

These results confirm the previous ones[2], insofar as postural oscillations were greater when the subjects were sitting in the 100% Sit condition than when they were standing. They are extended to the 30% Sit condition.

As the stability area is larger in sitting than in standing posture, this result suggests that the stability area is not the main stability factor. The pelvis mobility is reduced when the subjects are sitting, and more reduced when they are sitting with full ischio-femoral contact. Now, the longer the sway path, the less compensatory the regulation. Consequently, the sway path data suggest that the instantaneous compensation to the same respiratory perturbation is less efficient when the pelvis mobility is reduced.

Table 1. Sway Path (mm) in quiet breathing (QB).

	m	s	p
Sta	359	28	** **
30% Sit	438	58	NS
100% Sit	485	68	

Means (m), standard-deviations (s) and probability (p) are reported in standing (Sta) and sitting postures with full (100% Sit) and one third (30% Sit) ischio-femoral contact.

Table 2. Sway Path (mm) in deep breathing (DB).

	m	s	p
Sta	366	40	** **
30% Sit	470	78	NS
100% Sit	510	95	

Means (m), standard-deviations (s) and probability (p) are reported in standing (Sta) and sitting postures with full (100% Sit) and one third (30% Sit) ischio-femoral contact.
NS: non significant; **highly significant : $p < 0.01$

To conclude, body balance stability is enhanced by the postural chain dynamic mobility, even if balance perturbation is just provoked by respiration.

REFERENCES

1–Gurfinkel VS et al. (1971). In: Gurfinkel V.S., Fomin S.V. and Tsetlin M.L., eds. Models of the structural Functional Organization of certain Biological Systems. Cambridge: MIT Press, 382–395.

2–Bouisset S. and Duchene J.L. (1994). NeuroReport 5: 957–960.

3–Bouisset S and Le Bozec S (1999). In : Gantchev G.N., Mori S. And Massion J., eds. Motor Control, Today and Tomorrow, 275–291.

THE EFFECTS OF HEAD IMMOBILIZATION ON THE CO-ORDINATION AND CONTROL OF HEAD, TRUNK AND COM REORIENTATION DURING A DIRECTION CHANGE TASK

HOLLANDS M.A., SORENSEN K.L. & PATLA A.E.
Gait and Posture Laboratory, Department of Kinesiology, University of Waterloo, Canada

INTRODUCTION

Online steering is an integral component of adaptive locomotion and involves reorientation of the body toward the new travel direction in addition to modifications to stepping (such as step width regulation) which require movement of body centre of mass (COM). Patla et al.[3] previously reported that changing direction is accomplished by, first controlling the COM, then turning the head and finally by reorienting the upper body. However, COM displacement was *inferred* (from knowledge of trunk roll) and the protocol required participants to always turn in the same direction. The primary goal of the present study was to accurately describe COM (derived from knowledge of full body kinematics) during a steering paradigm that introduced uncertainty about required size *and direction* of the required locomotor adjustments. Prior to changing the direction of locomotion, subjects normally make anticipatory head movements towards the new travel path[2]. The second objective was to test the hypothesis that these head movements are made as part of the process of reorienting gaze[1,2,3]. If valid then one would expect that preventing the head from moving independently (by fixing it to the trunk) would result in the trunk starting to turn sooner in order to compensate.

METHODOLOGY

Participants (n=5) were instrumented with twenty eight infrared diodes placed bilaterally on various anatomical landmarks which were tracked using the OPTOTRAK motion analysis system. Knowledge of their positions over time allowed calculation of the following body parameters; head and trunk rotations (yaw, roll and pitch) and centre of mass (COM) and foot position in 3D space. For 50% of trials the participant's head was fixed to the trunk using a Ferno Universal Head Immobilizer. Participants walked at their natural self-selected pace along a 9 m straight travel path. Randomly, during 50% of trials they were visually cued to alter direction via lights placed on the floor at the end of each pathway. Figure 1.

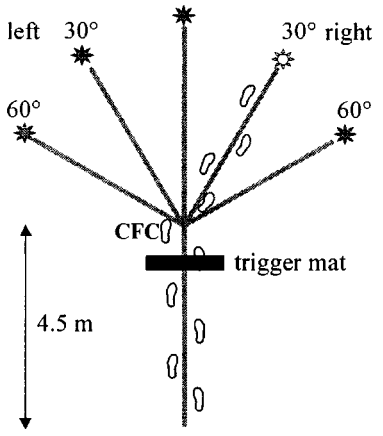

Fig. 1. Experimental paradigm.

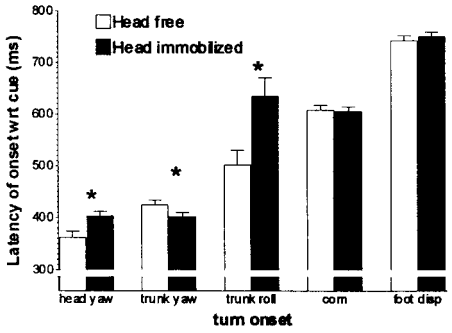

Fig. 2. Latency of reorientation onset with respect to cue light for various body parameters.

RESULTS

On average, during a turn, the contralateral foot (CFC on Figure 1) landed significantly further out laterally (mean 25 mm) away from turn direction prior to onset of COM displacement. Figure 2 shows mean latencies of reorientation onset with respect to cue light for various body parameters.

Effects of immobilizing head: On average, the head started to turn at same time as trunk. As hypothesised, mean trunk yaw reorientation onset was significantly earlier. Trunk started to roll significantly later after COM. Mean change in trunk roll over transition stride was significantly reduced. Other parameters were unchanged (amplitude of trunk yaw, foot and COM displacement, step timings etc.)

DISCUSSION AND CONCLUSION

The finding that there are no significant differences in participants' COM and foot displacement profiles between the head-free and head-immobilized conditions, despite the fact that the mean amplitude of trunk roll is significantly smaller in the latter, suggests that the contribution of the 'hip strategy' to COM control during steering is less important than previously thought. Acceleration of the COM in the new travel direction is achieved mainly through placement of the contralateral foot during the transition stride. The temporal sequence of body reorientation is consistent with previous findings that the head starts to turn in the direction of travel before the rest of the body. The fact that immobilizing the head results, on average, in earlier onset of trunk yaw reorientation supports our stated hypothesis that the head is moved first as part of the process of gaze realignment with the new travel path.

REFERENCES

1. Gibson (1958) *Brit. Journal of Psych 49* 182–189.
2. Grasso, R. et al. (1996) *Neuropreport 7* 1170–1174.
3. Patla et al. (1999) *Exp. Brain Res. 129(4)* 629–634.

EPIDURAL ANALGESIA WITH ROPIVACAINE AND BUPIVACAINE: CENTRE OF PRESSURE ANALYSIS OF STABILITY

LOITZ-RAMAGE B.[1], RONSKY J.[2], GILDENHUYS A.[2], MAURER J.[2], BREEN T.[3], YANG T.[4], ZERNICKE, R.[1]
[1]MCCAIG CENTRE FOR JOINT INJURY AND ARTHRITIS RESEARCH, CALGARY, [2]MECHANICAL AND MANUFACTURING ENG., UNIVERSITY OF CALGARY, CANADA, [3]DEPT. OF ANESTHESIOLOGY, DUKE UNIVERSITY MEDICAL CENTER, USA, [4]DEPT. OF ANESTHESIA, FOOTHILLS HOSPITAL, CALGARY, CANADA.

INTRODUCTION

Sensory feedback is an important factor in maintaining balance. Richardson et al. demonstrated that individuals with peripheral neuropathy had difficulty in maintaining single limb stance and demonstrated a significantly greater excursion of centre of pressure (COP) during single limb stance in comparison to age-matched controls.[1] The role of sensory feedback in maintaining postural stability is difficult to evaluate for conditions such as peripheral neuropathy due to the lack of individual control data. In this study, sensory impairment was induced using epidural analgesia, which allowed each subject's stability to be compared against his or her own control. The purpose of this study was to examine the static stability of individuals under epidural analgesia as part of a larger study that will examine the risk of falling under the effects of these drugs.

METHODS

Five subjects volunteered for the study. Each subject received an epidural infusion of ropivacaine on one day and bupivacaine on a second day. The order that the drugs were administered was randomized and the study was double blind. Epidural catheters were inserted 5 cm into the epidural space at the $L_{2,3}$ or $L_{3,4}$ interspaces by an experienced anesthesiologist. Volunteers received a solution of 0.08% local anaesthetic and 2 mg/ml fentanyl at an infusion rate of 10 ml/hr. Motion analysis was conducted prior to drug administration (control condition), and again at 0.5, 3, and 5 hrs after the initial injection. After 5 hrs, the drug was removed and 2 hrs later a final set of motion analysis data was collected. At each time point subjects were aligned with the axes of the force plate and asked to maintain a single limb stance for three 30-s trials on each leg.

Traditionally, velocity and total translation of COP have been used to measure postural stability. Riley et al. combined these measures to form a phase plane plot of COP velocity versus displacement for analysis of stability during quiet standing.[2] The researchers quantified the phase plane plots for comparison using a unitless stability parameter, s_r, derived from the standard deviations of the COP displacements and velocities. This parameter, given by Equation 1, was used to identify changes in stability due to epidural analgesia. In the anterior/posterior direction, standard deviations of COP displacements and velocities are denoted σ_{APd} and σ_{APv} respectively. Similarly, σ_{MLd} and σ_{MLv} are standard deviations in he medial/lateral direction.

$$\sigma_r = \sqrt{\sigma^2_{AP_d} + \sigma^2_{AP_v} + \sigma^2_{ML_d} + \sigma^2_{ML_v}} \qquad [1]$$

To test the effect of epidural drugs on stability, combined data for both drugs was analyzed using a general linear model with repeated measures (SPSS 9.0). Each drug was also analyzed independently.

RESULTS

Combined data for both drugs and all subjects (Fig.1) shows that average stability decreased significantly compared to control data at times 0.5, 3, and 5 hrs ($p=0.002$, 0.023 and 0.019 respectively). Stability at 7 hrs, 2 hrs after drug removal, was not significantly different from control ($p=0.108$). Bupivacaine affected stability throughout the entire time of infusion, but the effect of ropivacaine decreased after the initial injection.

DISCUSSION AND CONCLUSIONS

The stability parameter indicated significant decreases in stability due to the drugs when compared to the control condition. Single limb stance was proven to be an effective test of stability as it revealed changes caused by sensory impairment. The lasting effects of bupivacaine suggest that subjects were unable to accommodate to sensory impairment with this drug. Although drug levels remained constant between 0.5 and 5 hours, subjects were able to compensate for the loss of sensation under the effects of ropivacaine. These results suggest that bupivacaine has a differential effect that may increase the risk of falling due to sustained instability.

ACKNOWLEDGEMENTS: CRHA, NSERC, U of C

REFERENCES

1–RICHARDSON J.K. et al. (1996)-*Arch. Phys. Med. Rehabil.* 77, 1152–1156.
2–RILEY P.O. et al. (1995)- *J. Rehab. Res. Dev.*-32(3), 227–235.

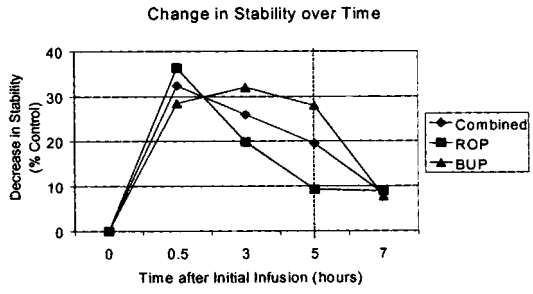

Fig. 1. Change in stability over time.

INTEGRATION OF A FEEDFORWARD CORRECTIVE COMMAND: SYNERGY BETWEEN POINTING AND POSTURE

MARTIN O.[1], TEASDALE N. [2], CORBEIL P.[2], SIMONEAU M.[3]

1Université de Bourgogne, Dijon, Franc e(email: omartin@u-bourgogne.fr); 2Université Laval, Québec, Canada; 3Northwestern University, Chicago, USA

INTRODUCTION

Postural and movement interaction processes are influenced by the level of predictability of the motor task and the environmental constraints imposed to the subjects[1–4]. In the present experiment, a pointing task from a standing posture was used. Subjects were submitted to double-step visual perturbations. The aim of the experiment was to examine if subjects modify the coordination between postural and focal commands after the first perturbation trial. Such changes would suggest a predictive rather than a reactive mode of control.

MATERIAL AND METHODS

Seven subjects performed right-hand pointings from a standing position to visual targets that could change position at hand movement onset. Two targets (LEDs), positioned along the sagittal axis, were 20 cm apart, 10 cm ahead and 10 cm beyond a distance corresponding to the length of the right arm extended in a pointing position (respectively within and beyond prehension space). One of the two targets was light up and the subject had to point as fast and as accurately as possible to the target. In the visual step-target condition, the perturbation occurred in 33% of the trials at hand movement onset, turning off the initial target and simultaneously turning on the other one. The elbow and hip joint angles were obtained from a Selspot II system.

RESULTS

In this presentation, the first pointing trial perturbed (visual double-step) was compared to the subsequent perturbed trials. Figure 1 shows perturbed trials from within to beyond the prehension space for a representative subject. For comparison purposes, two trials without perturbation (one for the near target and one for the far target) are also presented. The first perturbed trial is characterised by a nearly simultaneous break in the progression of the hip flexion and elbow extension. Then, the elbow extension and the hip flexion increase again before the subject reaches the far target. For the following perturbed trials (which were randomly presented), the uncertainty regarding the presence of a perturbation yields a control strategy characterized by earlier and much smoother hip and elbow angle adjustments. Similar behaviors were observed for all subjects.

DISCUSSION AND CONCLUSION

The initial coordinated postural and focal motor commands were certainly based on a rigid open-loop program. This program did not allow a rapid and optimal correction. The contextual uncertainty, however, was included into the program of the following trials allowing the on-line detection of a perturbation and rapid pointing and postural adjustments to reach new target. It is likely that these adaptations were integrated in a feedforward manner to allow a progressive and continuous updating of the pointing movement.

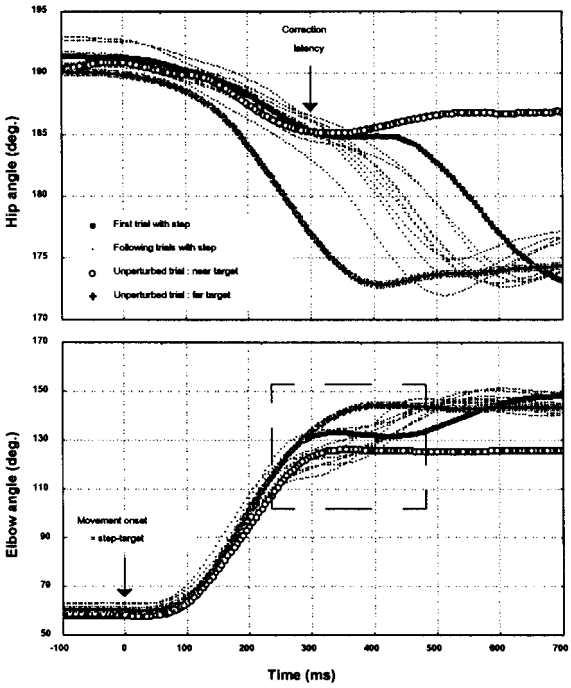

Fig. 1. Joint angles for hip (top panel) and elbow (bottom panel) for the first trial perturbed (thick lines) compared with following step-target perturbed trials (thick lines; n = 10). Two unperturbed trials for the near and the far targets are also presented. representative data from one typical subject.

ACKNOWLEDGEMENTS: Study supported in part by NSERC and FCAR.

REFERENCES

1–Lee W.A. et al. (1987) *Exp Br Res* 66: 257–270.
2–Massion J. (1992) *Prog in Neurobiol* 38: 35–56.
3–Martin O. et al. (2000) *Neurosci Lett* 281: 53–56.
4–Nougier V. et al. (1999) *Neurosci Lett* 260: 109–112.

ROTATION-EXTENSION STRATEGY IN DIRECTIONAL JUMPING

CALDWELL, G.E. AND JONES, S.L.
Department of Exercise Science, University of Massachusetts, USA.

INTRODUCTION

While human vertical jumping has been studied extensively, only recently has jumping in other directions been examined with experimental data[1] and/or simulation models[1,2]. Ridderikhoff et al[1]. used simulations of squat jumps (SJ) to illustrate that forward (long) jumping can be accomplished with the same muscle activity patterns used in vertical jumping if the SJ is initiated with a constant total body angular rotation. Their ROTEX simulation model (rotation followed by leg extension) produced kinematic and kinetic features similar to those produced in real forward jumps. Their data showed that SJs in different directions are performed with a common final extension phase, which is consistent with simulations on countermovement (CMJ) jumps[2]. It would seem that CMJs would be ideal for implementing the ROTEX strategy, with rotation initiated during the downward countermovement phase followed by powerful leg extension in the required direction. Therefore the purpose of the present study was to examine experimental data in directional CMJs for evidence of the ROTEX strategy proposed for SJs.

MATERIAL AND METHODS

Twelve subjects (age: 26 ± 5 yrs, mass 78 ± 9 kg, height 182 ± 8 cm) performed 3 maximal effort countermovement jumps (Fig. 1) in each of four directions: vertical (VJ, 90°), forward (FJ, 45°), intermediate (IJ, 70°) and backward (BJ, 120°). Ground reaction forces and selected muscle EMGs (1000 Hz), and 2D sagittal kinematic data (200 Hz) were collected. A linked segment rigid body model was used to calculate total body center of mass (CM) position and velocity along with the body's rotational kinematics (θ, dθ/dt) throughout each jump.

RESULTS

VJ kinematic and kinetic results were consistent with those reported in the literature. Further, takeoff characteristics (Fig. 1) for the directional jumps were similar to those reported by Ridderikhoff et al[1]. The subjects did rotate during both the countermovement and subsequent propulsive (final =300 ms before take-off) phases of each jump, with the exact rotation pattern depending on the jump direction (Fig. 2). Rotation during the countermovement was bi-phasic (P1 and P2), with a slow forward rotation (negative dθ/dt) followed by a rotation in the direction of the jump. This directional rotation continued as the CM accelerated rapidly in a similar manner during the propulsive (extension) phase of all jumps. The latter part of the propulsive phase was characterized by a positive angular acceleration (upward slope of dθ/dt) for all jumps. The EMG patterns (not shown) illustrated differences between jumps in the countermovement phase for tibialis anterior (TA), and to a smaller extent for gluteus maximus (GM). In the propulsive phase TA and hamstrings (HA) activity decreased with increasing takeoff θ while rectus femoris (RF) activity increased with increasing takeoff θ.

DISCUSSION AND CONCLUSION

All jumps began the countermovement with a forward rotation. The magnitude and velocity of this P1 rotation was indicative of the final jump direction, with FJ having the most rotation and BJ the least. The TA muscle was partially responsible for these differences in P1 rotation, while the GM was implicated in the change of rotation at the end of P1. During propulsion in the final 300 ms the FJ had lower RF and higher HA activity, leading to increased hip extension (see Fig. 1), which would slow down the forward rotation as shown in the last 200 ms (Fig. 2). As seen in previous CMJ simulations[2], the directional jumps showed unique preparation phases followed by a common final extension phase. However this common extension phase was produced by differing contributions from muscles RF, HA and TA. Therefore, although a rotation – extension pattern is used in these directional CMJs, the jumps are not performed with the VJ muscle activity pattern as proposed in the ROTEX strategy described for SJs[1].

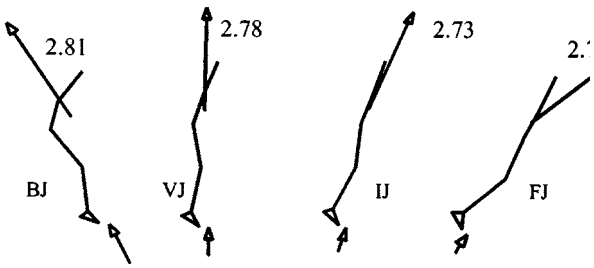

Fig. 1. Stick figures with CM velocity vector (m/s) at takeoff.

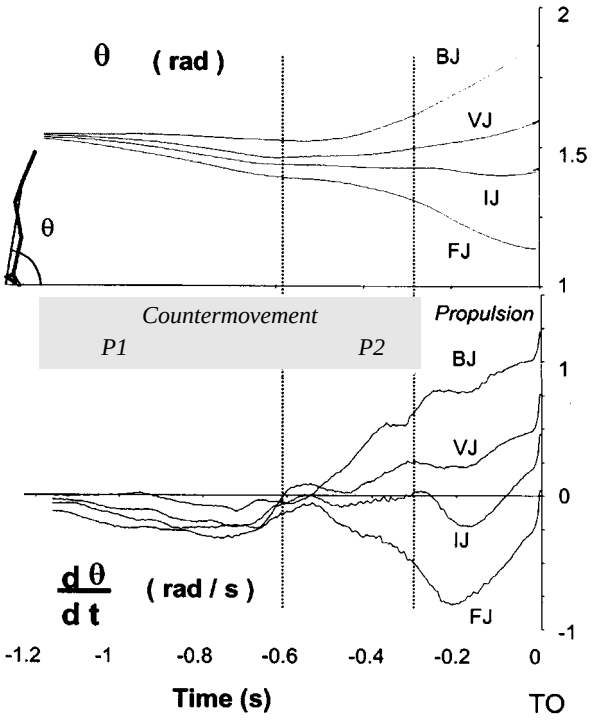

Fig. 2. Total body rotational kinematics.

REFERENCES

1–RIDDERIKHOFF A. et al. (1999). *Med. Sci. Sp. Ex.* 31, 1196–1204.
2–SELBIE W.S. and CALDWELL G.E. (1998). In: Proceedings of the *Third North American Congress on Biomechanics*, 461–462.

EFFECT OF FATIGUE ON PREFERRED AND MOST ECONOMICAL STRIDE FREQUENCY IN TREADMILL RUNNING

IAIN HUNTER AND GERALD A. SMITH
Biomechanics Lab, Oregon State University

INTRODUCTION

Economical running is of great importance to distance runners. Stride frequency and length play a significant role in how economical a runner can be. A large variation is apparent between distance runners in preferred stride rate. Trained runners have the ability to select a stride rate that is most economical in terms of VO_2[1].

Many aspects of a distance runner's technique are affected by fatigue. As one becomes fatigued, preferred stride frequency tends to decrease[2]. This brings up an interesting question of whether or not economical stride frequency is adjusted as preferred stride frequency changes. In a preliminary look at these relationships, this study compared stride kinematics and metabolic costs during a fatiguing run with particular focus on preferred versus most economical stride frequency and length.

METHODS

Two experienced runners ran at 75% VO_2 max for as many 10-minute stages as they could complete. The first stage began after five minutes. Each 10-minute stage consisted of two minutes of running at preferred stride rate, followed by a random order of two-minute intervals of plus and minus four and eight percent of the preferred rate found at the beginning of the stage. During the intervals of adjusted stride rate, a computer-based metronome was used to keep runners at the appropriate rate. Between each stage, subjects ran for 10 minutes without being monitored.

The runners were instructed to run as many stages as possible before stopping due to fatigue. VO_2 was recorded using a metabolic cart (SensorMedics 2900) during the second minute of each stride condition. The second minute was chosen to give the runners a fair amount of time to adjust biomechanically and metabolically to the new stride rate.

Second degree polynomial fit was calculated through the five data points at each stage as a function of stride rate. The minimum point of each curve represented the most economical stride rate.

RESULTS

As the runners were taken further from their preferred rate, in either direction, their metabolic cost increased. Figure 1 shows results for each stage of the runners. Preferred stride rate went from 1.288 Hz to 1.272 Hz for the first runner and from 1.536 Hz to 1.510 Hz for the second. As preferred stride rate shifted, most economical stride rate tended to follow the same shift. Stride length increases of 3–4 cm were observed between the first and last stages of the run.

DISCUSSION

These data support the idea that most economical stride rate coincides with preferred stride rate throughout a fatiguing run. A decrease in preferred stride rate (increase in stride length) was found in both subjects. As previous research has shown, most runners tend to follow this pattern of decreasing preferred stride rate as fatigue sets in. Despite a shift to a lower stride frequency, both runners remained at near optimal economy.

Despite fatigue during long distance runs, it appears that runners maintain an ability to optimize stride frequency and length to minimize metabolic cost throughout a run. It is likely that trained runners do not require a focus on modified stride kinematics for minimizing metabolic cost, even though some stride frequency and length changes likely occur when nearing exhaustion.

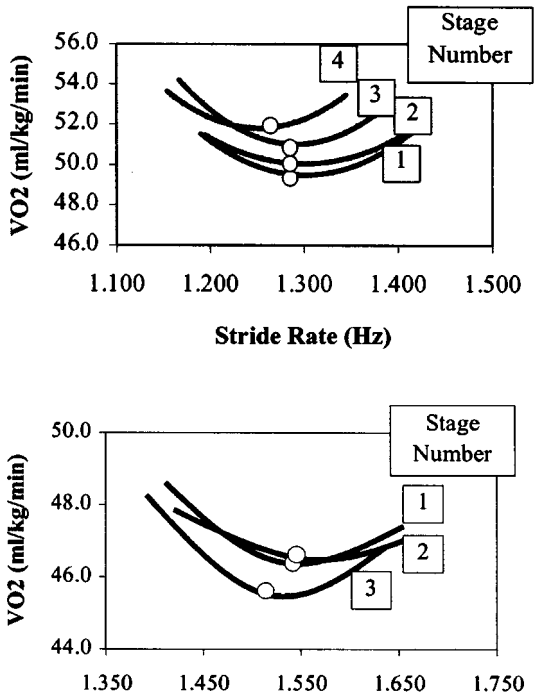

Fig. 1. VO_2 versus stride rate for both subjects. White circles represent preferred stride rate.

The data presented here are preliminary and will lead to future study exploring why preferred and optimal stride rate tend to decrease over the course of a fatiguing run.

REFERENCES

1–CAVANAGH, P.R. and WILLIAMS, K.R. (1982). The effect of stride length variation on oxygen uptake during distance running. *Medicine and Science in Sports and Exercise*, *14*, 30–35.

2–WILLIAMS, K.R., SNOW, R., and AGRUSS, C. (1991). Changes in distance running kinematics with fatigue. *International Journal of Sport Biomechanics*, *7*, 138–162.

THE RELATIONSHIP BETWEEN IMPACT FORCES AND RUNNING INJURIES

STEFANYSHYN D.J.[1], STERGIOU P.[1], NIGG B.M.[1], LUN V.M.Y.[2], AND MEEUWISSE W.H.[2]

[1]Human Performance Laboratory; [2]Sport Medicine Centre, University of Calgary, Calgary, Alberta

INTRODUCTION

Cushioning, the reduction of impact forces, has been studied intensively during the last 25 years. The results of these studies provided many surprising and unexpected results. Early associations of impact forces with musculo-skeletal injuries were either circumstantial in nature[1] or derived from experiments using animal models[2]. Results from *in vivo* experiments showed that a 1 Hz force signal could not maintain bone mass while a 15 Hz force signal produced new bone mass[3]. Obviously, there is a window of loading in which biological tissues react positively to the applied loads. Impact forces have a main frequency content between 10 and 20 Hz. Therefore, impact loading should have a positive effect on the development and maintenance of bone. Thus, it has been speculated that normal impact forces occurring during physical activities such as running might not be a major factor in the development of injuries in running[4]. The purpose of this investigation was to determine the influence of impact forces on injuries during running.

MATERIAL AND METHODS

Baseline biomechanical data were collected on 143 runners prior to the beginning of the summer running season. All subjects wore their own footwear, which they used during the running season. Kinematic data were collected using a 4-camera high speed (240 Hz) 3-dimensional motion analysis system. Reflective markers (3 per segment) were placed on the rearfoot, lower leg and upper leg. Kinetic data were collected (1000 Hz) using a force platform. Three trials were collected per subject. The running speed (4.0 $\pm$ 0.2 m/s) was monitored using two photo cells at shoulder height.

During a 6 month running period, subjects documented any injuries that developed. An injury was defined as a full day of missed training. Subjects were divided into three groups based on their impact forces and impact force loading rates: the bottom 25%, the middle 50% and the top 25%. Injury rates for the different groups were compared using a Chi-square test (α=0.05).

RESULTS

Of the original 143 runners who started the study, 69 completed the study. An additional 14 subjects dropped out of the study due to injury and were, therefore, still included in the injury analysis. Of the 83 runners, 69 or 83% sustained an injury during the six month training period. The subjects with high impact forces and loading rates did not have significantly more injuries than the subjects with low impact forces and loading rates (Figs. 1–2).

DISCUSSION AND CONCLUSION

The average injury rate of 83% is higher than previously reported values[1,3] primarily due to the injury definition used. This study does not support the commonly held belief that high impact forces and high impact loading rates are associated with running injuries. In fact there was a trend toward decreased injuries for high impact loading rates. This data corresponds well with previous data from another prospective study[3]. In this study, it was found that subjects with high impact loading rates had a significantly lower number of injuries. Thus, it is concluded that normal impact forces during running are not a major factor in the development of running related injuries. It may be that impact forces instead provide a signal to the human body which is used to tune the vibrations of the muscles of the lower extremities[3].

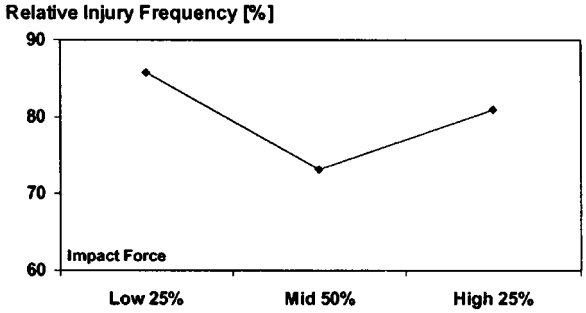

Fig. 1 Injury frequency as a function of impact force.

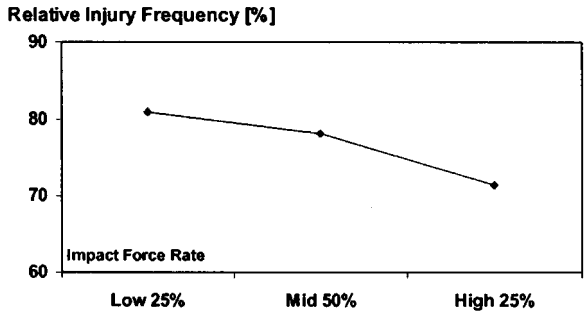

Fig. 2 Injury frequency as a function of impact force rate.

REFERENCES

1–JAMES S. et al. (1978) Am. J. Sport Med. 6:40–50.
2–McLEOD K. et al. (1990) Transactions Orthop. Res. Soc., 103.
3–NIGG B.M. (1997) Cur. Opinion in Orthop. 8:43–47.
4–RADIN E. et al. (1973) J. Biomechanics, 6: 51–57.

GAME ANALYSIS BY GPS SATELLITE TRACKING OF SOCCER PLAYERS

E.M. HENNIG AND R. BRIEHLE
Biomechanik - Labor, Universität Essen, Germany

INTRODUCTION

Soccer game analyses have been performed for many years by various researchers. Primarily, cinematographic or videographic recordings were used to determine distances by various players on the field (Ohashi et al., 1988). Due to the laborious nature of the analysis, single or only few games were evaluated in these studies. Therefore, most of the reported results were typical for a single team– but not necessarily representative data. Determination of the location on the earth by satellite tracking has become worldwide a well established orientation and guiding technique for aviation, on the sea, and to facilitate the navigation of vehicles on land. Modern, miniaturized GPS receivers are now available for determining locations on the earth for hikers. Such systems have been investigated for their suitability in determining distances and velocities during sport movements (Hennig and Sterzing, 1999). The performance and accuracy of GPS and DGPS system in various types of athletic movements was previously reported by these authors.

MATERIAL AND METHODS

70 soccer players were analyzed in 14 different games of different German soccer leagues. Because the soccer rules do not allow instruments being worn during official soccer games, training games (90 minutes duration) were chosen for the recordings. The players from 5 of the games were identified as "professionals" to indicate higher class soccer players (Regional-, Verbands-, Landesliga) and the players from the remaining 9 games were identified as "recreational players" (Bezirks-, Kreis-, Freizeitliga). Five typical player personalities were identified in each team. These players were equipped with the GPS units. For the defense typically a defense organizer (**L**ibero) and one to one **D**efenders are present. The defense organizer (libero) participates in the defense as well as in midfield activities. The left and right **W**ing **P**layers may have defensive as well as offensive tasks. The **P**lay**M**aker is a midfield player, preparing and participating in the attack on the opponents goal. The **F**orward is the goalgetter of the team. A GARMIN 12XL GPS receiver was used for data collection. The unit was worn by the players in a wide elastic waist band. The total weight of the receiver, including batteries, was 250 gram. The performance and accuracy of the Garmin GPS system was previously reported in Hennig and Sterzing (1999). For running and sprinting excellent results of less than 2% of the actually covered distance were measured. For slow motions - such as walking - the GPS measurements may overestimate the actual distances (around 10%). For all movement speeds, DGPS measurement accuracies were reported to be below 1%. However, these devices are yet too bulky and heavy to be carried by soccer players during a game. For each of the 70 soccer players 66 individual variables were calculated from the GPS recordings. Besides the total distance, covered by the various players in 90 minutes, movement velocities were calculated in equal 1m/s velocity intervals from 0 to 10 m/s (I,II,III,IV,V,VI,VII,VIII,IX,X).

RESULTS AND DISCUSSION

The average distance, covered by the 70 players was 10,600 m. This distance measurement compares well with the distances found by other authors for soccer game analyses. The shortest measured distance across the 70 players was 8.480 m and the longest distance 12.750 m during 90 minutes. For the first vs. the second half of the game players covered 4% more distance during the first half. As apparent in Figure 1, the playmaker and wing players cover the longest distances during 90 minutes, followed by forwards, liberos, and defenders.

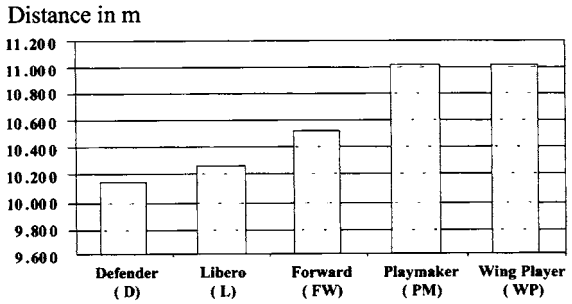

Fig. 1. Covered distances by player position (90 minutes).

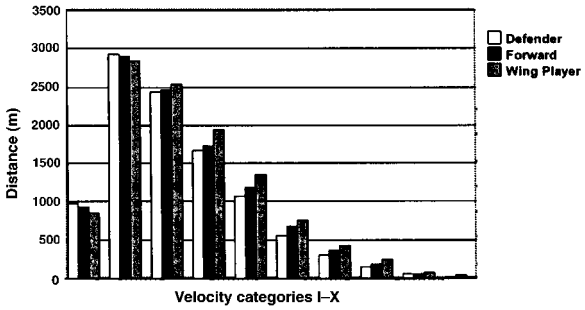

Fig. 2. Velocity profiles of players in different positions.

From all player positions, the wing players move longer distances at higher running speeds (Fig. 2). The professional players covered approximately 600 m more distance than the amateurs. Even more important, the velocity profile of the two groups showed for the professionals a distinct shift to higher velocities. The results from this study suggest that GPS tracking of soccer players provides valuable information about movement distances and velocity profiles of players. This information should be useful for a better understanding of the game and may also have consequences for coaching and footwear design.

This research was supported by a grant from Nike Inc., USA

REFERENCES

Hennig, E. M., Sterzing, T. F. (1999). The use of global positioning systems (GPS and DGPS) for the tracking of human motion. In W. Herzog & A. Jinha (Ed.), XVIIth Congress of the International Society of Biomechanics, (pp. 193). Calgary: Dept. Of Kinesiology, Univ. of Calgary.

Ohashi, J./Togari, H./Isokawa, M./Suzuki, S. (1988) - Measuring movement, speeds and distances covered during soccer match-play. In: Reilly, TH. et al.: Science and Football, London, S. 329–333.

CENTRIPETAL FORCE: MAJOR CHALLENGE IN PERFORMING SPRINGBOARD DIVES OF INCREASING DIFFICULTY

MILLER D.I.

School of Kinesiology, University of Western Ontario, London, Canada

INTRODUCTION

One strategy for being in medal contention in diving is to be able to perform high degree of difficulty (DD) dives with reasonable consistency. For example, Annie Pelletier (Canada) had the most difficult list of dives in the women's 3-m competition at the 1996 Olympic Games. She won bronze even though 8 of the top 10 finalists received higher scores before DD was factored in. If a diver is to adopt this strategy, what are the major factors that must be considered to successfully execute more difficult dives? The purpose of this study was to investigate the roles of vertical velocity, angular momentum and centripetal force associated with increasing the DD of non-twisting springboard dives.

MATERIAL AND METHODS

The flights of tuck (T) and pike (P) dives from the forward, back, reverse and inward groups (N=60) performed by the top four male and the top four female divers in the semifinals and finals of the 1996 Olympic 3-m competition were analysed. The performances had been videotaped using standard data collection procedures for quantitative planar analysis. A Peak5 system was employed to digitise segmental endpoints beginning 2 frames before last contact with the board in the takeoff and continuing at 1 frame intervals (1/30 s) until the diver disappeared from view in the flight phase. Gender specific regression equations were applied to locate segmental and total body centres of gravity (CG) and estimate segment moments of inertia.[1] Angular momentum (H_G) was calculated by summing local and remote body segment contributions. The diver's angular velocity (ω) while in a quasi-rigid position near mid flight of dives involving 2½ and 3½ revolutions was recorded. Total body moment of inertia with respect to the CG (I_G) and radius of gyration (k_G) were estimated from ω, H_G and mass (m). Maximum centripetal force ($Fc_{max} = m\ k_G\ \omega^2$) was expressed in terms of body weights (BW). H_G was normalised by dividing by mass $\times$ height^{2}and multiplying by 100.

RESULTS

As expected, vertical velocity of the diver's CG at the start of flight decreased as more somersaults were performed in a given position within a specific dive group[2]. However, it increased slightly between a 1½P and a 2½T and between a 2½P and a 3½T. The latter were associated with an increase of 1–2 normalised H_G units compared with an average of 8 more normalised H_G units for each additional forward and inward somersault pike and 11 more for each back and reverse somersault pike. In contrast to the small increase in vertical velocity and angular momentum between a 2½P and a 3½T was the requirement for more than 2 additional BWs (or Gs) of centripetal force. These relationships are illustrated in Table 1.

Table 1. Vertical velocity (m/s), ω (rad/s), normalised HG and Fc_{max} (BW) for high DD reverse and inward dives performed by 1996 Olympic male medallists.

	Rev 2½P DD 3.0		Rev 3½T DD 3.5		Inw 2½P DD 3.0		Inw 3½T DD 3.4	
	VV	ω	VV	ω	VV	ω	VV	ω
M1	5.5	***13.8***			4.3	***14.7***	4.4	***18.6***
M2	5.7	***15.5***	6.0	***19.8***			4.6	***19.0***
M3	5.7	***14.1***	6.0	***17.9***	4.5	***13.1***		
	H_G	*Fc*	***H_G***	*Fc*	***H_G***	*Fc*	***H_G***	***Fc***
M1	29	***4.7***			24	***4.7***	26	***6.8***
M2	29	***5.5***	31	***8.1***			26	***7.0***
M3	30	***4.7***	31	***6.9***	24	***3.9***		

DISCUSSION AND CONCLUSION

Fc_{max} values apply only briefly while the diver is acting as a quasi-rigid body and therefore do not have to be maintained throughout the entire flight. Unlike a pilot pulling out of an aircraft dive, blood is forced toward rather than away from the brain in competitive diving. Fc_{max} magnitudes, however, raise the question of the muscular strength required to pull into and maintain a tight pike or tuck. The ability to generate adequate levels of centripetal force appears to be a key challenge that must be met by divers attempting to gain a half point in DD by moving from a 2½ pike to a 3½ tuck. Aleshinsky[3] also alluded to the important role of centripetal force in executing multiple revolution jumps in figure skating.

ACKNOWLEDGEMENTS: This study was supported by US Diving, the IOC Medical Commission and the USOC.

REFERENCES

1–DE LEVA P. (1996)- *J. Biomech.* 29, 1223–1230.

2–SANDERS R.H. and WILSON B.D. *Int, J. Sport Biomech. 4*, 231–259.

3–ALESHINSKY S. (1990)-*Am. Skating World* (Aug.) 12–13, 21.

EFFECT OF HELMET GEOMETRY AND MATERIAL PROPERTIES ON IMPACT ATTENUATION OF ICE HOCKEY HELMETS

SPYROU E[1], PEARSALL DJ[1] AND HOSHIZAKI TB[2]
[1]Department of Physical Education, McGill University, Montréal, Canada; [2]Department of Human Kinetics, University of Windsor, Windsor, Canada.

INTRODUCTION

The ultimate goal of helmets in sport has been to reduce the risk of head injury by reducing energy transfer on impact. However, predicting impact absorption characteristics of helmets has proven to be difficult given the numerous material and geometric factors and their interactions[1]. The purpose of this study was to investigate the effect of geometric profile features (i.e. side inclination angle and top surface width), inner liner characteristics (i.e. liner type and density) and environmental conditions (i.e. energy of impact and multiple impacts) on the impact attenuating characteristics of the ice hockey helmet shell materials. To avoid confounding factors resulting from whole helmet testing[2,3] flat sectional samples representing typical ice hockey helmet materials and geometric profiles were evaluated.

METHODS

Samples consisted of a 2.5 mm thick shell with one of nine geometric formations (width & angle; Table 1), and a 12.5 mm thick liner (Vinyl Nitrile (VN) or Expanded Polypropylene (EPP) foams). The liners had two density levels: 80 and 96 kg/m^3. Each sample was impacted three times at three different levels of energy using a monorail drop test. (Table 1). Peak acceleration of the impactor was measured with a uniaxial accelerometer (2221 D, Endevco™). The transducer was capable of withstanding a shock of 1000 g_z and had a frequency response from 0 to 1000 Hz with a $\pm$ 1.5% variation.

DISCUSSION

The results revealed that shell geometry substantially affects the impact attenuation response, producing variations in performance ranging between 4 and 35%. Significant differences ($p < 0.05$) were observed for all main effects and two-way interactions for both liner types. The two geometric parameters appeared to modify the elasticity of the shell covering the liner, as similarly noted previously by Bishop[1,4]. Specifically, α was found to modulate the bending of the formation about its transverse axis while **w** was seen to modulate the bending occurring along the longitudinal axis of the formation. Hence, the two geometric parameters acted perpendicular to each other. In general, for all three trials and both liners, the 90°:16 mm geometry proved to be the best performance combination.

Further study of protective equipment design variables (e.g. height, shell thickness, and other geometric shapes) can aid complex design problems. An extension of this study would be incorporating samples to mimic the natural curvature of the actual helmet, to demonstrate the effect of helmet geometry in situ on impact attenuation.

Table 1. Summary of variables.

Indep. Variables	Dependent Variables Liner Foam Types	
	EPP	VN
Angle:α (º)	30, 60, 90	30, 60, 90
Width: **w** (mm)	8, 16, 24	8, 16, 24
Density(kg*m^{-3})	80, 96	80, 96
Impact energy (J)	30, 40, 50	15, 20, 25
Impact trials	3 per sample	3 per sample

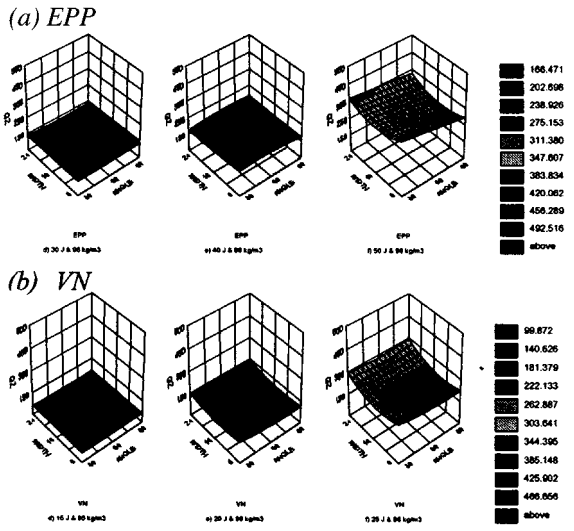

Fig. 1. Surface plots (quadratic estimate) for (a) EPP and (b) VN (96 kgm^{-3}). G_{max} versus a (30, 60, 90 degrees) and w (8, 16, 24 mm) of second trials. Note interaction of geometric variables with impact energy.

REFERENCES

1–Bishop PJ (1977) *J Safety Research. 9*, 159–167.
2–Newman JA (1993) *Accidental Injury: biomechanics and prevention.* (eds. Nahum & Melvin) 292–310.
3–Norman RW (1983) *Ex Sp Sci Rev 11*, 232–274.
4–Bishop PJ (1976) *Biomechanics V-B*, 299–305.

JOINT STIFFNESS DURING RUNNING WITH DIFFERENT FOOTFALL PATTERNS

HAMILL, J.[1], DERRICK, T.R.[2], AND MCCLAY, I.[3]
[1]Department of Exercise Science, University of Massachusetts; [2]Department of Health & Human Performance, Iowa State University; [3]Department of Physical Therapy, University of Delaware

INTRODUCTION

The stiffness of the lower extremity of humans and animals has often been approximated using the spring constant from a mass-spring model[1]. The stiffness value, however, is a linear combination of all structures that contribute to the compliance of the lower extremity. The actions of the ankle and knee joints are a major source of the compliance of the lower extremity during running. However, only the contribution of the ankle[2] to the stiffness of the lower extremity has been documented. In running there are different footfall patterns in which the ankle and knee joints may contribute differentially to the lower extremity stiffness. Stefanyshyn and Nigg[2] modeled the ankle as a torsion spring and reported differences in ankle stiffness during distance (heel toe pattern) and sprint (forefoot pattern) running. The purpose of this study was, therefore, to examine the joint stiffness of the ankle and the knee during running with different footfall patterns.

MATERIAL AND METHODS

Five young, healthy males served as subjects in this study. All subjects were free of injury prior to participation. Each subject was an active runner although only three could be considered skilled distance runners. The subjects all wore the same model of running footwear. Reflective markers were placed on anatomical landmarks for the purpose of defining the lower extremity joints. Each subject completed 5 trials at a locomotor speed of 3.5 m/s ($\pm$5%) in each of two running conditions: 1) heel toe footfall pattern (HS); and 2) forefoot footfall pattern (FF).

The experimental set-up consisted of five high-speed digital cameras operating at 200 Hz and an AMTI force platform operating at 1000 Hz. Running speed was monitored using a photoelectric cells placed 5 m apart.

Three-dimensional kinematic data of the reflective markers were obtained. However, since the primary motion was felt to be the flexion-extension actions of the joints, data analysis was limited only to the sagittal plane. Inertial parameters were determined using regression equations[3]. Joint moments were calculated using an inverse dynamics approach.

Leg stiffness (K_{leg}) was evaluated using the formula from McMahon and Cheng[4]. Stiffness for the ankle and knee joints was determined during both the shock absorbing and propelling phases of the support period by linearly fitting the respective slopes of the torque-angle profile. This calculation does not truly represent mechanical stiffness but can be considered a "quasi-stiffness"[5].

Since the sample size was well below that which would reveal statistically meaningful results, only mean values and trends in the data will be discussed.

RESULTS

The mean values and standard deviations of all computed stiffness values are presented in Table 1.

Table 1. Stiffness values (mean $\pm$ standard deviation).

		HT	FF
Leg[A]	K_{leg}	15.97 (2.51)	23.07 (5.52)
Ankle[B]	$K_{absorption}$	18.81 (2.86)	14.43 (3.99)
	$K_{propulsion}$	9.45 (1.64)	13.26 (3.54)
Knee[B]	$K_{absorption}$	17.93 (5.38)	22.47 (4.72)
	$K_{propulsion}$	13.24 (2.87)	12.15 (1.59)

A: kN/m; B: N.m/degree.

DISCUSSION AND CONCLUSIONS

During running, leg stiffness is greater when using a FF footfall pattern rather than a HT footfall pattern. However, these stiffness values do not truly reflect what is occurring in the joint actions during the shock absorbing phase and the propulsion phase of the support period.

It has been suggested that, based on the mass-spring model, the ankle joint is the dominant joint during locomotion[6]. During the shock absorbing period, this appears to be true only when using a FF footfall pattern. The ankle joint is certainly more compliant during FF running and less compliant during HT running. On the other hand, the knee joint stiffness exhibits the reverse pattern. That is, it is stiffer in the FF pattern and more compliant during the HT pattern. Both of these findings can be verified by evaluating the negative work done by each joint. A more compliant joint results in greater negative work done (i.e. shock absorption). Thus when the ankle is more compliant (FF), it is primarily responsible for shock absorption. In HT, the knee joint exhibits the greatest negative work done (i.e. more compliant) and thus is the primary shock absorber.

During the propulsion phase of the support period, the stiffness values for the ankle increased from the HT pattern to the FF pattern. The knee stiffness values remained basically the same.

These data lend support to the notion that an overall value of the leg stiffness, while giving some information on the action of the lower extremity, may not give a sufficient explanation to evaluate the inter-relationships of joint actions.

REFERENCES

1–Greene, P.R., McMahon, T.A. (1993) *J Biomechanics* 12:881–891.
2–Stefanyshyn, D.J., Nigg, B.M. (1998) *J Applied Biomechanics* 14:292–299.
3–Zatsiorsky, V.M., Seluyanov, V. (1983) *Biomechanics VIII-B*, pp. 1152–1159.
4–McMahon, T.A., Cheng, G.C. (1990) *J Biomechanics* 23:65–78.
5–Latash, M.L., Zatsiorsky, V.M. (1993) *Human Movement Science* 12:653–692.
6–Farley, C.T., Morgenroth, D.C. (1999) *J Biomechanics* 32:267–273.

COUPLES ARTICULAIRES SIGNIFICATIFS DES MOUVEMENTS DES MEMBRES INFÉRIEURS CHEZ LE RAMEUR

PUDLO P, BARBIER F, LEPOUTRE FX AND ANGUE JC
LAMIH UMR CNRS 8530, Université de Valenciennes et du Hainaut-Cambrésis, France

INTRODUCTION

L'évaluation du geste du rameur intègre souvent des données cinématiques (ex: le mouvement du rameur) et/ou dynamiques (ex: les forces développées par le rameur), qui sont une conséquence des actions musculaires. Les données utilisées sont alors des manifestations externes d'actions internes. La démarche retenue, afin d'approcher de telles actions internes, va reposer sur la quantification des couples articulaires, données calculées inobservables. Les couples articulaires au niveau des articulations du membre inférieur ont ainsi été calculés. Ce papier présente et décrit les premiers résultats obtenus.

MATÉRIEL ET MÉTHODE

Le dispositif expérimental est formé d'un ergomètre Concept II Modèle C et du système opto-électronique SAGA-3 muni de 4 caméras CCD 50Hz. Deux nouvelles barres de pieds indépendantes de l'ergomètre sont fixées à 2 plates formes de force 6 axes. Les capteurs mesurent les forces et les moments résultants selon les 3 directions de leur repère local. Le membre inférieur est modélisé en 3 dimensions. Les corps sont supposés rigides et articulés par des rotules sans frottement. Les caractéristiques inertielles et anthropométriques dérivent respectivement d'Hanavan[1] et de Dempster[2]. Le calcul des efforts articulaires est basé sur les principes de Newton-Euler. Le couple Cx, dit couple significatif du mouvement, pour chaque articulation du membre inférieur est défini en Figure 1. L'expérimentation a été menée sur un rameur de niveau régional pour une cadence de 14 coups par minute.

RÉSULTATS

La présentation se limite au couple articulaire Cx de la cheville pour la phase de propulsion. L'angle est l'angle que fait le pied avec la jambe (Fig. 2). La Figure 3 présente les variables Cx et pour la phase de propulsion.

DISCUSSION ET CONCLUSION

En début de propulsion Cx est négatif (Fig. 3). L'action de la jambe tend à étendre le pied. L'appui se faisant au début en bout de pied, l'angle n'augmente que faiblement (Fig. 3). En effet, d'une part l'angle diminue car le talon se rapproche de la barre de pied et d'autre part l'angle augmente à cause de l'extension du membre inférieur. L'action est motrice. Rapidement cependant le talon vient "heurter " la barre de pied. Cx devient positif et tend vers son maximum. L'action de la jambe tend à fléchir le pied. L'angle augmentant rapidement, l'action est résistante.

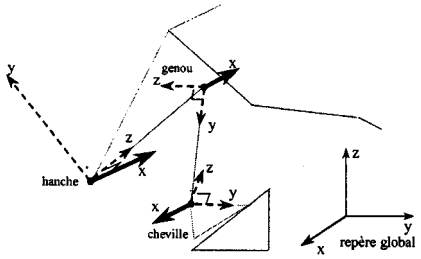

Fig. 1. Définition du couple Cx pour les articulations du membre inférieur.

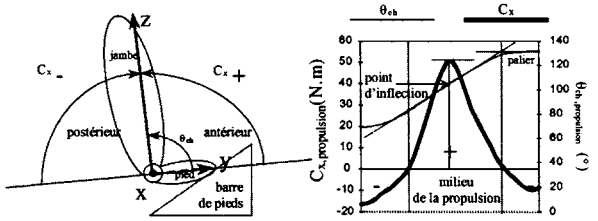

Fig. 2. *(left)* Description du couple Cx et de l'angle θ_{ch}.
Fig. 3. *(right)* Cx et θ_{ch}durant la propulsion.

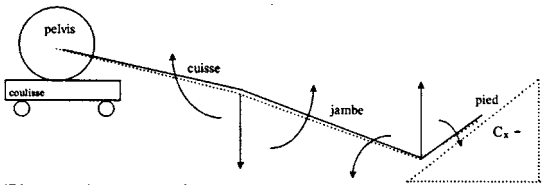

Fig. 4. Contribution du pied au verrouillage du genou.

Alors Cx positif décroît. L'action de la jambe tend toujours à fléchir le pied. L'angle augmente toujours (Fig. 3, le point d'inflexion de). La poussée se déplace alors peu à peu en bout de pied avec l'extension du membre inférieur. Enfin Cx est à nouveau négatif. L'action de la jambe tend à étendre la cheville. L'angle est maximal, l'action contribue au verrouillage du genou (Fig. 4).

Les couples articulaires significatifs ont permis d'expliquer les principaux mouvements observés pour le membre inférieur. Leur analyse apparaît donc comme une première étape pour mieux comprendre l'élaboration du geste du rameur et ainsi mieux appréhender les synergies musculaires.

RÉFÉRENCES

1–Dempster W.T., (1955), Space requirement of the seated operator, Wright Patterson Air Force Base, WASC-TR, 55–159.
2–Hanavan I.A., (1964), A mathematical model of the human body, AMRL-TR, 64–102, Aero Medical Research Laboratories, Wright Patterson, AF Base OHIO.

HISTORY DEPENDENCE OF FORCE PRODUCTION IN CAT SOLEUS

HAE-DONG LEE AND WALTER HERZOG
Human Performance Lab, Faculty of Kinesiology, University of Calgary, Canada

INTRODUCTION

Force depression following muscle shortening and force enhancement following muscle stretch have been well recognised and accepted phenomena in muscle mechanics. However, the exact mechanisms underlying these phenomena are not known [0, 0, 0, 0]. One possible way to gain insight into these mechanisms may be by studying force depression and force enhancement following stretch-shortening and shortening-stretch cycles. For example, it would be of interest to know whether stretch preceding shortening influences force depression; and whether shortening preceding stretch influences force enhancement, and if so, what relationship there may exist between the amount and speed of stretch (shortening) on the corresponding change in force.

The purpose of this study was to systematically study the effects of the amount and speed of stretch preceding shortening on force depression, and the effects of the amount and speed of shortening preceding stretch on force enhancement.

METHODS

Cat soleus muscles (n = 6) were used. The muscle contractions were achieved by electrical stimulation of the soleus nerve. The surgical implantation of nerve cuffs and experimental set up have been described elsewhere [0].

The protocols used to test the effects of the amount and speed of shortening preceding stretch on force enhancement were;

Test 1a: The muscles underwent a shortening-stretch cycle. All stretch phases were 4mm at a constant speed of 4mm/s. Shortening preceding the stretch occurred at a speed of 4mm/s and the amount of shortening varied from 2–8mm in 2mm increments (from 4, 2, 0, and –2mm to –4mm; Fig. 1).

Test 1b: The muscles underwent a shortening-stretch cycle as above (constant stretch of 4mm at 4mm/s), but the shortening preceding the stretch occurred at speeds of 4, 16, and 64mm/s over a constant amount of 4mm.

The protocols used to test the effects of the amount and speed of stretch preceding shortening on force depression were;

Test 2a: The muscles underwent a stretch-shortening cycle. All shortening phases were 4 mm at a constant speed of 4mm/s. Stretch preceding the shortening occurred at a speed of 4mm/s and the amount of stretch varied from 2–8mm in 2mm increments.

Test 2b: The muscles underwent a stretch-shortening cycle as above (constant shortening of 4mm at 4mm/s), but the stretch preceding the shortening occurred at speeds of 4, 16, and 64mm/s over a constant amount of 4mm.

RESULTS

Muscle shortening preceding stretch was found to influence force enhancement. The amount of force enhancement was systematically decreased with increasing amounts of shortening preceding the stretch (Fig. 1), whereas the speed of shortening preceding the stretch showed no effect on the amount of force enhancement.

The amount and speed of stretch preceding shortening had no effect on force depression.

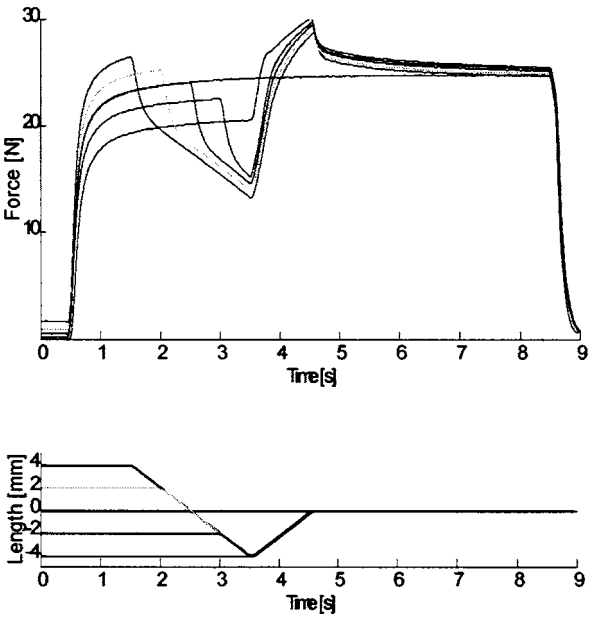

Fig. 1. Representative data of force-time histories for shortening-stretch contractions with different amounts of shortening preceding the constant stretch (Test 1a).

DISCUSSION AND CONCLUSIONS

The amount of shortening preceding stretch influences force enhancement in a dose-dependent manner. It appears that if the net length change in a shortening-stretch cycle is shortening (i.e. shortening > stretch), force is depressed compared to the corresponding isometric force at the same length. If the net length change is elongation (i.e. shortening < stretch), force is enhanced; and if there is no net length change (i.e. shortening = stretch), force appears to be about the same as the corresponding isometric force. The results of this study suggest that the mechanisms underlying force depression following muscle shortening are likely independent of the contractile history of the muscle, whereas the mechanisms underlying force enhancement following stretch depend specifically on the history of contraction, specifically the amount of shortening, a muscle undergoes before stretch.

ACKNOWLEDGEMENT: NSERC of Canada.

REFERENCES

1–Edman, K.P.A. et al. (1993) *J. Physiol*. 466–535–552.
2–Granzier, H.L.M. and Pollack, G.H. (1989) *J. Physiol*. 415, 299–327.
3–Herzog, W. & Leonard, T.R. (1997) *J. Biomech*. 30, 865–872.
4–Herzog, W. & Leonard, T.R. (1998) *J. Biomech*. 31, 1163–1168.
5–Maréchal, G. and Plaghki, L. (1979) *J. Gen. Physiol*. 73, 453–467.

THE EFFECT OF THE NUMBER OF STIMULI AND THE TIMING OF TWITCH APPLICATION ON THE VARIABILITY IN INTERPOLATED TWITCH TORQUE

SUTER ESTHER, HERZOG WALTER, WIMMER USCHI
Faculty of Kinesiology, The University of Calgary, Canada

INTRODUCTION

Superimposing an electrical twitch on a contracted muscle has been used to assess activation of various muscle groups (1,2). The interpolated twitch torque (ITT) decreases as muscle activation increases. Some variability in the ITT has been found for identical twitch stimulation and similar muscle force levels. It was hypothesized that the variability in ITT is related to the timing of the twitch application with relation to the firing sequence of the motor units. Furthermore, by increasing the number of applied twitches, the variability in ITT was speculated to be decreased.

MATERIAL AND METHODS

Experiment 1: The influence of timing of twitch application on the ITT amplitude was tested by applying electrical stimulation trains with a superimposed single twitch to the triceps surae muscle. The subject's left foot was fixed in 10° dorsi flexion on a strain gauged foot plate. Stimulation trains of 1200ms and pulse width of 0.8ms were applied at frequencies of 4, 8, 12, 16, 20, 35 and 50 Hz and two different voltages to simulate a range of motor unit firing conditions. Approximately 800ms into the train, a single supramaximal twitch of 0.8ms was superimposed. The timing of the superimposed twitch was systematically varied and occurred A) 5ms after a train stimulus; C) in the middle of two train stimuli, and E) 5ms before a train stimulus. For trials B and D, the superimposed twitches were placed in the middle of A and C, and C and E, respectively. The ITT evoked by the single twitch was calculated as the difference between the highest torque amplitude within 200ms of twitch application and the torque immediately before twitch application. ITTs for different conditions were compared using repeated measures ANOVA.

Experiment 2: To assess the effect of number of the twitches applied on the variability of the ITT, twelve subjects performed isometric knee extensor contractions at 50% MVC. During the force plateau, square wave pulses of 240V and 0.8ms duration were applied either as single twitches, doublets, triplets or quadruplets. Inter pulse intervals for the multiple twitches were 8ms. Five trials were performed for each condition in a random order. The ITT was normalized to a twitch applied to the resting muscle (RTT). Muscle activation (MA) was calculated as (1-ITT/RTT). Mean MA and variability (SD) in MA were calculated for each condition and subject. Differences in MA and SD between conditions were calculated using ANOVA.

RESULTS

Experiment 1: Trial E (i.e. single pulse superimposed 5ms before train pulse) produced consistently higher ITTs for all stimulation frequencies and both voltages used while the ITTs of the other four conditions did not differ from each other (Fig. 1).

Experiment 2: Table 1 shows the mean MA and SD for each condition. There was a significant effect of number of twitches on MA ($F=30.1$ $p<0.001$) and SD ($F=7.3$, $p=0.02$). The ITT was lowest for the single twitch condition, which resulted in the highest MA. ITT increased significantly and MA decreased as the number of twitches increased. The variability in MA was highest for the single twitch and decreased for the multiple twitch conditions. The differences in MA and SD were significant for single twitch vs. triple and quadruple twitches.

Table 1. Mean values and variability (SD) in muscle activation (MA) for the four different stimulation conditions.

Condition	Count	MA (%)	SD (%)
Single	12	60.7	4.3
Double	12	50.3	3.1
Triple	12	45.9	3.0

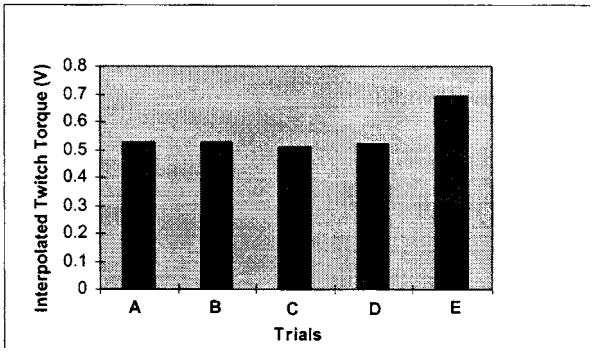

Fig. 1. Interpolated twitch torque in Volts (V) for the five different timing conditions.

DISCUSSION AND CONCLUSIONS

The present study was aimed at exploring timing of twitch application as a possible source of the variability in ITT observed during constant muscle activation and stimulating conditions. We found that a stimulus applied immediately before a subsequent train pulse resulted in higher ITT amplitudes compared to all other conditions. It is speculated that the single twitch, which is stronger than the train twitch, caused potentiation of the subsequent train twitches. This finding confirmed that the time point of twitch application in relation to the firing sequence of the motor units is crucial with respect to the resulting twitch response. The variability in ITT was significantly reduced when a quadruple twitch was applied instead of a single twitch. By applying multiple twitches to a contracted muscle, the probability of evoking a maximal, potentiated twitch response from an individual motor unit is increased and as a result, the total ITT will be more consistent and closer to the theoretical maximum.

In summary, our results supported the idea that part of the variability in the ITT is related to the timing of the twitch application with respect to the firing of the motor units. Using multiple twitches instead of a single twitch may significantly reduce the variability in the ITT. The observation that multiple twitches evoke a more consistent ITT is new and has important practical implications.

REFERENCES

1–Belanger et al. 1981 *J Appl Physiol, 51*:1131–1135.
2–Allen et al., 1998, *Muscle & Nerve, 21*:318–328.

LONG-TERM H-REFLEX ADAPTATION UNDERLYING MOTOR SKILL ACQUISITION

SCHNEIDER C., MERCIER I. AND CAPADAY C.
Centre de Recherche Université Laval-Robert Giffard, Québec (QC), Canada.

INTRODUCTION

In naïve subjects walking backwards, the Soleus (SOL) H-reflex reaches nearly the same amplitude during the swing phase as during the stance phase[1]. This is a surprising result since during the swing phase of backward walking the SOL is silent, as it is during forward walking. But, in the swing phase of normal walking, the H-reflex is shut-off [1]. Backward walking on a treadmill is a novel and unusual motor task for naïve subjects. Would daily training at this task modify the H-reflex modulation pattern?

MATERIAL AND METHODS

Eight subjects walked backwards on a treadmill for 15 min. daily, excluding weekends. They were tested every 3 days throughout a backward training program. The electromyographic activity (EMG) of the SOL (ankle plantar flexor) and Tibialis anterior (TA, ankle dorsiflexor) were recorded. Electrogoniometric recordings at the hip, knee and ankle joints allowed to acquire the time course of the leg angles. To determine the modulation pattern of the SOL H-reflex during the backward cycle, H-reflexes were elicited in 50 ms increments starting from toe contact (pressure activated switch). Four H-reflexes were averaged per increment. Only one electrical stimulus was delivered per step to the tibial nerve and the inter-stimulus interval varied from one to three steps. The stimulation intensity was monitored by a time-amplitude window discriminator.

RESULTS

1–SOL and TA EMG patterns and electrogoniometric traces of the three joints during backward walking were similar to those described in the literature[2,3].

2–The SOL H-reflex modulation pattern became more reciprocal with time of training (see following figure). In naïve subjects (Day 1), the H-reflex amplitude in the swing phase was higher than during the stance phase. Within 10 days of training, the reflex modulation pattern was adapted to the motor pattern: the SOL H-reflex was extinct when the SOL was silent, as shown in forward walking[1]. Note the phase shift of the H-reflex increase during swing, without any significant change of the walking EMG pattern. Neither was modified the angular course of the whole lower limb.

3–The H-reflex adaptation was not due to persistent changes in the spinal cord circuits. Indeed, the Hmax/Mmax ratio measured during quiet standing (control) is not modified, in any significant respect, over the course of the adaptation process.

4–The H-reflex adaptation remarkably persisted during at least the 6 months following the training program.

DISCUSSION AND CONCLUSION

In naïve subjects, increase of the H-reflex in the late swing phase of backward walking may reflect behavioural uncertainties in estimating moment of toe contact and maintaining balance within a relative postural instability. Adaptation is not due to peripheral changes as EMGs and kinematics profiles remained unaltered. Our working hypothesis is that the H-reflex reflects adaptive changes in the motor commands, rather than persistent changes in the reflex circuits, as it has been reported for the primate H-reflex[4] and for the vestibulo-ocular reflex[5]. One may hypothesize, for example, that the corticospinal tract may be more active during the backward swing phase for naïve subjects acting in new biomechanical constraints. This adaptive phenomenon may prove to be a useful model for studying the neural mechanisms of motor learning and adaptation in man.

REFERENCES

1–SCHNEIDER C. et al. (2000). *J. Neurophysiol*. (in press).
2–THORSTENSSON A. (1986). *Exp. Brain Res. 61*:664–668.
3–WINTER D.A. et al. (1989). *J. Mot. Behav. 21*:291–305.
4–WOLPAW J.R. (1997). *TINS 13*:137–142.
5–LISBERGER S.G. (1998). *Cell 92*:701–704.

EMG SPASMS ASSOCIATED WITH SUPRASPINOUS LIGAMENT STRAIN DURING STATIC LUMBAR FLEXION

SOLOMONOW, M., WILLIAMS, M., ZHOU, B., BARATTA, R.V. AND HARRIS, M.

Bioengineering Laboratory, Louisiana State University Health Sciences Center, New Orleans, Louisiana, USA

INTRODUCTION

It is well known that certain types of Low Back Pain/Disorders (LBP/D) are associated with spasms of the paraspinal muscles. It is thought that muscle overuse during intense occupational activities are responsible for the spasms and associated pain. One such high risk activity is static flexion performed by individuals such as roofers, brick layers, mechanics, etc.

We hypothesize, however, that prolonged static flexion results in creep or excessive strain in the spinal ligaments and discs and that such creep/strain excite the afferents[1,2] within the above viscoelastic tissues. The afferents, including nociceptors, reflexively excite the paraspinal muscles, inducing spasms and possibly pain due to sub-acute injury to the tissue, even without muscle overuse.

METHODS

Six cats were anaesthetized, and the skin over the lumbar spine resected. Fine wire EMG electrodes pairs were inserted into the lumbar multifidus muscles. A hook was inserted around the L-4/5 supraspinous ligament and connected to an MTS 858 unit operating in a displacement mode. The MTS unit was programed to stretch the ligament in its physiological elongation range, and maintain it for 50 minutes while recording EMG from six lumbar levels (a cat has seven lumbar vertebrae), as well as the displacement force. Ligament length subjected to 0.5N load was measured before and at several times after the 50 minutes test.

RESULTS

The force recorded from the ligament exhibited tension-relaxation immediately after the application of the displacement. The tension-relaxation displayed an exponential decrease of force with asymptotic trajectory reaching 41% of the initial force at the end of the 50 minutes. EMG recording also displayed initial discharge that decreased exponentially, in parallel to the tension-relaxation, decaying to 5% of its original peak to peak amplitude in 5–6 minutes. Large, random and unpredictable EMG spasms were recorded thereafter, throughout the remainder of the 50 minutes. The spasms appeared on and off in a given lumbar level, as well as different levels. Spasms were also visible in the spinalis and longissimus muscles, and lasted even after the removal of the displacement applied to the L-4/5 supraspinous ligament.

A mean residual strain of 8.9% ($\pm$ 1.78) was recorded after the 50 minutes test. The residual strain did not fully recover even after three hours of rest.

DISCUSSION

In this paradigm, a passive anterior flexion was applied to the lumbar spine while elongating the supraspinous ligament. EMG spasms, some with amplitude 7–10 times larger than the initial reflexive EMG recorded from the same muscle appeared and persisted after 6–7 minutes of flexion with complete absence of voluntary activation or work of the muscles (the feline was anaesthetized).

The residual strain in the ligament indicates that a possible sub-acute damage was present in the tissue, which may have excited the muscles reflexively by the nociceptive afferents.

Complete rest showed partial exponential recovery of the tension-relaxation in the ligament similar to that described by McGill and Brown.[3] A complete recovery did not occur in three hours. The residual strain also recovered partially (45%). Short stretch tests (5 sec.) of the supraspinous ligament during the three hours of rest show initial reflexive hyperexcitability of the multifidus muscle in the first hour, followed by an exponential recovery thereafter.

A bi-exponential model fitted to the tension-relaxation and EMG shows that even after 24 hours of rest a full recovery of ligament and muscular function is not possible.[4, 5, 6]

CONCLUSIONS

The results of this study demonstrate that tension-relaxation or creep in the lumbar viscoelastic structures developed by passive prolonged static loading can induce spasms and possibly also pain, even without muscle overuse.

The results also support that long periods of rest are required to allow creep/tension-relaxation to recover before physiologically normal functions are restored.

It is shown that sub-acute, sprain like injury to the ligaments can elicit spinal disorders. Such sub-acute injuries are not possible to diagnose with conventional protocols. The results also support that rest is a valid treatment of such LBD.

REFERENCES

1–Rhalami, W., Yahia, H., Newman, N. and Isler. *Spine*, 18:264–267, 1993.
2–Jackson, H., Winklemann, R. and Bickel, W. *JBJS*, 48A:1272–1281, 1966.
3–McGill, S. and Brown, S. *Clin. Biomechanics*, 7:43–46, 1992.
4–Solomonow, M. et al. *Spine*, 24:2426–2434, 1999.
5–Gedalia, U. et al. *Spine*, 24:2461–2467, 1999.
6–Solomonow, M. et al. *Clin. Biomech*. (In press).

FORCE TRANSMISSION IN UNIPENNATE SKELETAL MUSCLE

W. HERZOG, T.R. LEONARD, A. STANO
Human Performance Lab, Faculty of Kinesiology, The University of Calgary, Calgary, Alberta, Canada

INTRODUCTION

It is universally accepted that force production in a single, isolated fibre from skeletal muscle occurs along its long axis. There is no reason to believe that this situation should be different for a fibre inside a muscle. Therefore, it has typically been assumed that the resultant force in a muscle is in the fibre direction. For unipennate muscle, this assumption implies that force transmitted to the aponeuroses and tendon of the muscle (i.e. what people refer to as the muscle force, Fm) corresponds to the projection of the fibre force, Ff, onto the aponeuroses; i.e. Fm=Ff cos(?), where ? is the angle of pinnation. However, if this was the case, aponeuroses of a unipennate muscle should approach during contraction, and for reasons of volume preservation, the muscle should expand in the direction perpendicular to the fibre plane. However, such muscle force deformation has never been observed. Based on theoretical considerations (Epstein and Herzog, 1998), we hypothesized that the resultant force of a muscle should not be along the fibre direction but should be along the collagen fibril direction in the aponeuroses. The purpose of this study was to test the above hypothesis by measuring the three-dimensional force of a unipennate muscle acting along its aponeuroses.

METHODS

Cat medial gastrocnemius, MG, muscles (n=10) were used for these experiments. The muscles were isolated and prepared for tendon force measurements as described before (Herzog and Leonard, 1997). In addition, two metal plates were glued to the medial and lateral aponeuroses of this unipennate muscle. The lateral aponeuroses plate was attached to a three-dimensional force measurement device for recording of the resultant forces acting on MG for isometric contractions at five different lengths and three different deformation states, representing the entire physiological range of MG.

RESULTS

The three-dimensional forces measured on the lateral aponeurosis of cat MG were, on average, in the fibre plane and along the collagen fibril direction of the aponeurosis (Fig. 1). This result

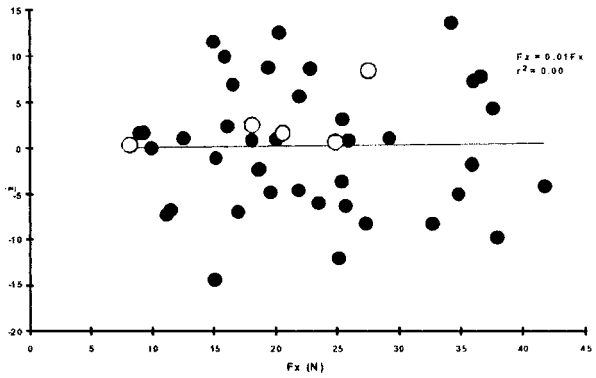

Fig. 1. Scatter diagram of the forces in the fibre plane acting on the lateral aponeurosis of cat MG. The x-axis is along the aponeurosis.

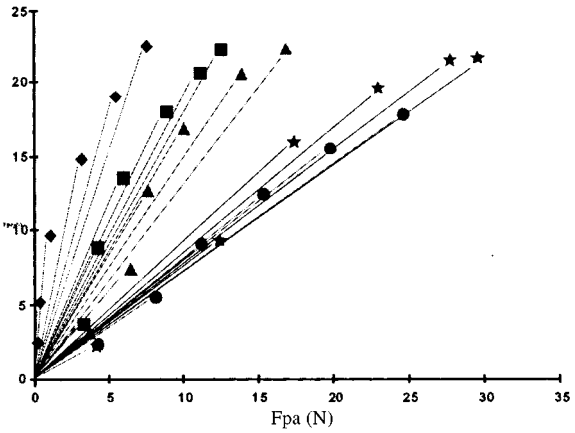

Fig. 2. Forces perpendicular (Fpe) and parallel (Fpa) to the fibre direction at five muscle lengths and for six distinct force levels of each length.

was observed independent of the magnitude of muscle force (Fig. 2), muscle length, and deformation state (not shown).

DISCUSSION

Most theoretical research on muscle contraction suggests that muscle forces act along the fibre direction. As a consequence, it has been assumed that muscle and fibre force are related by Fm = Ff cos(). However, the results of this study suggest that this relationship does not hold. When investigating where this misconception had originated, it became obvious that in most theoretical derivations of whole muscle force, the force constraints associated with kinematic constraints, such as volume preservation, were not considered properly. Although researchers claimed to have considered these constraint forces (Otten, 1988; Woittiez et al. 1984), they did so by using a free body diagramme approach, an approach that almost certainly must lead to failure because of the non-intuitive nature of the constraint forces. We have demonstrated here experimentally, and elsewhere theoretically, using a virtual work approach (Epstein and Herzog, 1998), that the resultant forces in unipennate skeletal muscle have been misinterpreted for a long time.

ACKNOWLEDGEMENTS: NSERC of Canada

REFERENCES

1–Epstein M., Herzog W. (1998) Theoretical Models of Skeletal Muscle:Biological and Mathematical Considerations. John Wiley and Sons, New York.
2–Herzog, W. and Leonard, T.R. (1997) *J. Biomech. 30*:865–872.
3–Otten, E. (1998) *Exer. And Sport Sci. Rev. 16*:89–137.
4–Woittiez et al. (1984) *J. Morphol. 182*:95–113.

MUSCLE FATIGUE DURING CONCENTRIC AND ECCENTRIC CONTRACTIONS

PASQUET B., CARPENTIER A. AND DUCHATEAU J.
Laboratory of Biology and Research Unit in Neurophysiology, Université Libre de Bruxelles, Belgium

INTRODUCTION

Fatigue is a common feature in everyday activities and the factors influencing its deleterious effects are diverse and task-dependent. Therefore, the extent to which the impairment of each possible site, ranging from the central nervous system command to the actin-myosin interactions, might contribute to fatigue during concentric (shortening) and eccentric (lengthening) contractions is largely unknown. Nonetheless, recent observations (Tesch et al., 1990; Hortobagyi et al., 1996) suggest that the decline in muscle force is less during fatigue protocols involving eccentric (ECC) contractions compared with concentric (CON) ones. The purpose of the present work was to further investigate this difference in fatigability by comparing the changes in central and peripheral processes during CON and ECC contractions.

MATERIAL AND METHODS

Ten subjects took part in this investigation and performed, at one week interval, two standardised fatigue tests (CON or ECC) of the ankle dorsiflexor muscles during isokinetic imposed movements. Each fatigue test consisted in 5 sets of 30 maximal contractions at a constant 50°/s velocity and for a 40° range of motion. The frequency of contraction was one every 3.5s and one minute rest was allowed between each set. The torque produced by the dorsiflexors and the surface EMG of the tibialis anterior were recorded throughout the fatigue tests. The relative importance of peripheral and central mechanisms to muscle fatigue was assessed in isometric conditions by comparing, before and after each set, maximal voluntary contractions (MVC) and electrically-induced contractions in response to single and paired stimuli. Central fatigue was tested by the interpolated-twitch method (Belanger and McComas, 1982).

RESULTS

The results showed that within each set, CON contractions led to a greater loss of force and decreased EMG activity than ECC muscle contractions. This difference was particularly pronounced during the first four sets of contractions but appeared to be smaller during the last set (cf Figure). At the end of the tests, the decline in torque and EMG was significantly greater ($P<0.05$) for CON contractions (-31.6% and -26.4%, respectively) than for ECC contractions (-23.8% and -17.5%, respectively). After the successive sets of contractions, the MVC was found to be progressively reduced and to a greater extent in CON condition. Muscle activation was not affected since neither the interpolated-twitch method nor the voluntary EMG/Mwave ratio was changed during the two fatigue tests. Although no significant difference in Mwave amplitude occurred during the two tests, the twitch contractile properties were more affected by CON contractions than by ECC ones.

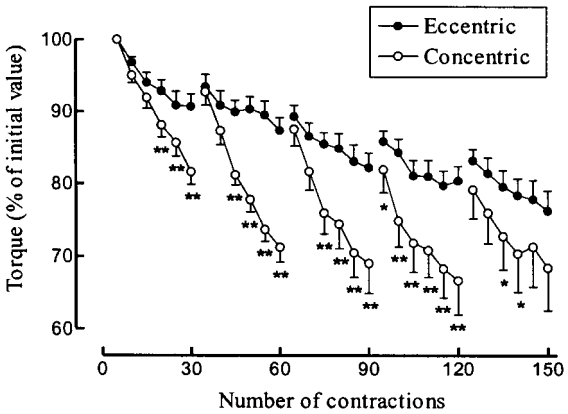

DISCUSSION AND CONCLUSION

This work, showing a greater muscle fatigability for CON contractions and a different time course of force decline compared with ECC contractions, confirms and documents previous study (Tesch et al., 1990). In addition, the results indicate that the difference in fatigability is more pronounced for a few number of contractions, but declines when a greater number are performed. This observation suggests that different mechanisms are involved in the two fatigue tests. Since there was no evidence of impaired central activation in this study, the force decline observed during the two fatigue tests should reflect mainly peripheral alterations. The absence of changes in Mwave amplitude in the two tests suggests that the force decline was related to mechanisms located beyond the neuromuscular junction and muscle membrane conduction. It is concluded that the greater alterations in the contractile properties observed during CON contractions indicate that intramuscular mechanisms, probably related to a larger energy requirement, are more affected and explains the greater fatigability of shortening compared to lengthening contractions.

This work was supported by the FNRS

REFERENCES

1–Belanger A.Y. and McComas A.J. J Appl Physiol 51: 1131–1135, 1981.
2–Enoka R.M. J Appl Physiol 81: 2339–2346, 1996.
3–Hortobagyi T., Tracy J., Hamilton G. and Lambert J. Int J Sports Med 17: 409–414, 1996.
4–Nardone A., Romano C. and Schieppati M.: J. Physiol. 409: 451–471, 1989.
Tesch P.A., Dudley G.A., Duvoisin M.R., Hather B.M. and Harris R.T. Acta Physiol Scand 138: 236–271, 1990.

MUSCLE FORCE QUANTIFICATION BY PARTITIONING USING SURFACE EMG

BAKER N. AND RONSKY J.
Department of Mechanical and Manufacturing Engineering, University of Calgary, Calgary, Canada.

INTRODUCTION

A method for quantifying patellofemoral (PF) joint contact stress under physiologic load, non-invasively and *in vivo* has been developed[1]. Load applied at the heel during a magnetic resonance (MR) scan is used as input to a lower leg and PF joint model to estimate joint contact force and stress. Previous work neglected the hamstrings contribution to joint contact force. In the absence of ACL integrity, hamstrings may be more active than in healthy knees to secure joint stability[2,3]. The purpose of this work is to quantify muscle force contributions for use in the model of PF joint contact force.

METHODS

Standard surface EMG protocol was used to record the muscle activation patterns of the rectus femoris (RF), vastus lateralis (VL), vastus medialis (VM), medial hamstrings (MH) and lateral hamstrings (LH). Isometric knee extension and flexion contractions were performed on a Biodex dynamometer (Shirley, NY) at flexion angles of 15° and 30° (0° = full extension). The subject was supine to mimic the MR scan. A maximal voluntary contraction (MVC) was performed and the torque was gravity corrected. Submaximal target torque levels (50, 30, 20 & 10% of MVC) for flexion and extension were displayed for the subject to match. EMG signal root mean square (RMS) was calculated over a 1.5s contraction captured from the force plateau. RMS was normalized to the MVC for each submaximal contraction.

The extension or flexion force was partitioned to the active muscles: RF, VL & VM or MH & LH, respectively, based on the magnitude of each RMS EMG signal[4]. A 2nd order polynomial was fit to data from three trials at a unique flexion angle to describe each muscle's EMG-force relationship during extension or flexion. MVC and 30% isometric leg press contractions were performed on the Biodex to mimic the MR set-up. EMG signals were recorded and used to calculate muscle forces from the predetermined EMG-force relationship.

RESULTS

EMG-force relationships were obtained for LH & MH (flexion) and VM, RF & VL (extension) for one subject with no knee injury history (Fig. 1). Results were consistent between trials. The relationships for 15° and 30° were similar, with higher force magnitudes observed at 30°. The EMG-force relationships were used to calculate leg press force from the normalized RMS EMG.

DISCUSSION AND CONCLUSIONS

It was assumed that all force during a contraction was generated by the superficial agonist muscles. Antagonist activity was small (average 3.5 ± 3.4% of the agonist activity) during all contractions. Force production from deep muscles (e.g. vastus intermedius) is distributed among the other agonists and total force acting on the PF joint will not change. VL force is twice as high as VM and RF for knee extension. MH and LH forces are similar in magnitude for flexion. Hamstrings activity for the leg press is minimal for this particular subject but may be higher in the case of ACL-deficiency. Future application of this work will be to compare PF contact characteristics between normal and unstable (ACL deficient) knees using this method to quantify muscle forces for input to the PF joint contact force model.

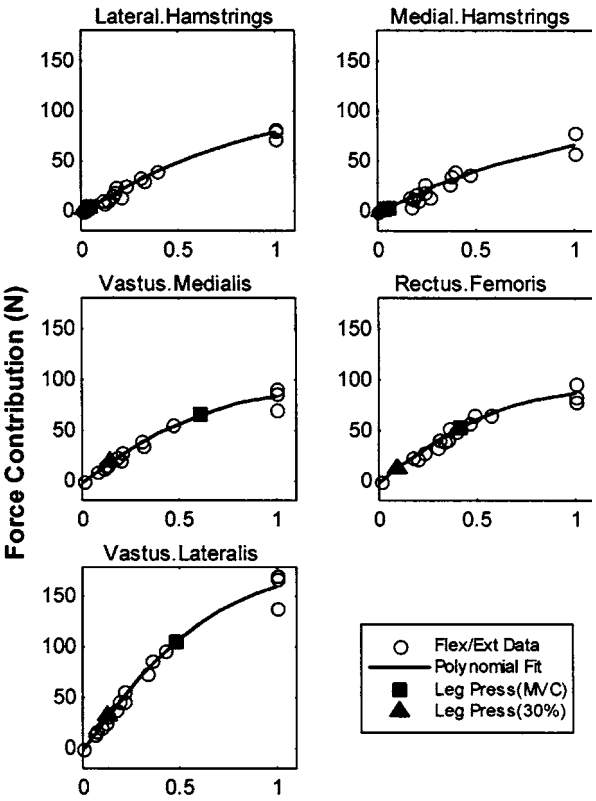

Fig. 1. Subject-specific EMG-force relationship at 30°.

ACKNOWLEDGEMENTS Financial: NSERC; Technical: M. Maitland, E. Suter

REFERENCES

1–RONSKY J.L. (1994). Ph.D. dissertation, University of Calgary, Calgary AB.
2–WEXLER G. et al. (1998). *Clin. Orthop. Rel. Res*. 348, 166–175.
3–KÅLUND S. et al. (1990). *Am. J. Sports Med*. 18, 245–248.
4–McGILL S.M. et al. (1986). *Spine 11*, 666–678.

ELECTROMYOGRAPHY: AN OBJECTIVE TOOL TO ANALYSE SEAT COMFORT IN CARS

LINO F.[1], MUR. GUERRI A.[2], BLAISE T.[3], AND LE COZ J-Y.[1]
[1]Laboratory of Accidentology, Biomechanics and human behaviour. PSA PEUGEOT CITROEN – RENAULT (LAB), Nanterre, France; [2]CEESAR, Nanterre, France; [3]FAURE-CIA, Etampes, France

INTRODUCTION

During the three last decades, many researchers have tried to measure dynamic comfort in sitting position, especially in driving condition1,2. Two types of research have been investigated: objective and subjective approaches. The former uses physiological or mechanical assessment techniques, the latter makes use of sensorial methods based on questionnaires. In most of the cases, studies deal with comfort during long-term driving by combining the two approaches3,4. In all these papers, researchers observe and measure subject behaviour without interfering. The originality of our work is to create the discomfort phenomenon by using a vertical transitional vibration which simulates road short events. In other words, the purpose of this work is to find an objective tool to analyse seat transient comfort.

MATERIAL AND METHODS

Fifteen healthy subjects (11 men and 4 women) between 20 and 35 years participated in this experiment. The subjects sat on a seat which is fixed on a vibrator bench. Nine different seats were tested. The seats have been chosen in the way to modify cushion foam thickness and hardness. The subjects posture were standardised (see Figure 1), with hands on thighs. The test lasted about one hour per subject. A triangular order signal has been used for the experiment. The triangular form was chosen to be closer to road short events such as sleeping policemen or trenches. The transitional vibration has been reproduced forty times for each seat. During the test, electromyograms (EMG) were recorded from six trunk and neck muscles. Pairs of bipolar surface electrodes (Red Dot, diameter 10 mm, disposable) were applied over the surface of Oblicuus Externus, Erectores Spinae and Sternocleidomastoidus on the right and left sides of the body. The signals were amplified by a home-made physiological amplifier and band-pass filtered (20–350 Hz). Signals were digitized on-line over 16-bit resolution at 840 Hz and stored in a laboratory computer. After each mechanical stimulation, the first stage consisted of counting and comparing the number of EMG bursts for each seat. The initial hypothesis is based on the following relation: “the more the number of EMG bursts increases the more the discomfort increases.

RESULTS

We apply a statistical method based on linear multiple regression to find the best model which optimises the comfort relation between EMG index (number of EMG bursts for the fifteen subjects and the six muscles) and the mathematical function f(t,h) which links thickness (t) and hardness(h) of the foam.

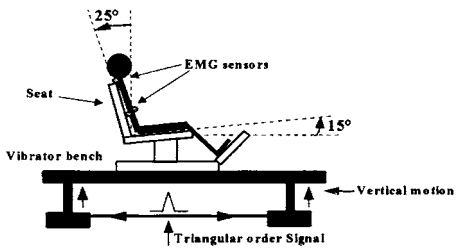

Fig. 1. Experimental device.

Table 1. Multiple regression results.

Variable	Correlation Coef.	SD	Fischer test	Probability
EMG index	0,991	0,003	30,99	HS

HS: High Significant; SD: Standard Deviation.

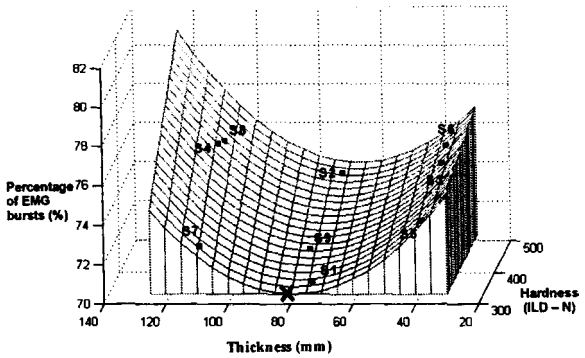

Fig. 2. Answer curves for the seats panel.

A summary of the results is shown in Figure 2. This figure is a planar representation of the best regression model solution described in Table 1. The crux X defines the best comfort position associated to the mathematical model. According to the results, the S1 seat with its low hardness and medium thickness presents the best comfort. On the contrary, a group of seats composed by S3, S4, S6 and S8 is closer to the maximal discomfort area.

DISCUSSION AND CONCLUSION

When EMG is used during long term driving, the quality of results is rather poor because of inter-individual signal variability1. On the contrary, when a stimulation is well-defined to create an EMG answer, the electromyography technique shows very good characteristics of repeatability and could contribute to improve the process of seat design. Future experiments should be done to validate this approach and improve fit.

REFERENCES

1. LAMOTTE T. and al. (1996) Ergon., 3, 5, 781–796.
2. PARK S.J. and KIM C.B. (1997) SAE., paper n°970595: 143–151.
3. WILDER D. and al. (1994) Appl. Ergon., 25, 2, 66–76.
4. GYI D.E. and PORTER J.M. (1999) Appl. Ergon., 30, 99–107.